



UNIVERSIDADE ESTADUAL DE CAMPINAS

Faculdade de Engenharia Mecânica

JOSÉ DOUGLAS ALVES DE LIRA

**Exergetic cost of an operating sugarcane power
plant**

**Análise de custo exergetico de uma usina no setor
sucroalcooleiro**

Campinas

2022

JOSÉ DOUGLAS ALVES DE LIRA

Exergetic cost of an operating sugarcane power plant

Análise de custo exergetico de uma usina no setor sucroalcooleiro

Dissertation presented to the School of Mechanical Engineering of the University of Campinas in partial fulfillment of the requirements for the degree of Master in Mechanical Engineering, in the area of Thermal and Fluids

Dissertação de Mestrado apresentada à Faculdade de Engenharia Mecânica de Universidade Estadual de Campinas como parte dos requisitos exigidos para obtenção do título de Mestre em Engenharia Mecânica, na área de Térmica e Fluidos

Orientador: Prof. Dr. Waldyr Luiz Ribeiro Gallo

ESTE TRABALHO CORRESPONDE A
VERSÃO FINAL DISSERTAÇÃO DE
MESTRADO DEFENDIDA PELO ALUNO
JOSÉ DOUGLAS ALVES DE LIRA, E ORI-
ENTADO PELO PROF. DR. WALDYR LUIZ
RIBEIRO GALLO.

Campinas

2022

Ficha catalográfica
Universidade Estadual de Campinas
Biblioteca da Área de Engenharia e Arquitetura
Rose Meire da Silva - CRB 8/5974

L67e Lira, José Douglas Alves de, 1992-
Exergetic cost of an operating sugarcane power plant / José Douglas Alves de Lira. – Campinas, SP : [s.n.], 2022.

Orientador: Waldyr Luiz Ribeiro Gallo.
Dissertação (mestrado) – Universidade Estadual de Campinas, Faculdade de Engenharia Mecânica.

1. Exergia. 2. Biomassa. 3. Energia termelétrica. 4. Termodinâmica. I. Gallo, Waldyr Luiz Ribeiro, 1954-. II. Universidade Estadual de Campinas. Faculdade de Engenharia Mecânica. III. Título.

Informações para Biblioteca Digital

Título em outro idioma: Análise de custo exergetico de uma usina no setor sucroalcooleiro

Palavras-chave em inglês:

Exergy

Biomass

Thermoelectric energy

Thermodynamics

Área de concentração: Térmica e Fluídos

Titulação: Mestre em Engenharia Mecânica

Banca examinadora:

Waldyr Luiz Ribeiro Gallo [Orientador]

Joaquim Eugênio Abel Seabra

Antônio Garrido Gallego

Data de defesa: 29-07-2022

Programa de Pós-Graduação: Engenharia Mecânica

Identificação e informações acadêmicas do(a) aluno(a)

- ORCID do autor: <https://orcid.org/0000-0002-9284-140X>

- Currículo Lattes do autor: <http://lattes.cnpq.br/7265874691157855>

**UNIVERSIDADE ESTADUAL DE CAMPINAS
FACULDADE DE ENGENHARIA MECÂNICA**

DISSERTAÇÃO DE MESTRADO

**Exergetic cost of an operating sugarcane power
plant**

**Análise de custo exergetico de uma usina no setor
sucroalcooleiro**

Autor: José Douglas Alves de Lira

Orientador: Prof. Dr. Waldyr Luiz Ribeiro Gallo

A Banca Examinadora composta pelos membros abaixo aprovou esta Dissertação de Mestrado:

Prof. Dr. Waldyr Luiz Ribeiro Gallo

Departamento de Engenharia Mecânica – Universidade Estadual de Campinas

Prof. Dr. Joaquim Eugênio Abel Seabra

Departamento de Engenharia Mecânica – Universidade Estadual de Campinas

Prof. Dr. Antônio Garrido Gallego

Departamento de Engenharia Mecânica – Universidade Federal do ABC

A Ata de Defesa com as respectivas assinaturas dos membros encontra-se no SIGA/Sistema de Fluxo de Dissertação/Tese e na Secretaria do Programa da Unidade.

Campinas, 29 de Julho de 2022

DEDICATION

This work is bigheartedly dedicated to my beloved mother, grandfather, and especially to my grandmother, that entered her eternal sleep. They have been my source of inspiration, giving me the strength to never give up, and providing their moral and financial support.

ACKNOWLEDGEMENTS

To my mother Raquel, my grandfather José Rozendo, and Rafaela all your support.

To my fiancée who provided emotional support and shared her words to encourage me to finish this study. For putting up with me at times when even I couldn't stand myself. Also, thanks to her mother, aunt Marcia and her sister, Isis, who gave me support in this journey.

To my roommates Felipe and Israel, I miss our days talking about thermodynamics and spending weekends doing things together. Thank you for helping me with this work. To my friends Igor, Luciano, and Matheus for their support.

To my Advisor Prof Dr. Waldyr L. R. Gallo, for his patience, calmness, and understanding, for his dedication, and for his love of teaching. You are one of the most amazing human beings I've had the pleasure of meeting on my journey. Also, thank you for teaching me to be methodic about thermodynamics.

To Prof. Dr. Antônio Gallego, Prof. Dr. Joaquim E. A. Seabra, and Prof Dra Silva Nebra for their questions and contributions to making this work better.

This study was financed in part by the Coordenação de Aperfeiçoamento de Pessoal de Nível Superior – Brasil (CAPES) - Finance Code 001

Einstein about Thermodynamics: “It is the only physical theory of universal content, which I am convinced, that within the framework of applicability of its basic concepts will never be overthrown.”

RESUMO

Um dos principais desafios do mundo passou a ser produzir energia limpa, barata e ecologicamente correta para alcançar o desenvolvimento sustentável. A indústria sucroenergética tem mostrado grande potencial para produzi-la utilizando biomassa. Para suprir a produção de açúcar e álcool necessária, suprir todas as necessidades de energia elétrica e até mesmo para vender energia elétrica à rede, sugere-se operar com pressão de vapor superaquecido superior a 60 bar. No entanto, a avaliação do processo de conversão de energia de forma mais eficiente depende do desenvolvimento de diversos parâmetros termodinâmicos. Diante desses desafios, foi desenvolvida uma análise de custo exergético e exergético de uma usina de cana-de-açúcar para identificar as perdas do sistema e por quais razões essas perdas ocorrem no processo de conversão de energia. Este sistema processa mais de 9.000 toneladas de cana-de-açúcar por dia e está equipado com três caldeiras e sete turbinas a vapor de contrapressão. Hoje, esta usina opera com um sistema de cogeração de baixa eficiência baseado em um ciclo de vapor com vapor superaquecido a 22 bar e temperaturas em torno de 285°C. Nesta usina, nenhuma energia elétrica é vendida à rede e o sistema de cogeração deve suprir todas as necessidades de energia elétrica, bem como as necessidades de energia térmica. Para avaliar o desempenho deste sistema e propor modificações para aumentar a eficiência global, cujos dados foram coletados in situ, o procedimento de cálculo e as propriedades termodinâmicas são compilados no Engineering Equation Solver (EES). Os resultados da análise de exergia demonstram que (1.) A taxa de destruição de exergia através dos gases de escape representa 14.59% da exergia do combustível. Essa destruição de exergia pode ser reduzida usando a temperatura dos gases de exaustão para aumentar a temperatura da água que é alimentada nas caldeiras. (2.) A destruição de exergia em turbinas e válvula de expansão é de 2.71% e 0.36%, respectivamente. (3.) As turbinas estão operando em condições de carga parcial e a válvula de expansão é um dispositivo puramente dissipativo. Por outro lado, o custo exergético pode ordenar os componentes, de acordo com sua destruição de exergia, e mostrar quais componentes devem ter prioridade nas medidas de aprimoramento para aumentar a eficiência do sistema. Os resultados de custo exergético demonstram que (4.) O elemento com maior prioridade são as três caldeiras, com uma diferença de custo relativa de 3.79, 3.79 e 3.58, respectivamente (5.) Os resultados sugerem que quanto mais exergia é destruído para produzir o fluxo, mais caro é o custo exergético unitário; então, o custo exergético está aumentando através do sistema até os produtos finais, (6.) Considerando a energia elétrica como um produto, o custo exergético unitário deste produto é cerca

de 3 vezes maior em relação a outros sistemas que produzem o mesmo produto (7.) Os outros componentes mais bem classificados são as turbinas do sistema e a expansão válvula. Portanto, substituir a turbina menos eficiente por um motor elétrico, desativando a válvula de expansão e enviando seu consumo de vapor para a turbina, que é acoplada ao gerador elétrico, parece ser interessante, pois essa turbina tem capacidade para isso. As modificações propostas foram avaliadas e os resultados demonstram que: (8.) Obteve-se um excedente de energia 10,69% maior que a potência do caso real (9.) As eficiências de cogeração de energia e exergia no caso real e no caso proposto são: 62.56% – 17.14% e 63.99% – 18.37%, respectivamente, e (10.) A análise de custo exergético mostra que a formação de custos através do sistema de configuração proposto diminuiu 8.54% em relação ao caso base. Desta forma, este estudo indica que as modificações propostas se mostraram eficazes do ponto de vista termodinâmico e podem ser implementadas para disponibilizar a energia excedente para venda à rede como um projeto futuro. Essas modificações são baseadas apenas na alteração das condições de operação, e não requerem altos investimentos para alterar toda a configuração do sistema de cogeração, ou seja, aumentar as condições de trabalho de pressão para mais de 60 bar.

Palavras-chave: Exergia, Biomassa, Energia Termelétrica, Termodinâmica

ABSTRACT

One of the main challenges in the world has become to produce clean, cheap, and environmentally friendly energy to achieve sustainable development. The sugarcane industry has shown great potential to produce it using biomass. In order to provide the required sugar and alcohol production, supply all-electric power needs, and even for selling electric energy to the grid as well, it is suggested to operate with superheated steam pressure higher than 60 bar. However, the evaluation of the energy conversion process more efficiently depends on the development of several thermodynamics parameters. Facing these challenges, an exergy and exergetic cost analysis of a real-world sugarcane power plant was developed to identify the system losses and for what reasons those losses occur in the energy conversion process. This system process over 9000 tons of sugarcane per day and is equipped with three boilers and seven back pressure steam turbines. Today, this power plant is operating with a low-efficiency cogeneration system based on a steam cycle with superheated steam at 22 bar and a temperature around 285°C. In this power plant, no electric power is sold to the grid and the cogeneration system must supply all-electric power needs, as well as the thermal power needs. To evaluate the performance of this system and propose modifications to increase the global efficiency, which data was collected in situ, calculation procedure and thermodynamics properties are compiled in Engineering Equation Solver (EES). The exergy analysis results demonstrate that (1.) Exergy destruction rate through exhaust gas represents 14.59% of fuel exergy. This exergy destruction could be reduced by using the exhaust gas temperature to increase the water temperature that is fed in boilers. (2.) Exergy destruction in turbines and expansion valve are 2.71% and 0.36%, respectively. (3.) Turbines are operating at partial load conditions and the expansion valve is a purely dissipative device. On the other hand, the exergetic cost can rank the components, according to their exergy destruction, and show which components should have priority in enhancement measures to increase the efficiency of the system. The exergetic cost results demonstrate that (4.) The element with the highest priority is found to be the three boilers, with a relative cost difference of be 3.79, 3.79, and 3.58, respectively (5.) Results suggest that the more exergy is destroyed to produce the flow, the more expensive is the unit exergetic cost; then, the exergetic cost is increasing through the system to the final products, (6.) Considering electrical power as a product, the unit exergetic cost evaluated here is about 3 times higher compared to the values found in the literature; (7.) The other top-ranked components are the turbines for mechanical power and the expansion valve. Therefore, replacing the less efficient turbine with an electric

motor, deactivating the expansion valve, and sending their steam consumption to the turbine, which is coupled to the electric generator, seems to be interesting, since this turbine has the capacity to do it. The proposed modifications were evaluated and the results demonstrate that: (8.) A surplus energy of 10.69% greater than the power output of the actual case was obtained, which could be sold to the local electric distributor (9.) The energy and exergy cogeneration efficiencies in the real case and proposed case are: 62.56% – 17.14% and 63.99% – 18.37%, respectively, and (10.) The exergetic cost analysis shows that the cost formation through the proposed configuration system has decreased by 8.54% comparing to the base case. In this manner, this study indicates that proposed modifications have been proved to be effective from a thermodynamics point of view and can be implemented to make the surplus energy available for sale to the grid as a future project. Since these modifications are based only on the change of the operation conditions and do not require high investments to change all cogeneration system configurations i.e., increase pressure working conditions above 60 bar.

Keywords: Exergy, Biomass, Thermoelectric energy, Thermodynamics

LIST OF FIGURES

1.1	“The interactions among exergy, economy, and environment” (Soltanian et al., 2020) Copyright 2021, with permission from Elsevier. License Number: 5094941357396	22
1.2	“Relationship between exergy destruction and economic loss/resource depletion” (Soltanian et al., 2020). Copyright 2021, with permission from Elsevier. License Number: 5094941357396	22
2.1	Brazilian sugar exports by the harvest in million tons – source: (CONAB, 2020)	31
2.2	Brazil ethanol exports by the harvests in million liters – source: (CONAB, 2020)	31
2.3	Brazilian Ethanol imports by harvest - source: (CONAB, 2020)	32
2.4	Participation of bagasse in electricity generation – Source: (EPE, 2019a)	33
2.5	Self-consumption and energy exported by cogeneration systems fueled by bagasse – Source: (EPE, 2019a)	35
2.6	“Kalina cycle System 11 (KCS-11) integrated with the cogeneration plant of the considered 3500 TCD sugar factory” (Singh, 2020). Copyright 2021, with permission from Elsevier. License Number: 5102580565293	38
2.7	“Variations of increases in net power output, cogeneration energy efficiency, and cogeneration exergy efficiency of the cogeneration-Kalina integrated system with the decrease in moisture content of bagasse” (Singh, 2020). Copyright 2021, with permission from Elsevier. License Number: 5102580565293	38
2.8	“Distribution of irreversibility in each equipment using 8 regenerators in scenarios C2 and C3” (Pérez et al., 2018). Copyright 2021, with permission from Elsevier. License Number: 5102581381928	39
2.9	“Exergy efficiency of solar collectors on day of maximum efficiency”(López et al., 2021). Copyright 2021, with permission from Elsevier. License Number: 5102591118737	39

2.10	“Impact of pinch point temperature difference on exergy efficiency and cost rate”(Karimi et al., 2020). Copyright 2021, with permission from Elsevier. License Number: 5102611353245	40
4.1	generic subsystem adapted from (Torres, 1999)	54
5.1	Block diagram of the thermodynamic analysis of the system.	56
5.2	Sugarcane power plant configuration.	58
6.1	Unit exergetic cost considering power generation as a product	77
6.2	Top-ranked Relative Cost Differences at each control volume in the system .	79
6.3	Proposed modification plant	82
A.1	An example of a <i>simple graph</i>	97
B.1	An example of a directed graph.	99
B.2	Another example of a directed graph.	99
A.1	General information about BPST attached to the generator	147
B.1	General information about BPST	148

LIST OF TABLES

2.1	The World's top 10 sugarcane-producing countries – Average 2018 – 2020 .	28
2.2	The World's top 10 sugarcane consumers in 2019	29
2.3	World Fuel Ethanol Production and Consumption in Billions Litres	29
2.4	Critical review on cogeneration systems fueled by biomass	42
3.1	Standard chemical exergy at reference-environment	47
4.1	Thermoeconomic theories reported in the literature	49
5.1	Technical specifications of the boilers at nominal conditions	57
5.2	Technical specifications of the TX-2040ME/20 turbine at nominal conditions	59
5.3	Technical specifications of the TX-10000/20 turbine at nominal conditions .	59
5.4	Working conditions and site data of cogeneration system	59
5.5	Characteristics of sugarcane bagasse (Cortes-Rodriguez et al., 2017a)	60
5.6	Energy balance for each component	62
5.7	Standard chemical exergy at reference-environment	64
5.8	Exergy destruction rate for control volume	64
5.9	Fuel and product exergy definitions of the cogeneration system	66
5.10	Equations for exergetic cost balance of the cogeneration system	67
6.1	Flow identification and thermodynamic properties.	70
6.2	Non-Material flow identification	71
6.3	Energy and exergy balance for the boilers and efficiency on energy and exergy base.	72
6.4	energy and exergy balance for turbines and efficiency on energy and exergy base.	73
6.5	Exergy balance of the analyzed cogeneration system and the percentage ratio of exergy to fuel exergy input	73
6.6	Flow identification and thermodynamic properties.	74
6.7	Exergy, exergetic cost and unitary exergetic cost of each flow	75
6.8	Unit exergetic cost and relative cost difference of each control volumes . . .	78
6.9	Flow identification and thermodynamic properties of the proposed case . . .	81

6.10	A comparison between the exergy destruction on the analysed cogeneration system and the proposed case.	83
6.11	Effect of proposed changes on net power output, net electrical efficiency on energy and exergy based and cogeneration efficiency on energy and exergy based.	83
6.12	Exergy, exergetic cost, and unitary exergetic cost of each flow for the proposed case	85
6.13	A comparison between the unit exergetic cost of the reference system and the proposed case.	86
6.14	Unit exergetic cost and relative cost difference of all control volumes from the proposed case	87

LIST OF ABBREVIATIONS AND ACRONYMS

ASME	The American Society of Mechanical Engineers
BECCS	Bioenergy with carbon capture and storage
BPST	Back pressure steam turbine
CONAB	National Supply Company
CV	Control Volume
EEA	Exetended Exergy Accounting
EPE	Energy Research Company
FPS	Fuel-Product-Loss
GHG	Greenhouse Gas
IEA	International energy agency
LCA	Life Cycle Assessment
LER	Reserve Energy Auction
NREL	National Renewable Energy Laboratory
SIN	National Integrated System
Unicamp	University of Campinas

LIST OF SYMBOLS

A	Incidence Matrix
B	Boiler
e	Specific Exergy
e	A column-vector of the energy flow rate associated to the j-th flow
E	Energy
\dot{E}	Exergy flow rate
\dot{H}	Energy transfer rate associated with enthalpic flow
h	Specific enthalpy
HHV	Higher heating value
LHV	Lower heating value
\dot{m}	Mass flow rate
m	A column-vector of the mass flow rate associated to the j-th flow
P	Pressure
\dot{Q}	Heat transfer rate
R	Universal Gas Constant
s	Specific entropy
T	Temperature
T	Turbine
u	Specific internal energy
\dot{W}	Power transfer rate
wt	Weight

ϵ	A column-vector of the exergy flow rate associated to the j-th flow
ϵ	Efficiency based in the second law
\mathcal{E}	Set of graph edges
\mathcal{E}	Set of the m flows in the thermodynamic system.
\mathcal{G}	directed simple graph
η	Efficiency based in the first law
κ	Unit Exergy Consumption
ζ	Set of distinct graph nodes.
ζ	Set of n devices or process in the thermodynamics system.

LIST OF SUBSCRIPT AND SUPERSCRIPT

\mathbf{A}_F	Fuel Incidence Matrix
α_{ij}	Element of matrix \mathbf{A} at the i-th row and j-th column.
\mathbf{A}_L	Loss Incidence Matrix
\mathbf{A}_P	Product Incidence Matrix
B	Boiler
CH	Chemical exergy
cog	Cogeneration
CV	Control Volume
\mathbb{C}_0	Base configuration
\mathbb{C}_1	Proposed configuration
d	Destruction
dist	Distillery Process
\dot{E}^*	Exergetic cost of Flow rate
E_j	Exergy flow rate associated with work or heat
eg	Exhaust gases
el	Electrical
f	Fuel
\mathbf{f}^*	Exergetic cost of fuel
\dot{H}_b	Enthalpic flow to carry out the phase change of water into superheated steam
\dot{H}_f	Enthalpic flow supplied by the fuel

h_0	Enthalpy at dead state
in	Inlet
iso	Isoentropy process
M_w	Moisture content in bagasse
MM_{ap}	Apparent molecular mass of mixture
net	net electrical energy
p^*	Exergetic cost of product
PH	Physical exergy
P_0	Surrounding environmental pressure
\dot{Q}_{all}	Energy losses associated with moisture in the fuel, convection, and radiation losses from the boilers surface.
sugar	Sugar Production
s_0	Entropy at dead state
T_0	Surrounding environmental temperature
u_0	Specific internal energy at dead state
v_0	Specific volume at dead state
v_0	system surrounding environment
w_{ash}	Bagasse weight percentages of ash
w_c	Bagasse weight percentages of carbon
w_h	Bagasse weight percentages of hydrogen
w_o	Bagasse weight percentages of oxygen
w_s	Bagasse weight percentages of sulphur
ϵ_d^*	A column-vector of the exergy destruction cost flow rate associated to the j-th flow

η_{iso}	Isentropic efficiency of turbines
κ_{d}	Diagonal Matrix contained the exergy unit consumption of each subsystem
ϕ_{dry}	Ratio chemical exergy to the LHV

CONTENTS

1	Introduction	21
1.1	Aim	24
1.2	Objectives	25
1.3	Dissertation outline	25
2	Literature review	27
2.1	Biomass	27
2.2	The Sugarcane Industry	28
2.3	Brazilian international market of sugar and alcohol	30
2.4	Brazilian electricity using cogeneration systems in Sugarcane Industry	32
2.5	Literature Review On Sugarcane industry	35
3	Thermodynamic Analysis	44
3.1	Energy and Exergy Analysis	44
3.2	Environment	46
3.3	Physical flow exergy	46
3.4	Chemical Exergy	47
3.5	Exergetic Efficiency	48
4	Exergetic Cost Analysis	49
4.1	Exergetic cost analysis	49
4.2	Theory of Exergetic Cost - TEC	50
4.3	Productive Structure – Fuel-Product-Loss	50
4.3.1	<i>Fuel Incidence Matrix</i>	51
4.3.2	Vector of Flows of type <i>Fuel</i>	51
4.3.3	<i>Product Incidence Matrix</i>	52
4.3.4	Vector of Flows of type <i>Product</i>	52
4.3.5	<i>Loss Incidence Matrix</i>	52
4.3.6	Vector of Flows of type <i>Loss</i>	53
4.3.7	<i>Exergy Destruction Vector</i> as a function of f , p and l	53
4.3.8	<i>Unit Exergy Consumption Matrix</i>	53
4.4	Exergy Cost Definition through Propositions	53

4.5	Exergetic cost of Control volumes	54
5	Thermodynamic & Exergetic Cost Modelling	56
5.1	Description of the cogeneration power plant.	56
5.2	Fuel properties	60
5.3	Assumptions for energy and exergy analysis	61
5.3.1	Energy Analysis	61
5.4	Exergy Analysis	63
5.5	Energy and Exergy Efficiencies	64
5.6	Exergetic cost analysis	65
6	Results and Discussion	69
6.1	Performance of the sugarcane power plant	69
6.2	Exergetic cost analysis	74
6.3	Proposed modifications based on exergy and exergetic cost analyses	79
6.4	Exergy and exergetic cost analyses of the proposed modifications	80
7	Conclusion and Future studies	89
	Bibliography	91
	Appendix	96
APPENDIX A	Theory of Exergetic Cost - Physical Structure	97
APPENDIX B	Theory of Exergetic Cost - Physical Structure as a Directed Graph	98
APPENDIX C	Theory of Exergetic Cost - Mass Balance over all Aggregation Levels in Matrix Form	101
APPENDIX D	Theory of Exergetic Cost - Energy Balance over all Aggregation Levels in Matrix Form	102
APPENDIX E	Theory of Exergetic Cost - Exergy Balance over all Aggregation Levels in Matrix Form	103
APPENDIX F	Theory of Exergetic Cost -Exergetic Cost Balance per Proposition \mathcal{P}_1	104
APPENDIX G	Theory of Exergetic Cost – Appending (n-m) equations using propositions	105

APPENDIX H	Theory of Exergetic Cost - Complete System of Equations in Terms of Unit Exergy Cost κ^*	106
APPENDIX I	EES Source Code	108
Annex		146
ANNEX A	Catalog of the BPST attached to the generator	147
ANNEX B	Catalog of the BPST attached to the machines	148
ANNEX C	General characteristics of the boiler	149

1 INTRODUCTION

Energy is the most basic human need and energy conversion processes with increased efficiency have become extremely important in the last decades. The annual outlook report issued by the U.S. Energy Information Administration ([Center, 2020](#)) reported that generation levels from renewable sources are expected to reach more than 2000 billion kilowatt-hours by 2050.

Currently, the planet has nearly 8 billion inhabitants (2021), and Our World in Data estimates predict a population of 11 billion by 2100 ([Roser, 2013](#)). According to ([Rosa; Ordonez, 2021](#)), population growth alone could account for a 1% per year increase in energy demand. According to ([IEA, 2018](#)), most energy use comes from non-renewable sources.

The growth of renewable energy is needed in recent years due to its less carbon-intensive and more sustainable energy system and is becoming increasingly popular because of the adverse environmental effects of greenhouse gas emissions from the use of fossil fuels ([Rahman; Velayutham, 2020](#)).

Population growth, technological development, and industrialization result directly in increasing energy consumption. As a result, to reduce CO₂ emissions, improved designs and operation of the energy conversion process are highly needed. Thermodynamic indicators like energy, exergy, and exergy based on the first and second laws of thermodynamics are generally considered as the most natural ways to determine the sustainability of renewable energy projects ([Dadak et al., 2016](#)).

Among the approaches mentioned, exergy-based methods rooted in the laws of thermodynamics have been proven capable of providing invaluable insights into thermodynamic, economic, and environmental aspects ([Soltanian et al., 2020](#)). However, determining the sustainability and productivity facets of an energy resource through the standard exergy analysis has been criticized for its ineffectiveness in quantifying the exergy of externalities ([Aghbashlo et al., 2018b](#)).

To overcome it, a novel approach called Extended Exergy Accounting (EEA) was introduced, and it can be employed to cover the deficiencies of exergy theory and consider the externalities in terms of exergy ([Aghbashlo et al., 2018b](#)) ([Sciubba, 2001](#)). Thus, exergy is uniquely treated as the confluence of economy, environment, and sustainable development

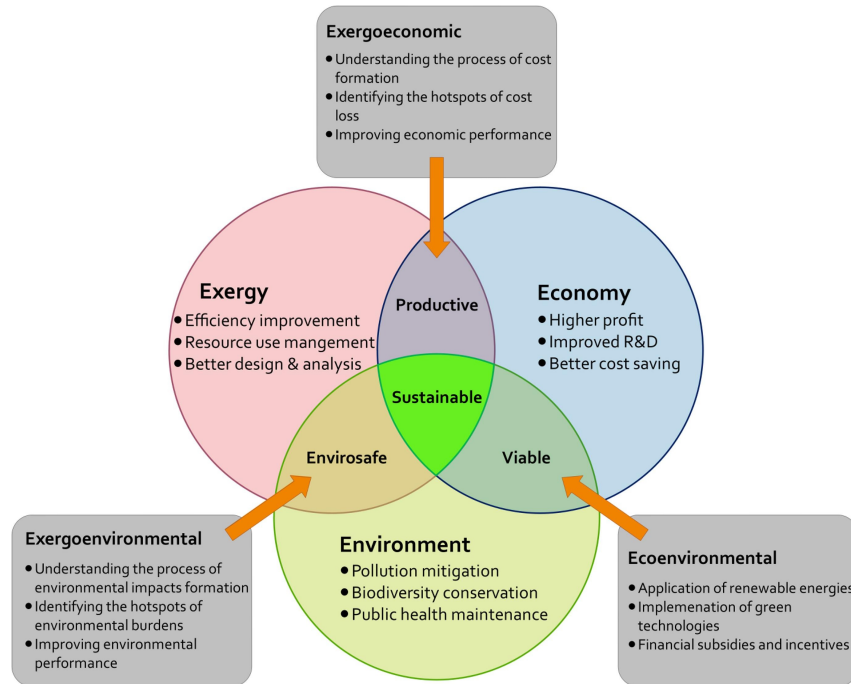


Figure 1.1 – “The interactions among exergy, economy, and environment” (Soltanian [et al.](#), 2020) Copyright 2021, with permission from Elsevier. License Number: 5094941357396

as shown in the Figure 1.1. As can be seen in Figure 1.2, with the increasing sustainability

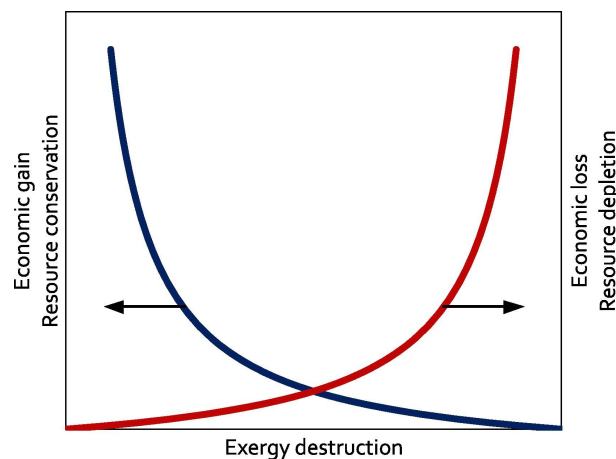


Figure 1.2 – “Relationship between exergy destruction and economic loss/resource depletion” (Soltanian [et al.](#), 2020). Copyright 2021, with permission from Elsevier. License Number: 5094941357396

and decreasing environmental impact, the exergy efficiency of a process must increase (Dincer, 2011) (Dincer; Rosen, 2005) .

In most countries, thermal power plants are playing a crucial role in energy production (Kumar, 2017). Thus, increase thermal power plant’s performances is an objective in terms of economic, energy policy, national security, fuel reserve, and environmental concerns

([Erdem et al., 2009](#)). Moreover, according to ([Dincer; Abu-Rayash, 2020](#)), co-generation systems thermal power plants present a chance to improve decentralized electricity generation, avoid transmission losses, and system flexibility can be increased. Furthermore, GHG emissions are limited by co-generation very strongly and enhance processes, leading to substantial cost savings and affordable electricity rates ([Dincer; Abu-Rayash, 2020](#)).

In Brazil, using a cogeneration system has become a practice adopted by the sugarcane and ethanol agroindustry. The most common cogeneration system includes a steam boiler, back-pressure steam turbines, or turbogenerator. The sugarcane bagasse is burned into furnaces to produce steam for power generation. In these systems, the superheated steam supplies the back-pressure steam turbines to generate electrical power. The low-pressure steam leaving the turbines flows to heating devices as mill drives in the sugar or ethanol production stages.

As previously stated, the impacts of industrial activities on the environment have become increasingly recurrent and the main challenge of the world has become to produce clean, cheap, and environmentally friendly energy to achieve sustainable development. Sugarcane has great potential in the supply of clean energy from the bagasse of sugarcane, ethanol, fertilizers from vinasse, alcoholic distillate, and bio-based bulk materials(bio-plastic) among other derivatives

In Brazil, the sugarcane sector is the world's largest producer of sugarcane worldwide ([ISO, 2022](#)). The Sugarcane sector is considered to be one of the most important economic sectors in Brazil due to its large domestic and international market of sugar and ethanol production ([CONAB, 2020](#)). According to ([ISO, 2022](#)), the sugar product obtained from sugarcane accounts for nearly 80% of global sugar production. In addition, the sugarcane sector plays a strategic role in energy security and the country's environmental performance ([Picoli et al., 2016](#)). The importance of the sugarcane sector in energy security countries occurs because the bagasse is the main biomass used for electricity generation in Brazil ([CONAB, 2020](#)).

According to ([IEA, 2019](#)) the energy matrix of the world is mostly based on non-renewable fuels. In Brazil the consumption of energy from non-renewable sources (53.8%) is higher than that from renewable (46.2%) and when considering the offer of renewable sources, 18% was derived from sugarcane biomass ([EPE, 2019b](#)). According to ([EPE, 2019b](#)) the Brazilian electric matrix in 2019 is even more renewable than the energetic one, being: 64.9% hydro, 9.3% natural gas, 8.6% wind, 8.4% sugarcane biomass, 3.3% coal, 2.5% nuclear, 2% oil and 1% solar. A review article reported by ([Ferreira et al., 2018](#)) has concluded that the contribution

of the sugarcane biomass to the Brazilian electricity matrix could be increased.

To understand the importance of this sector in the national interconnected system, in 2019, the cogeneration system fueled by bagasse injected about 2.6GW average into the National Interconnected System(SIN) (EPE, 2019a). Also, in Brazil, there are about 366 Sugarcane power plants in operation in 2019, eight more than in the 2018 year. Of all of the plants that export energy to the National Integrated System (SIN), about 60% operate exclusively in free contracting environments, 17% operate in the Regulated contracting environments, and 23% sell to both contracting environments (EPE, 2019a). It is also important to state that, according to the National Energy Balance (EPE, 2021), in 2020, about 181622×10^3 tonnes of bagasse were obtained; however, only 30824×10^3 tonnes of this bagasse was used for electricity generation, which represents about 17% on average of the total production. This indicates that the electricity generation using bagasse can be increased.

With such a large volume of bagasse being produced, the sugarcane sector exhibits significant economic potential for electricity generation in Brazil and might have a positive effect on energy generation to meet the country's energy demand using renewable resources. However, this potential is not reached because of various factors such as high technological demands, unavailability of needed capital, and lack of expertise. The use of high technological systems for cogeneration systems coupled with optimization allows the production of surplus bagasse (Ensinas et al., 2007). Note that, this potential is not reached because, generally, the low-efficiency cogeneration system based on a steam cycle with superheated steam at 22 bar and 300°C is still used (Ensinas et al., 2007) (Macedo, 2001). According to (Ensinas et al., 2007), cogeneration systems operating with superheated steam with pressure above 60 bar are the best to attempt the plant energy requirement and produce electric surplus energy that can be sold to the grid.

1.1 Aim

The present work aimed to analyze a sugarcane power plant that produces sugar, ethanol, and electric energy using the First and Second Laws of Thermodynamics and the Exergetic cost analysis. The electric energy in this sugarcane power plant is for self-consumption. With the results obtained from these analyses, a new configuration proposal was proposed and evaluated using these analyses to produce an electric energy surplus. The importance of the Second Law of Thermodynamics and Exergetic cost methodologies to develop systems that ef-

fectively use renewable energy resources is apparent. These method is well suited for furthering this goal. Because of the importance of the sugarcane sector in Brazil's economy, the use of adequate methodology is needed to design new systems and to reduce the inefficiency of existing systems.

1.2 Objectives

The Objectives of this work are:

- Evaluate the performance of a sugarcane power plant using the mass, energy, exergy, and exergetic cost analyses with experimentally obtained variables.
- Examined the performance of the sugarcane power plant through various thermodynamics parameters such as global efficiency, electric to heating ratio, exergy destruction, and so forth.
- A new configuration proposal to minimize the exergy destruction and increase the power generation without high investments.
- Evaluate these modifications and its benefits

1.3 Dissertation outline

- Chapter 2: The second chapter presents the reader with a brief bibliographic review of the main concepts relevant to this work, such as the origin of biomass as an energy source, and the importance of the sugarcane industry to the international market of sugar and alcohol, Brazilian electricity using bagasse. This chapter shows that the use of bagasse has a small consumption in order to produce energy generation and shows that sugarcane cogeneration systems might have a positive effect on energy generation to meet the country's energy demand. To finish this chapter, a literature review on the sugarcane industry using thermodynamics analysis is presented.
- Chapter 3: In the third chapter, the thermodynamics methodology used in this work is presented. First, a brief comment on the main applications of thermodynamics in engineering is presented. Then, key concepts of thermodynamics are presented, such as heat, work, property, entropy, exergy, restricted equilibrium, unrestricted equilibrium, exergy destruction, reversible process, system efficiencies, and environment.

- Chapter 4: In the fourth chapter, the exergetic cost methodology used in this work is present. First, a brief comment what is thermoeconomic analysis and its history. Second, a table showing the various thermoeconomic theories reported in literature is presented. Then, key concepts of the theory of Exergetic Cost are presented, such as physical structure, the mass, energy, exergy and exergetic cost balances of all aggregation levels in matrix form, definitions of fuel, product, loss, unit exergy consumption, and the propositions. The fuel, product, and loss incidence matrix are also presented in this chapter. To finish this chapter, the exergy cost definition through propositions is presented.
- Chapter 5: In the fifth chapter, thermodynamic modeling is presented. First, is presented the cogeneration system, its working conditions, the fuel properties, and the assumptions made for the energy and exergy analysis. Second, the energy and exergy equations for each control volume are presented in tables. Then, energy and exergy efficiencies are presented. To finish this chapter, the four propositions used to determine the missing equations of the exergetic cost balance are presented as well as all exergetic cost equations to each control volume in a table are presented.
- Chapter 6: In the sixth chapter, presents the results and discussion. A brief comment on how the flow and thermodynamic properties were obtained is presented. First, the results and discussions applying the energy, exergy and exergetic cost balance of the current cogeneration system are presented. Then, the proposed modifications based on the previously results are briefly explained. To finish this chapter is presented a comparison of the experimentally originated data with those calculated from the generalized model using the exergy and exergetic cost analyses.
- Chapter 7: Finally, the seventh and last chapter records the conclusions obtained about the study and its prospects.

2 LITERATURE REVIEW

This chapter will be presented a literature review of the sugarcane industry. This chapter will approach the position reached by Brazil in the top countries of sugarcane production, sugarcane consumers, ethanol production, and the importance of the Brazilian international market of sugar and alcohol. Then, a brief literature review on the Brazilian electricity using cogeneration systems in these sectors will be presented. In this part, important definitions are presented. In closing the chapter, a brief literature review using the laws of thermodynamics is presented in the Literature review on sugarcane industry subchapter.

2.1 Biomass

The use of biomass as an energy source must have started between 350,000 and 320,000 years ago. At that time, the use of biomass was primordial for human beings, and their evolution. Its own means of obtaining and using it progressed together from firewood collected to cooking, heating, protection, and even to modern practices of silver-agricultural and industrial production, transforming and using biofuels to generate heat, motive power, and electricity ([Shimelmitz et al., 2014](#)).

Sugarcane bagasse is the main biomass used for electricity generation in Brazil for some reasons: (1.) Due to the quantity and economy, because its availability relies on the sugar and ethanol production with a large domestic and international market ([CONAB, 2020](#)); (2.) because the ethanol and sugar industry established on the national soil. From a historical perspective, In 1975 a remarkable impact on the introduction of biofuels in the Brazilian national market was the National Alcohol Program (Proálcool) ([EPE, 2015](#)).

Remark 1 (Proálcool – ([EPE, 2015](#))). *It is considered a pioneering biofuel program, and its main objective was to produce a national alternative fuel, since, after the oil shocks in 1973 and 1979, this product and its derivatives had a considerable price increase, strongly impacting the balance of payments. With the Proálcool program, the national sugar-energy industry was consolidated and expanded, becoming an international reference.*

According to ([Mauricio, 2016](#)), In the beginning of Proálcool program, sugarcane production in Brazil grew almost 9 times. In 2015, The area used to plant sugarcane in Brazil

was 9 million hectares average, resulting in a production of 658.4 million tons of sugarcane, 117.8 million tons of bagasse and 102.1 million tons of straw were produced (Mauricio, 2016).

Given the relevance of the sugarcane industry, a brief literature review will focus on it and its technology.

2.2 The Sugarcane Industry

Sugarcane production top ten countries can be seen in Table 2.1. These countries are responsible for almost 70% of all sugarcane production and Brazil is the world's largest producer of sugarcane. Sugarcane is a thin plant in a cylindrical shape with large leaves. This plant can reach up to six meters in height. This plant produces two essential products for the world economy sugar and alcohol. The sugar product obtained from sugarcane accounts for nearly 80% of global sugar production (ISO, 2022). The sugarcane sector is crucial to Brazil since almost seven hundred thousand people are employed in this sector ¹.

Table 2.1 – The World's top 10 sugarcane-producing countries – Average 2018 – 2020

Rank	Country	Production (tonnes)
1	Brazil	752714698
2	India	385273676
3	Thailand	113681347
4	China	108535400
5	Pakistan	71520939
6	Mexico	56709426
7	Australia	3206854633
8	USA	31019373
9	Columbia	30255807
10	Indonesia	29171276

Source: United Nations Food and Agriculture Organization, FAOStat, 2022.

According to (ISO, 2022), the world sugar trade averages about 65 millions tonnes/year and accounts for 60% of internationally trade volumes. The international marketing of sugar is led by India, EU-28, China, and Brazil, which together dominate 70% of the world trade in 2019 (Table 2.2).

¹ Employment data provided by Observatorio da cana

Table 2.2 – The World's top 10 sugarcane consumers in 2019

Rank	Country	Production (mln tonnes)
1	India	25.1
2	EU-28	18.11
3	China	16.20
4	Brazil	10.55
5	USA	10.24
6	Indonesia	6.9
7	Russia Fed.	5.95
8	Pakistan	5.35
9	Mexico	4.09
10	Egypt, Arab Rep.	3.19

Source: International Sugar Organization, ISO, 2022.

Table 2.3 shows the global ethanol production and consumption from 2012 to 2020. Ethanol global production continue to increase through the years, reaching a new record in 2018. Global production has reached 108.2 billion liters, up to 100.6 billion liters in 2017.

Table 2.3 – World Fuel Ethanol Production and Consumption in Billions
Litres

	2012	2013	2014	2015	2016	2017	2018	2019	2020
Production	82.6	86.8	93.2	97.2	97.1	100.6	108.2	107.1	98.6
US	50.4	50.4	54.3	56.1	58.2	60.0	60.8	59.7	52.7
Brazil	20.6	23.9	25.0	26.7	24.9	25.1	30.7	32.3	30.1
Others	11.6	12.5	13.9	14.4	14.0	15.5	16.6	15.1	16.3
Consumption	80.7	86.6	91.2	98.9	98.6	99.0	105.3	105.7	92.7
US	48.8	50.0	50.9	52.8	54.3	54.4	54.4	55.1	47.8
Brazil	17.8	21.5	24.1	28.8	26.2	25.6	29.7	31.8	28.6
Others	14.1	15.1	16.2	17.3	18.1	18.0	21.2	18.17	16.3

Source: International Sugar Organization, ISO, 2022.

This represents the highest increase in production year from year change since 2012. On the other hand, the consumption balance in 2018 was lagged behind the production number by around 3 billion liters, at 105.3 billion liters.

In 2020, Ethanol global production was 98.6 billion liters and began lagged behind the production number for the last three years. Compared to the global record in 2018, a decrease of 9%. The Ethanol global consumption was 92.7 billion liters. Compared to 2019, this represents a reduction of 12.3%. A decrease in worldwide Ethanol production and consumption can be explained due to the COVID-19 pandemic crisis.

Note that, over the years, Ethanol production in Brazil increased by 49% and US increased by 20%. In the same period, Ethanol global production increased by 31%. In this manner, it is possible to state that

the sugarcane sector drove the production, once the previous large increases in Ethanol production were given by this sector. According to (CONAB, 2020), this increase is explained by various factors, such as the increased production observed in relation to previous harvests, a result of the recovery of crops in the north-northeast regions, and a result of good weather conditions in the center-west in recent harvests

Remark 2 (Ethanol Production in Brazil – (ISO, 2022)). *Brasil is the world leader in fuel ethanol production from sugarcane.*

Remark 3 (Ethanol Production in USA – (ISO, 2022)). *Ethanol production in the US is predominantly grains-based, most commonly made from corn.*

2.3 Brazilian international market of sugar and alcohol

Sugarcane can be considered as to be the one of the great alternatives for the biofuels sector because its great potential in the production of ethanol and its by-products. The Brazilian national sugar and ethanol industry, operates in a positive and sustainable environment.

As previously stated, Brazil is the world's largest producer of sugarcane worldwide and has great importance to the Brazilian economy. According to the Monitoring of the Brazilian sugarcane crop through December 15 2020 released by the National Supply Company (CONAB) estimated that 665.1 million tons of sugarcane have been grinding in the 2020/2021 harvest, up to 3.5% from the 2019/2020 harvest.

Remark 4 (CONAB). *Responsible to provide relevant information to help the federal government to manage public policies aimed at the sugar-energy sector and to provide important data to the sector itself. CONAB is designated by the ministry of agriculture, livestock, and supply and exist since 2005, promoting surveys and quarterly evaluations of the Brazilian sugarcane crop.*

Due to the Coronavirus pandemic, the market demand forced a change in the ethanol-sugar production ratio. According to (CONAB, 2020), in the 2020/2021 harvest, the total ethanol production has suffered a reduction of 7.9% compared to the previous harvest and the sugar production in the 2020/2021 harvest increased 40.4% to that produced in the previous harvest.

During the 2020/2021 harvest, Brazil's leading destination for sugar exported was China (17.2%) of the sugar production. Then, the sugar exported had numerous destinations highlighting the participation of countries such as India (6.9%), Bangladesh (6.6%), Algeria (6.3%), Indonesia (6.3%), and Nigeria (4.6%)) (CONAB, 2020). According to them, Brazil exported, on average, about 70% of its sugar production in the last five harvests, being the world's largest exporter and producer of the commodity. Following Brazil, the main competitors in the international sugar market are India and Thailand.

After three consecutive harvests of reductions in sugar exports (2016/2017 to 2019/2020), a recovery rate in the 2020/21 harvest occurred (Figure 2.1). According to (CONAB, 2020), this happened because of the interest rate high exchange rate, and appreciation of sugar products in the international market. Because of these factors, the increase contribute to the advanced sale of sugar in the international market and maintained export stations at high levels during this harvest.



Figure 2.1 – Brazilian sugar exports by the harvest in million tons – source: (CONAB, 2020)

On the other hand, in the 2020/2021 harvest, Brazilian ethanol exports increased by 49.2%, compared to the same period in the last harvest Figure 2.2. According to (CONAB, 2020) the main reason for the

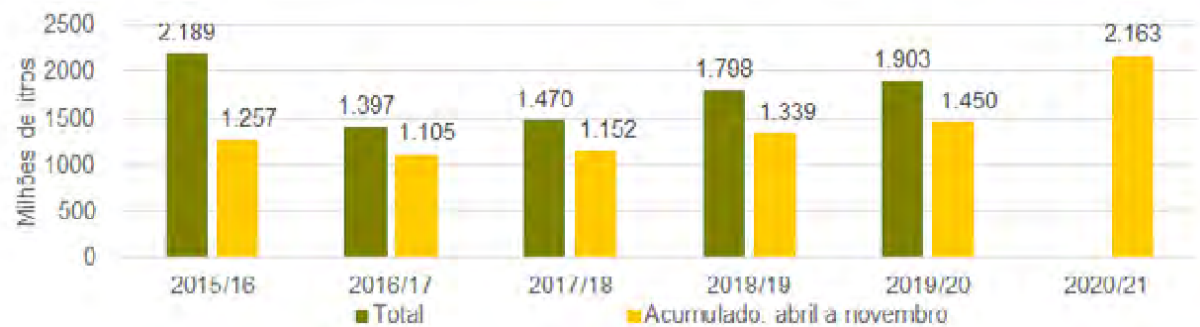


Figure 2.2 – Brazil ethanol exports by the harvests in million liters – source: (CONAB, 2020)

growth of Brazilian ethanol exports comes from the devaluation of the real against the dollar, as previously stated. The increase in ethanol exports occurs despite the estimate of a 14.3% reduction in national production of the biofuel in the 2020/21 harvest. As can be seen in Figure 2.2, Brazil exported around 2.2 billion liters of ethanol in the 2020/2021 harvest. This ethanol was exported to various countries, highlighting to United States (40.1%), South Korea (33.4%), and the Netherlands (9.4%), which together accounts for 82.9% of the total ethanol exportation. The rest of the exported ethanol was obtained by countries such as Japan, Philippines, Nigeria, Colombia, Ghana, Cameroon, Congo, and others (CONAB, 2020).

Highlight to the ethanol imports that has a decreased by 65.1% in the 2020/21 harvest, compared to the same period last harvest as can be seen in (Figure 2.3). This performance of biofuel imports was influenced by the devaluation of the real against the dollar, favoring the search for the product within the Brazilian market (CONAB, 2020). Also, this decrease can be explained due to a fact of the sharp reduction in ethanol consumption during this harvest because of the COVID-19 pandemic crisis.

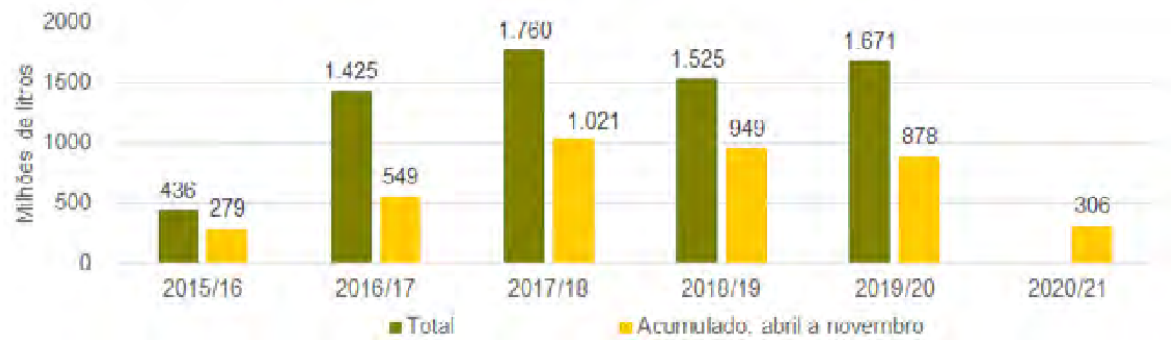


Figure 2.3 – Brazilian Ethanol imports by harvest - source: (CONAB, 2020)

2.4 Brazilian electricity using cogeneration systems in Sugarcane Industry

In Brazil, the sugarcane sector plays a strategic role in energy security and the country's environmental performance (Picoli et al., 2016). The sugarcane industry is one of the most important economic sectors in Brazil, a position reached in large measure due to high efficiency and competitiveness in the first-generation ethanol production process (Ensinas et al., 2007) (Palacios-Bereche et al., 2013). Sugarcane is currently the main renewable energy source in Brazil (Seabra et al., 2011). Sugar mills produce various co-product as bagasse, filter mud, and molasses.

Definition 1 (Bagasse – (Rein et al., 2016)). *The bagasse is a fibrous residue of sugarcane, which is obtained after crushing and extract the sugar juice. Each tonne of sugar can produce 250kg of bagasse.*

Definition 2 (Molasse – (Rein et al., 2016)). *Is a viscous substance in the final stage of crystallization, where no additional sugar can be obtained by a further process. This sub-product is an agricultural product and it is hard to determine its exact composition but in general consists of water, sugar, glucose, and fructose. The molasse is defined as*

1. *Molasse A being the syrup after the first crystallization process.*
2. *Molasse B the product obtained after the second crystallization process.*

Each 100 tonnes of sugar can produce 3-4 tonnes of molasses.

In the past, bagasse wastes were burned as a means of solid waste disposal but this has been changing because of their calorific characteristics, which are used as the principal raw materials in cogeneration plants (Frías et al., 2011). Today, the primary use of bagasse is to use as an energy source in mill cogeneration systems to provide the energy requirements of sugar and ethanol processes (Seabra; Macedo, 2011).

Remark 5 (The use of Bagasse – (EPE, 2021)). *According to the National Energy balance, in 2020 about 181622×10^3 tonnes of bagasse were obtained; however, only 30824×10^3 tonnes of this bagasse was used for electricity generation, which represents about 17% on average of the total production. This indicates that the electricity generation using bagasse can be increased. – [Click here](#) and go to the page 54 for more information.*

Definition 3 (Cogeneration – (Moran et al., 2010)). *Is a process that produces power – electrical and/or mechanical energy – and useful thermal energy for a certain process . To accomplish that cogeneration system is fed by a primary energy source into a thermal device. After that, a combustion reaction occurs to transform the chemical energy of the fuel into a mechanical shaft, which is converted into electrical energy using generators.*

Remark 6 (Types of cogeneration system). *There are two types of cogeneration systems:*

1. *Cogeneration system as a topping cycle. In this system, the steam is used to first produce power and then the thermal energy is used to obtain the final product. Thermal energy is the by-product of the cycle. The cogeneration system as a topping cycle is used in most cogeneration systems.*
2. *Cogeneration system as bottoming cycle: In this system, the thermal energy, at high temperature, is produced to carry out a specific industrial process. In this process, some of the waste heat is recovered into a heat exchanger to be used in a turbine generator to produce electricity. Typical areas of application are: ceramic, cement, steel and so forth.*

The participation of thermal generation fueled by bagasse has increased remarkably on the national scene. Figure 2.4 shows the share of bagasse in electricity generation in 2018/2019. As can be seen in Figure 2.4

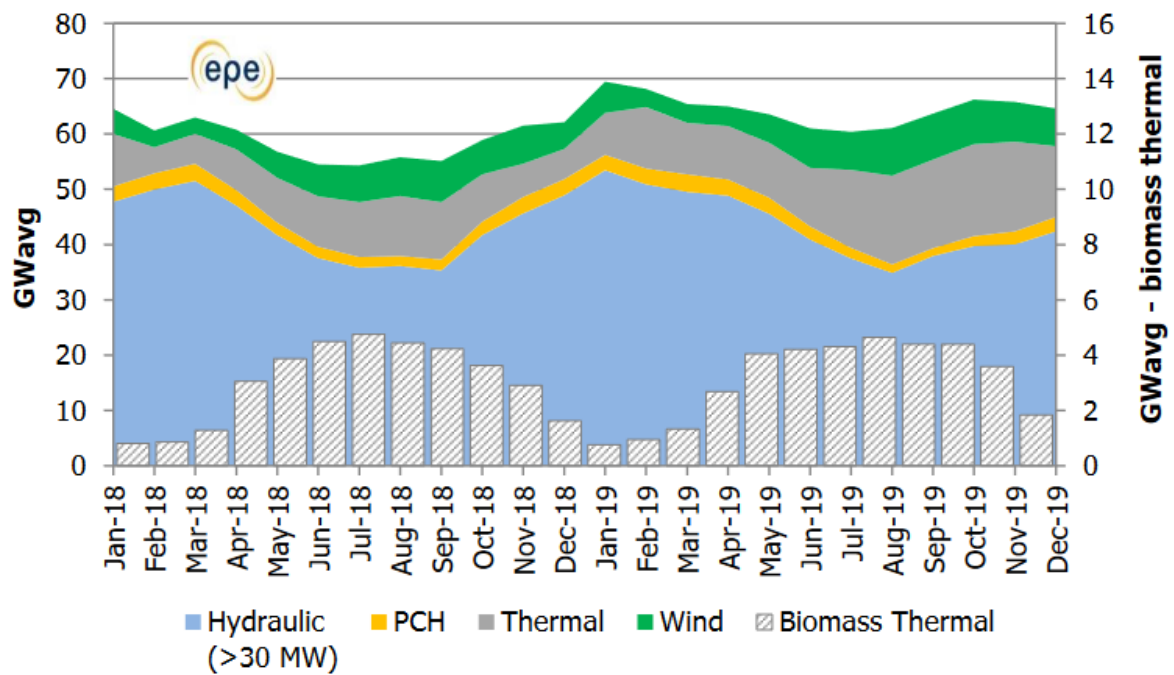


Figure 2.4 – Participation of bagasse in electricity generation – Source: (EPE, 2019a)

in the 2019 period (January to December), the national electricity matrix remained at the same level as the previous year (3.8%). The cogeneration system fueled by bagasse, injected about 2.6GW average in to the National Interconnected System(SIN) (EPE, 2019a). This shows an increase of about 4.5% compared to that verified in 2018. Note that, the period in which the cogeneration system using biomass increases its electricity generation is concomitant with the drought. Then, the biomass system and Hydraulic system are complementary to each other because the Hydraulic system increases its electricity generation during the flood Figure 2.4.

In Brazil, the use of cogeneration systems has become a practice adopted by the sugarcane and ethanol agroindustry using sugarcane bagasse, given the need for energy independence because of the systemic crises in the electrical sector and its energy-self-sufficiency characteristic (Dantas, 2010).

The most common cogeneration system includes a steam boiler and back-pressure steam turbines or turbogenerators. To drive the boilers, the bagasse is used to be burned into furnaces to produce steam for power generation. The superheated steam supplies the back-pressure steam turbines to generate electrical power and the low-pressure steam leaving the turbines flows to heating devices as mill drives in the stages of sugar or ethanol production.

Remark 7 (Types of turbines used in Sugarcane industry (Smith; Botermans, 2013)). *Two types of turbines are used in sugarcane industry:*

1. *The back-pressure steam turbine is used in a system that intends to manufacture sugar and or ethanol. This turbine gives a quantity of steam depending on its load at constant exhaust pressure. The exhaust vapor is in a superheated state and contains high heat energy to be used in the specific process to produce a final product - sugar or ethanol*
2. *Extraction condensing turbine. In this process, the steam required to produce the final product is given in the extraction mode. The steam not consumed by the process is sent to a condenser. After the condensing process, the water is sent to the boilers. This turbine produces more power than the last one.*

With such large volumes of sugarcane being produced, the sugarcane sector exhibits significant economic potential for electricity generation because in Brazil, A still significant portion of the cogeneration system in the sugar-energy sector, uses industrial processes and low-efficiency cogeneration plants, consuming biomass with the main objective of meeting the energy demands (heat and electricity) of the unit, with little or no surplus (Ensinas et al., 2007) .

The self-consumption and energy exported by cogeneration systems fueled by bagasse in 2012/2019 seasons is shown in Figure 2.5. Note that there was an increase in electricity generation using bagasse, driven by an improvement in electricity exports, with the participation of self-consumption being stable over the 2012/2019 period (Figure 2.5).

Remark 8 (Regulatory Mechanisms and Incentive Policies – (EPE, 2019a)). *To improve the competitiveness of sources from biomass and stimulate the growth of bioelectricity generation, the Brazilian government created regulatory mechanisms and incentive policies. In 2018, the first energy auction dedicated to biomass helped contract over 590MW on average, the maximum amount recorded scheduled for 2009 and 2012. This was realized by the reserve energy auction(LER).*

Definition 4 (Reserve Energy Auction(LER)). *The reserve energy auction was realized between 2009/2015 to contracted projects through alternative sources such as small hydroelectric plants, wind, biomass plants, and so forth. This program was used as an incentive for the construction of projects to generate specific energy sources, allowing the development of the respective supply chain.*

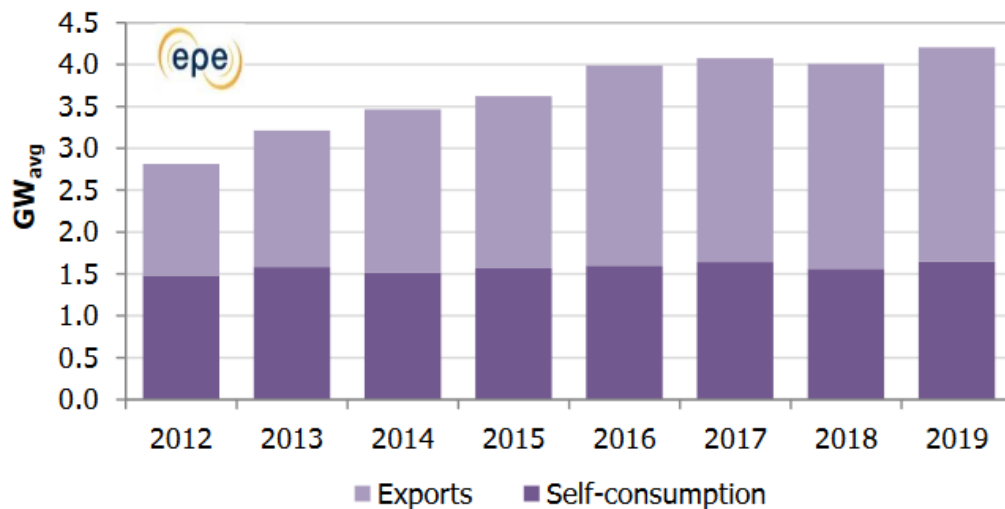


Figure 2.5 – Self-consumption and energy exported by cogeneration systems fueled by bagasse
– Source: (EPE, 2019a)

There are about 366 Sugarcane power plants in operation in 2019, eight more than in the 2018 year. Of all of the plants that export energy to the National Integrated System (SIN), about 60% operate exclusively in free contracting environments, 17% operate in the Regulated contracting environments, and 23% sell to both contracting environments (EPE, 2019a).

Then the sugarcane bagasse cogeneration might have a positive effect on energy generation to meet the country's energy demand using renewable resources (see Remark 5). However, this potential is not reached because of various factors such as High technological demands, unavailability of needed capital, and lack of expertise. The use of high technological systems for cogeneration systems coupled with optimization allows the production of surplus bagasse (Ensinas et al., 2007).

One important factor that this potential is not reached is because, generally, the low-efficiency cogeneration system based on a steam cycle with superheated steam at 22 bar and 300 ° C is still used (Ensinas et al., 2007) (Macedo, 2001). With better technologies in cogeneration systems, as being operating with live steam pressure higher than 60 bar attempts to the plant energy requirement and producing surplus that can be sold to the grid (Ensinas et al., 2007). Given the relevance of the sugarcane industry in bioelectricity generation, a brief literature review will be presented next.

2.5 Literature Review On Sugarcane industry

The efficiency of a cogeneration process should be evaluated in terms of its sustainability and use of energy resources (Palacios-Bereche et al., 2013). As previously stated, low-efficiency cogeneration is still being used in the sugarcane industry. Concerns about the importance of energy efficiency took Europe to identify and promote measures and technologies that might guarantee achieving primary energy saving of 20% in the energy efficiency directive 2012/27/EU. In this document, the cogeneration system has great importance in energy consumption because it can contribute to reducing substantially energy consumption in final uses of energy by thermal

machines and heat engines ([Directive, 2012](#)) ([Paredes-Sánchez et al., 2019](#)). Currently, there are a remarkable amount of literature available on the sugarcane industry and cogeneration systems to understand how to increase the thermodynamics efficiency of cogeneration systems.

([Rodriguez, 2014](#)) evaluated the efficiency of boilers fueled by bagasse using Thermodynamics's First and Second Laws. In his experimental work, data were obtained from an installed industrial plant located in the State of Sao Paulo. In the First Law of Thermodynamics, the loss method was used as established in the standards ASME PTC 4-2008 and EN 12952-15:2003. His work detailed thermal losses through the boiler walls. Also, he evaluated the uncertainty of the performed determination. In his work, the procedures used in the bagasse fuel analysis are reported using ASTM standards realized in the Technological Research Institute and the University of Sao Paulo. LHV obtained in his work was evaluated to be 6.2MJ/kg with sugarcane bagasse composition on a dry basis. He evaluated six boilers at the same pressure on average (about 65 bar) and temperature varying from 477 to 507 °C. His results suggest that the second law efficiency of the boiler as to be $24.5\% \pm 0.6$, $24.8\% \pm 0.6$, $25.7\% \pm 0.6$, $25.8\% \pm 0.6$, $27.1\% \pm 0.6$, and $26.6\% \pm 0.6$ in the boilers one to six, respectively. He obtained these results using a steam bagasse ratio of 2. He suggests that losses by radiation and convection as be 34.7% using HHV and 44.8% using LHV for the data measured. Using the same parameters, the energy analysis of the boilers as to be $89.8\% \pm 0.3$, $88.6\% \pm 0.3$, $85.9\% \pm 0.4$, $85.5\% \pm 0.5$, $89.2\% \pm 0.3$, and $87.3\% \pm 0.4$. These results shows the importance of applying exergy analysis to understand the irreversibility in real processes.

On the other hand, ([Arnao, 2007](#)) evaluated the thermodynamic performance of the bagasse boiler operating at 6.5MPa and 500 °C, to reduce the cost of your exhaust gas energy recovery system. For this, the characterization of the bagasse was carried out; sugarcane bagasse samples were obtained through the extraction processes: Mill and Diffuser were used in order to determine the influence of these processes on the particle characteristics. Also, bagasse properties such as higher calorific value, exergy, peak or step start temperature, and auto-ignition temperature was determined. Boiler performance was determined by applying the First and Second Laws of Thermodynamics. In the First Law analysis, the boiler efficiency was determined using the method: (i) Inputs and Outputs (based on standards ASME PTC 4 - 1998) and (ii) the Energy Balance, both calculated on the basis of lower (LHV) and higher (HHV) calorific values. In the first law analysis, his results suggests that the largest portion of energy losses corresponds to the exhaust gases using LHV as to be 10.21% and the boiler first law efficiency using LHV as to be 86.45%.

([Cortes-Rodriguez et al., 2017a](#)) studied an experimental efficiency analysis in sugarcane bagasse boilers using the first law of thermodynamics. The methodology used to evaluate the efficiency is using the energy losses method, based on ASME PTC 4-2008 and EN 12952-15:2003 standards. This data were obtained from boilers installed in sugarcane sector in the state of Sao Paulo, Brazil. In the boiler efficiency, various tests were carried out as Fuel ultimate analysis, proximate analysis of fuel, ashes, flow temperature determination at inlet and outlet of boilers, measurement of gases combustion composition, unburned materials, measurement of boiler wall temperature, and presence of unburned matter in the ash. Results suggests that, the First Law Efficiency using LHV base (%) vary between 87.3 ± 0.4 to 89.8 ± 0.3 . The steam/fuel ratio (kg/kg) using in this work vary between 1.9 and 2.0.

On the other hand, ([Cortes-Rodriguez et al., 2017b](#)) presented an experimental work to evaluate efficiency analysis of sugarcane boiler fueled by bagasse, using the First and Second law of Thermodynamics. To

evaluate this work, primary measurements required for the determination of boilers' performance were: Measurement of mass flow, temperature, and steam pressure of the boiler, the flow temperature, proximate and ultimate analysis of the fuel, proximate analysis of ashes, boiler wall external temperature, and composition of the combustion gases. In his work, They presented two methodologies to evaluate the bagasse of exergy. Results suggest that the exergy loss in the combustion process reaches a value of 53% because of the irreversibilities generated, high moisture content in the fuel.

([Leal et al., 2013](#)) studied the importance of the sugarcane industry in Brazil. They suggest that the sugarcane straw provides one-third of the total primary energy of sugarcane in the field and its use is mainly wasted by burning in the pre-harvest or left on the ground. Through their results, they conclude that the impacts scenario and the economic value indicate that the optimal soil can be considered depending on local conditions, agricultural practices, natural landscape characteristics, and the planned end use. The main contribution of their work is to shed some light on the field to help understand the importance of the various impacts of straw mats on the soil, the availability and quality of straw, the economics of straw recovery and use, and the main criteria for determining straw quantity.

([Seabra et al., 2010](#)) compared the techno-economic performance for thermochemical and biochemical conversion of sugarcane remainder, considering future conversion plants adjacent to sugarcane mills in Brazil. The process models developed by the National Renewable Energy Laboratory were adapted to reflect the composition of Brazilian raw materials and used to estimate the cost and performance of these two conversion technologies. Their results suggest that, despite the apparent cost-competitiveness of ethanol production, these processes have to compete with different options for biomass use.

([Chum et al., 2014](#)) related in their work that the global biofuel production grew rapidly from 2007 to 2012, led by the United States and Brazil, the two largest fuel ethanol production systems in the world using corn and sugarcane, respectively. Their work provides information on the characteristics of the Brazilian sugarcane industry and corn industry in the US. Their results suggest that sugarcane industry and corn ethanol systems are improving energy production and reducing GHG emissions over time. Also, Brazilian sugarcane systems have exceeded American corn systems based on the renewable energy ratio production indicator, although both systems improve with a shift towards greater bioenergy production (i.e., electricity).

On the other hand, ([Neto; Gallo, 2021](#)) studied the potential impacts of biogas production from anaerobic digestion of vinasse and its impact in various contexts to understand the use of the biogas for power generation and the potential of this energy source compared with fossil oil power plants in terms of various terms such as energy, costs, and greenhouse gases emissions. Their results suggest that an incentive program could make the use of vinasse biomethane as an alternative fuel feasible in small plants with minimal impacts, proving remarkable emission reductions.

To identify exergy lost through the exhaust gas and understand the effect of moisture of bagasse, ([Singh, 2020](#)) has evaluated through exergy analysis the application of Kalina cycle for increase exergy performance of a bagasse-fired cogeneration plant in the sugarcane industry. This system process 3500 tons of sugar cane per day and its capacity is 16MW (Figure 2.6.) His study suggests that 5.20% is lost through exhaust gases and that the integrated Kalina cycle avoids that waste, and overall exergy efficiency increased by 0.32%. In addition, the parametric study realized by him suggests that the power output increases by 3531.5 kW, cogeneration

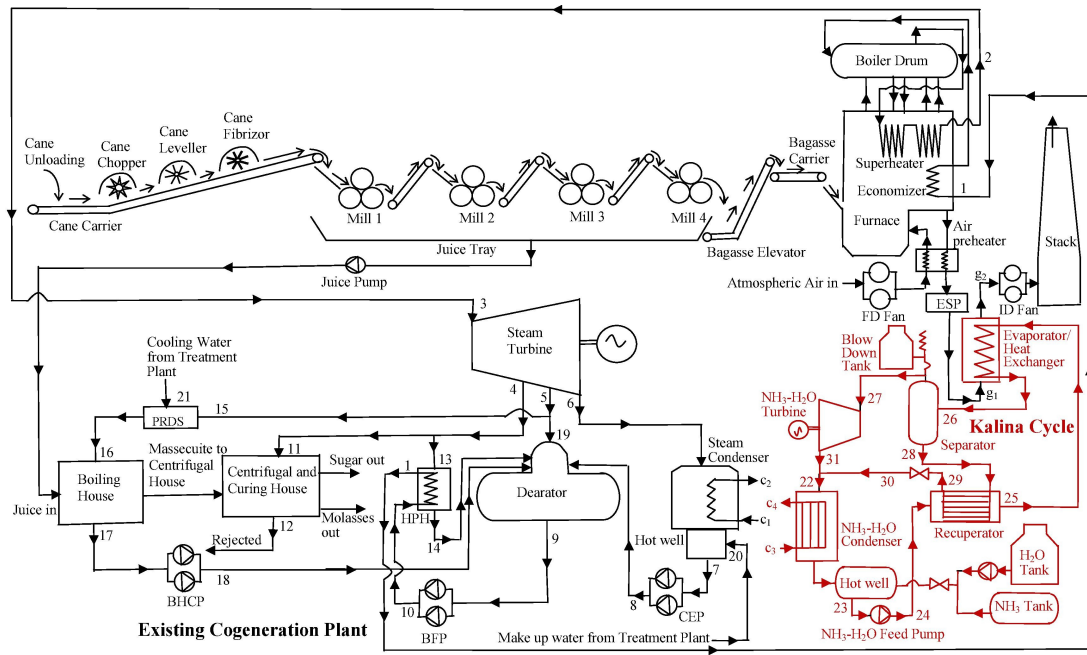


Figure 2.6 – “Kalina cycle System 11 (KCS-11) integrated with the cogeneration plant of the considered 3500 TCD sugar factory” (Singh, 2020). Copyright 2021, with permission from Elsevier. License Number: 5102580565293

energy efficiency by 3.6%, and cogeneration exergy efficiency by 2.9% if the moisture content in the fuel decrease to nil (Figure 2.7.)

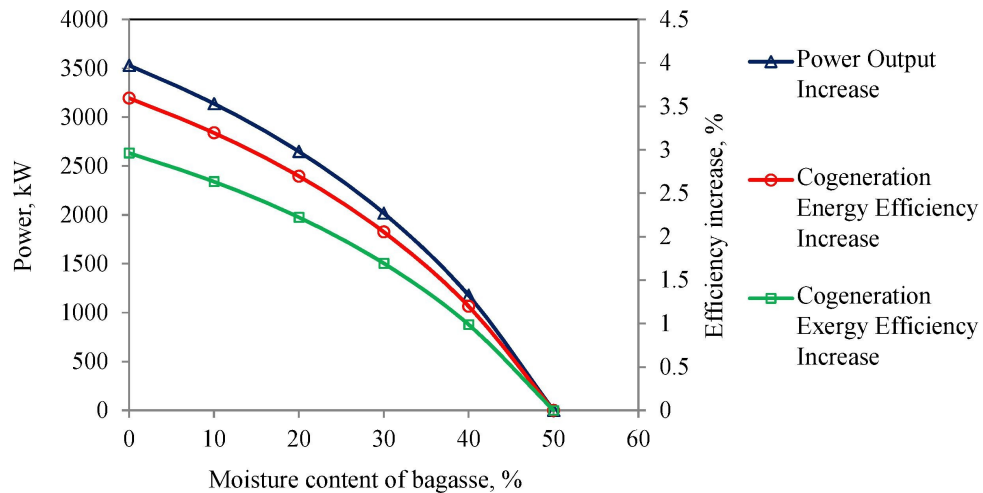


Figure 2.7 – “Variations of increases in net power output, cogeneration energy efficiency, and cogeneration exergy efficiency of the cogeneration-Kalina integrated system with the decrease in moisture content of bagasse” (Singh, 2020). Copyright 2021, with permission from Elsevier. License Number: 5102580565293

A technical and economic evaluation of incorporating the reheating and regeneration to increase efficiency in a sugarcane cogeneration system producing sugar and ethanol was reported by (Pérez et al., 2018). Four scenarios were evaluated in the study to quantify gains by implementing heating and regeneration alternatives:

(1.) The base case, (2.) Reheat, (3.) Regenerative, and (4.) Simultaneous reheating and regeneration. Their results

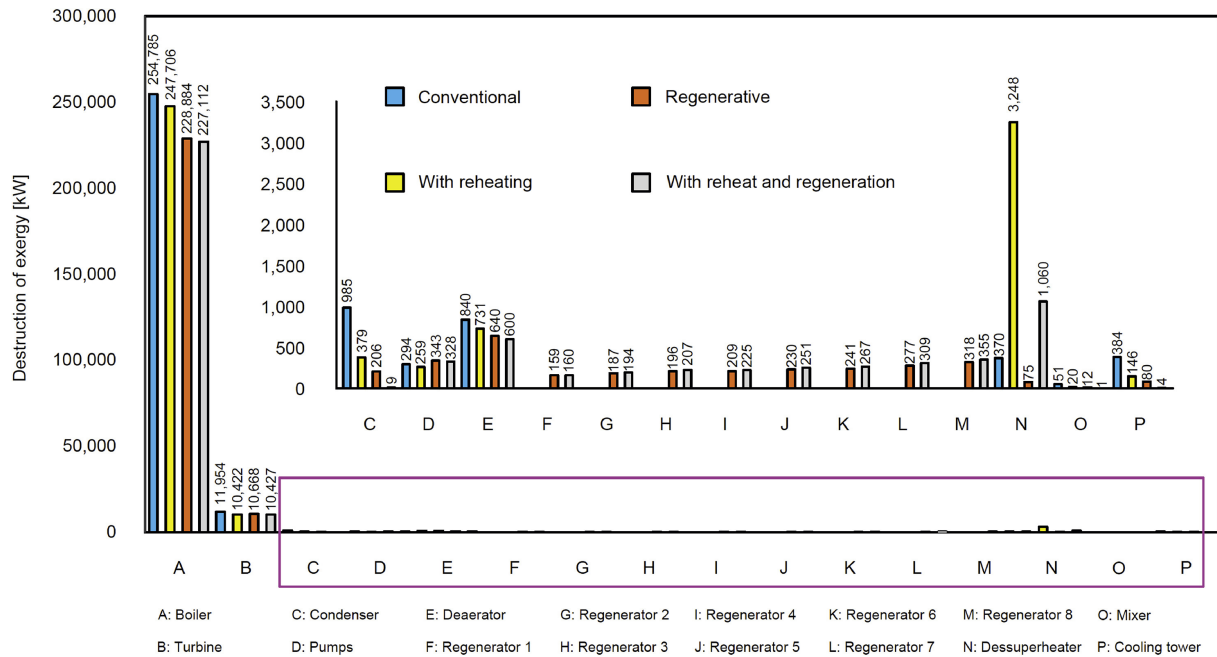


Figure 2.8 – “Distribution of irreversibility in each equipment using 8 regenerators in scenarios C2 and C3” (Pérez et al., 2018). Copyright 2021, with permission from Elsevier. License Number: 5102581381928

suggest that boilers have the highest exergy destruction rate. The combination of reheating and regeneration (scenario 4.) contributes to reducing irreversibility in the boiler (Figure 2.8.) In addition, economic analysis has shown that regenerative heating with three regenerators is preferred over a reheating implementation.

In the context of the sugarcane cogeneration system, (López et al., 2021) evaluated two different types of solar thermal collectors and compared them using the exergy analysis method. This system is located in Columbia and produces about 250kg per ton of milled sugarcane, and this source is used as fuel for the steam generators. Their results suggest that the inclusion of solar thermal collectors reduces the fuel consumption by 1.1%. In addition, the overall exergy efficiency can be increased by 1.66% (Figure 2.9.)

A biomass-based combined heat and power plant integrating a downdraft gasifier, a solid oxide fuel cell, a micro gas turbine, and an organic Rankine cycle was evaluated using exergy, and exergoeconomic analysis by (Karimi et al., 2020). This system is fueled by rice straw. Their results suggest that the highest pinch point temperature cause the lowest exergy efficiency and ORC cost rate (Figure 2.10). In addition, the total cost rate was found to be 10.2 \$/h and working optimum conditions was obtained by multi-objective optimization.

The main concern for the ethanol process residues carried (Fukushima et al., 2019) to evaluate an energy analysis of the sugarcane industry considering vinasse concentration and incineration. They studied the integration of a vinasse concentration and incineration system into the conventional sugar industry. They use the Aspen Plus software to simulate the production process to analyze various scenarios considering vinasse concentration with a multiple-effect evaporator system, vinasse incineration with salt recuperation, and heat integration. Results suggest that the steam produced with vinasse incineration contributes to supplying the energy demand for

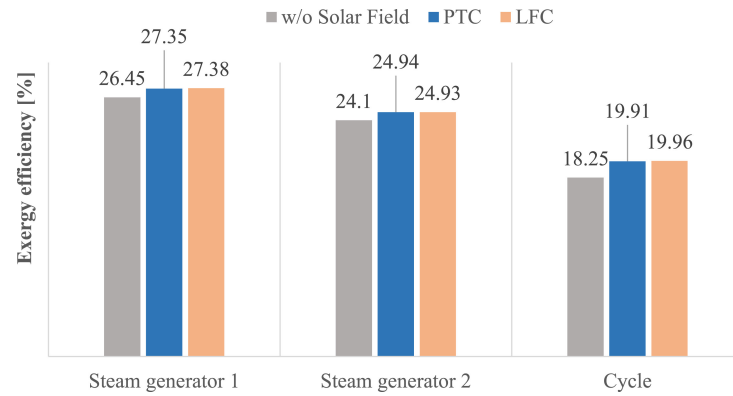


Figure 2.9 – “Exergy efficiency of solar collectors on day of maximum efficiency”(López et al., 2021). Copyright 2021, with permission from Elsevier. License Number: 5102591118737

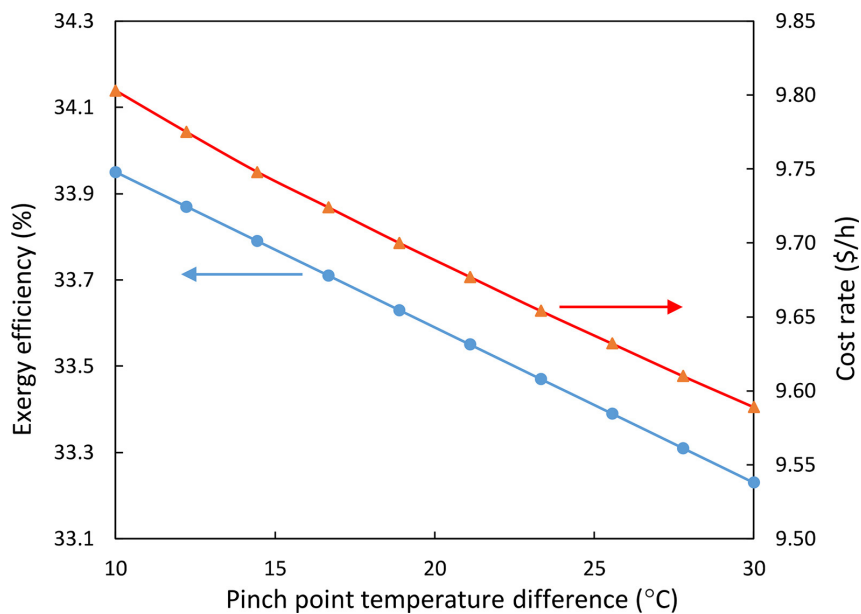


Figure 2.10 – “Impact of pinch point temperature difference on exergy efficiency and cost rate”(Karimi et al., 2020). Copyright 2021, with permission from Elsevier. License Number: 5102611353245

vinasse concentration; integrates the concentration systems without additional utility consumption, and the heat integration allows for reducing the number of effects on vinasse and juice concentration systems.

To analyze the opportunities and buried the context of government initiatives, institutions, and prevailing regulatory frameworks in Brazil and Nepal, (Khatriwada et al., 2012) studied the complementarity between hydroelectricity and surplus electricity from the sugarcane industry. They suggest that electricity from cogeneration can be a good complementary for hydroelectric electricity, helping foster diversification on the generation side and enhancing the security of electricity supply based on local resources.

(Ortiz et al., 2020) studied an exergy analysis and techno-economic optimization of bioethanol production using various routes. In the study, the global analysis of bioenergy configuration was evaluated, ranking the sugarcane systems focused on key performance indicators. Their results suggest that chemical reactions, fer-

mentation, and combustion systems represent the principal destroyed exergy in ethanol production and electricity generation in the sugarcane industry as an energy input in the cogeneration unit.

On the other hand, ([Velásquez et al., 2013](#)) evaluated exergo-environmental analysis of liquid biofuel production processes for five different kinds of biomass. They apply the exergy method to evaluate the combined production of sugar and ethanol from sugarcane, ethanol production from amylaceous and lignocellulosic materials obtained from the banana plant, and biodiesel and kernel oil production from the fresh fruit bunches of the African oil palm. Results suggest that the use of renewable materials doesn't guarantee that the process is renewable.

([Batlle et al., 2021](#)) evaluated and compare using energy, economic, and environmental analysis using Life Cycle Assessment of the integrated production of palm and sugarcane ethanol. LCA method was evaluated using SimaPro v.8.0.3 software and impacts were quantified using the IMPACT 2002+ method. The energy was evaluated using the First Law of Thermodynamics and economic analysis was evaluated using the fixed capital investment index. Their main highlight are: (1.) The environmental impacts and fossil energy use in the product life cycle to be reduced, (2.) Integrated biorefinery reduces GHG emissions due to the sustainability of products, (3.) The integrated scenario has a better ratio of bioenergy produced, (4.) The integrated biorefinery increase ethanol production by up to 31%, and (5.) The improved scenario has a better energy rate by up to 3.82% in the global efficiency system.

([Souza et al., 2018](#)) studied the sugarcane industry as an alternative to producing clean energy profiles in Latin America and the Caribbean. Their work aims to understand the potential of various approaches to energy production using bagasse as fuel and its implication for the environmental aspects. Their results suggest that with a minor investment, bagasse may increase the electricity access in many countries and might be an alternative to replace fossil fuel. Using bagasse as source to electricity generation, they conclude that sugarcane offers a large potential as renewable energy because it promote the GHG emissions savings.

To understand the potential of sugarcane in modern energy development in southern Africa, ([Souza et al., 2016](#)) evaluate the potential of sugarcane to replace traditional biomass and fossil fuel and enlarge the access to electricity in Southern Africa. In their work, they considered two scenarios in order to produce energy using sugarcane to explore the potential to produce clean energy and GHG emissions savings. Also, they evaluate the potential of cogeneration bioelectricity using bagasse as fuel. Their results suggest that the sugarcane sector can contribute to enhancing electricity access in the long term. Also, benefits regarding the reduction of fossil fuel use and external dependency on fossil fuel import and saving GHG emissions can be achieved.

To determine the physio, chemical, and thermal properties of sugarcane dry cleaning system residue and bagasse from milling in cogeneration systems, ([Camargo et al., 2020](#)) studied these residues as biomass for combustion in boiler, because characteristics of these residues are relevant for the analysis of thermal power plants using First and Second Law of Thermodynamics. These authors suggest that the bulk density and mean particle size of bagasse are important for boiler supplying system design. Also, the chopped straw with a moisture content of around 40% implies a heating load during the combustion process in the boiler. On the other hand, ([Bizzo et al., 2014](#)) analyzed how bagasse is produced from sugarcane, presented the physical properties and characteristics of bagasse, and estimate their energy potential, and their use as an energy source in the production of ethanol. In their work, they suggest that understand the characteristics of bagasse to determine the energetic potential of this fuel. Also, characteristics of bagasse depend on some factors as plant species, the method used to harvest the crop,

the juice extraction process and so forth.

(Milão *et al.*, 2019) analyzed a large-scale sugarcane industry using thermodynamic and financial assessments by coupling the production of bioenergy to carbon capture and storage (BECCS). The industry was analyzed to assess ethanol production, power production, heat demand, water demand, carbon dioxide intake, profitability, and resource utilization. These authors suggest that in a conventional sugarcane biorefinery 1000t/h of sugarcane generates 284MW of net electricity exportation, with 0.7tCO₂ per ton of sugarcane. Also, the results suggest that the BECCS reconfiguration compared to the conventional biorefinery leads to negative emissions.

In order to understand the effects of the reduction process steam demand and water usage in sugar and ethanol production from sugarcane through heat integration, (Pina *et al.*, 2017) evaluate various plant configurations of sugar and ethanol production plants using exergy analysis to quantify the reduction irreversibility generation owing to the heat integration procedure. The simulation procedure was performed using ASPEN PLUS software to evaluate the mass, energy, and heat integration using the Pinch method to minimize the utility consumption. Their main highlights show the potential reduction in water usage and steam consumption resulting from heat integration. Their results suggest that a reduction in steam consumption was about 34% and 37% for both cases and it leads to a remarkable increase in the bagasse surplus when using a backpressure steam turbine. When the condensing steam turbine is adopted, a surplus of electricity is obtained.

Finally, several works approaching cogeneration systems in sugarcane industry are reported in Table 2.4.

Table 2.4 – Critical review on cogeneration systems fueled by biomass

Ref	Capacity (MW)	Energy	Exergy	Exergoeconomic	Findings
(López <i>et al.</i> , 2018)	50	✓	✓	x	Evaluated two configurations of hybrid solar-sugarcane cogeneration. Base configuration exergy destruction was 11.10% greater than improved case. 8.50 GWh of extra electricity was obtained in the improved case.
(Lira; Gallo, 2021)	10	✓	✓	x	Evaluated two configurations to improve the technical performance of the system. No energy in the base case is sold to the grid, and with proposed changes, a power surplus of 2314 kW, which is 22.51%, was obtained.
(Palacios-Bereche <i>et al.</i> , 2020)	—	✓	✓	✓	Evaluated two cases to improve the technical, economic performance of the system. Exergy results show that energy and exergy efficiencies are in the same range. The economic analysis concluded that vinasse incineration presents economic feasibility.

Continued on next page

Table 2.4 – continued from previous page

Ref	Capacity (MW)	Energy	Exergy	Exergoeconomic	Findings
(Prestipino et al., 2021)	—	✓	✓	x	Two cases were evaluated to improve thermodynamics parameters. An improvement in overall exergy by 5% was obtained compared to the base scenario. An LCA was conducted and concluded that the CO ₂ -eq impact is magnitudes lower than electricity from the national grid.
(Gholamian et al., 2016)	—	✓	✓	x	Evaluated through a parametric study, a co-generation system composed of a biomass gasifier, gas turbine, an S-CO ₂ cycle, and a domestic water heater. Results suggest the highest exergy destruction occurs in the combustion chamber, and using wood as biomass leads to a higher exergy efficiency at the expense of a higher CO ₂ emission.
(Oyekale et al., 2020)	—	✓	✓	✓	They investigated optimization potentials through exergy and exergoeconomic analysis. Results suggest that exergetic efficiency amounts to about 11%. Cost product of electricity was obtained as 10.5c€/kWh and 12.1c€/kWh for conventional and integrated exergoeconomic approaches, respectively.
(Soltanian et al., 2019)	—	✓	✓	✓	Evaluated by exergoeconomic analysis of biorefinery that produces lactic acid and power. Results suggest that about 52% of total cost due to exergy destruction occurs in the steam generation, and unit exergoeconomic cost of lactic acid and power was found out to be 8.55 USD/GJ and 15.61 USD/GJ, respectively.
(Palacios-Bereche et al., 2013)	—	✓	✓	✓	Evaluated a proposed ethanol production scheme by integrating it into the conventional process by exergy analysis and exergetic cost. Results suggest that by introducing bagasse enzymatically, its exergy destruction and losses represent a significant portion. In integrating first and second-generation ethanol production, exergy costs of the final products are higher than in conventional cases.

Continued on next page

Table 2.4 – continued from previous page

Ref	Capacity (MW)	Energy	Exergy	Exergoeconomic	Findings
(Dogbe et al., 2018)	—	✓	✓	x	Evaluated by exergy analysis of a cogeneration system in the sugarcane industry. Results suggest that the cogeneration system is found to be the main responsible for exergy destruction and that the exergetic performance of the mill can be increased by adopting a single-stage crystallization.
(Aghbashlo et al., 2018a)	—	✓	✓	x	Evaluated a lignocellulosic biorefinery annexed to a sugar mill by an exergy analysis. Results suggest that exergetic efficiency was found to be 44.73%. The lactic acid production unit is found to be the main responsible for exergy destruction 16.30%.

✓ – Included ; x – Not included

3 THERMODYNAMIC ANALYSIS

This chapter will be presented the main concepts of energy and exergy analysis. In this chapter, the difference between these methodology are presented, main definitions are presented. Then, the concepts of environment, physical flow exergy, chemical exergy, and exergetic efficiency is presented.

3.1 Energy and Exergy Analysis

One of the main applications of thermodynamics in engineering is associated with processes and flows of matter from one thermal plant component to another. Traditional analyses are **energy analysis** and **exergy analysis**.

In energy analysis, work and heat are two possible energy interaction between a system and its environment - i.e. The First Law of Thermodynamics deals work and heat as equivalent. Although they have the same units, they are fundamentally different. Also, the First Law of Thermodynamics gives no indication about which direction spontaneous processes can occur. This gap is filled by the Second Law of Thermodynamics.

The Second Law of Thermodynamics introduces a new property called entropy. Many are the consequences of the Second Law such as: (1.) indicates which direction spontaneous processes can occur; (2.) indicates what processes and chemical reactions can occur; (3.) indicates that heat transfer is accompanied by entropy transfer, whereas work occur with absence of entropy transfer; (4.) the limits to energy conversion into various energy forms, carrying to the concept of energy quality; consequently, it leads to the exergy method.

Definition 5 (Entropy - (Callen, 1998)). *In classical thermodynamics entropy is simply a measure of disorder. In statistical mechanics, is the number of microstates in which a system undergoes transitions, and share uniform probability of occupation, increases to the maximum permitted by the imposed constraints.*

Remark 9 (Entropy). *From Definition 5 entropy increase to the maximum permitted by imposed constraint; however, the statement that entropy never decreases is valid only to adiabatic processes. Thus, entropy can be decreased if $\Leftrightarrow \delta Q < 0$.*

According to (Enrico; Wall, 2007), Tait and Lord Kelvin (1868) had defined something related to exergy, but no discussion on this concept was put forward. In 1879 Gibbs was the first to introduced new a thermodynamic function called “Available energy”. Gouy and Stodola (1889) achieved an expression for “Énergie utilisable” – useful energy – just as the difference between the entropy and a reference temperature. As a consequence of this work, the dissipated work concept was introduced. Duhem (1904) and Caratheodory (1909) involved in Gibbs’ availability.

In the meantime, various works related to Gouy-Stodola’s were published by Jouget into thermal machines (1906 – 1909). Later, Fran Bošnjakovic published his contribution by introducing a property called “Arbeitsfähigkeit” – Work Potential. Rosin and Fehling (1929), Emden(1938), and Rant(1947) calculated the exergy of fuels and provided an application of exergy analysis to chemical process. According to (Enrico; Wall, 2007) exergy theory had an extraordinary development from 1970s’ to 1990’s.

Exergy analysis is a method that uses the conservation of mass and combines the First with the Second Law of Thermodynamics to design and analyze energy systems.

Definition 6 (Exergy (Kotas, 2013)). *Is a measure of the maximum capacity of a system to perform useful work as reach the equilibrium with its surroundings - i.e. the potential of a system or flow to cause change due to being in disequilibrium with its surroundings.*

Definition 7 (Exergy (Tsatsaronis, 2007)). *The maximum theoretical useful work that can be obtained as the system is brought into complete thermodynamic equilibrium with the environment .*

From Definition 6 and Definition 7 the system can come into thermodynamic equilibrium with the environment in two ways (a.) Restricted Equilibrium and (b.) Unrestricted Equilibrium.

Definition 8 (Restricted Equilibrium - (Kotas, 2013)). *State where the system is brought into mechanical and thermal equilibrium with the environment. The temperature and pressure of the system and environment must be equal, but chemical equilibrium is not satisfied. Also, kinetic and potential energy must be zero. This state is referred as to be the environmental state.*

Definition 9 (Unrestricted Equilibrium - (Kotas, 2013)). *State where the system is brought into mechanical, thermal, and chemical equilibrium with the environment. The chemical potentials of the system and environment must be equal. Under these conditions, the equilibrium is completely satisfied. This state is referred as to be the dead state.*

Understand the nature of irreversibilities will provide a better understanding of total exergy destruction.

Remark 10 (Exergy Destruction). *The exergy destruction is distributed among the system components, and provides a quantitative measure of those which are contributing most to overall system inefficiency.*

The concepts of reversible and irreversible processes are, respectively:

(1.) Reversible process: The ideal process, which can never be realized fully but is useful conceptually and it is easier to describe in mathematical terms than an irreversible process. (2.) Irreversible process: Every real process takes place irreversibly - i.e. irreversible process occur accompanied by an increase in entropy in the system. The increased in irreversibilities occur because (a.) dissipation of work into internal energy of the system and it is caused by solid or fluid friction, mechanical or electrical hysteresis, ohmic resistance, and so forth; (b.) spontaneous non-equilibrium processes, in which a system tends to move in an unrestrained manner from a state of non-equilibrium to one of equilibrium and it is caused by chemical reactions, free diffusion, unrestrained expansion, and equalization of temperature (Kotas, 2013).

Remark 11 (Reversible process (Kotas, 2013)). *A reversible process is used as a standard of perfection which represents a limit to the performance of an actual process. This process is free of dissipative effects, and the work performed by the system or on the system is optimal. Note that, according to the Second Law of Thermodynamics, the entropy of the system and its surroundings in any adiabatic process is greater than or equal zero.*

$$\Delta S \geq \frac{Q}{T} \Rightarrow \Delta S \geq 0 \quad (3.1)$$

Think a specific process denoted by X then,

$$\Delta S_X = S \quad (3.2)$$

Now, the reverse process of X can be happen and it is denoted by Y , then,

$$\Delta S_Y = -S \quad (3.3)$$

Then, the net entropy change for a reversible process is

$$S - S = 0 \quad (3.4)$$

The use of exergy method is essential to reach efficient energy resource use, since such method predict the locations, types, and real magnitudes of wastes and losses to be determined. According to (Rosen, 1999) this method can reveal whether or not, and by how much, is possible to design more efficient energy systems by reducing the inefficiencies in existing systems, and contributes to achieving energy security in an environmentally acceptable way.

Remark 12 (System efficiencies). *Increasing systems efficiencies reduce emissions. The emissions reductions are achieved by increasing system efficiencies. Thus, reducing the requirement for new facilities for the production, transportation, transformation, and distribution of the various energy forms will be achieved.*

3.2 Environment

The environment must be defined because when a system undergoes a process, it will interact with the environment, that is, the system will be affected by its surroundings. (Moran et al., 2010) suggests that including every detail of the environment in the exergy analysis would be not practical, thus, simplifications are made to obtain a model result. To illustrate this important concept the environment is:

a very large body or medium in the state of perfect thermodynamic equilibrium. This conceptual environment has no gradients or differences involving pressure, temperature, chemical potential, kinetic or potential energy and, therefore, there is no possibility of producing work from any form of interaction between parts of the environment (Kotas, 2013).

Due to its complexity, ideal models of environmental are needed. (Kotas, 2013) suggest that the environment interact with the system through:

1. Thermal interaction as a reservoir at temperature T_0 .
2. Through mechanical interaction as a reservoir of unusable work.
3. Through chemical interaction as a reservoir of a substance of low chemical potential in stable equilibrium.

3.3 Physical flow exergy

The physical flow exergy may be defined formally as:

Definition 10 (Physical exergy of system – (Kotas, 2013)). *Equal to the maximum amount of work obtainable when the stream of substance is brought from its initial state to the environmental state defined by P_0 and T_0 , by physical processes involving only thermal interaction with the environment.*

Note that the physical flow exergy does not depend on the chemical composition. The physical flow exergy is:

$$e^{PH} = (h - h_0) - T_0 (s - s_0), \quad (3.5)$$

h_0 and s_0 are the enthalpy and entropy at environmental state (P_0, T_0). The physical exergy of the system is always greater than or equal to zero even when $T < T_0$ and $P < P_0$.

However, the physical flow exergy can be less than zero. This can be demonstrated by the following

$$\begin{aligned} e^{PH} &= (h - h_0) - T_0 (s - s_0) = u + Pv - u_0 - P_0v_0 - T_0(s - s_0) \\ &= u - u_0 + Pv - P_0v_0 + P_0v - P_0v - T_0(s - s_0) \\ &= \underbrace{(u - u_0) + P_0(v - v_0) - T_0(s - s_0)}_{\mathbb{X}} + v(P - P_0) \end{aligned}$$

if $\mathbb{X} < |v(P - P_0)|$ for $P < P_0 \Rightarrow e^{PH} < 0$. The physical significance of negative values to e^{PH} indicates that net work is needed to undergoes the system to restricted equilibrium.

3.4 Chemical Exergy

As discussed above, physical exergy is obtained when a system is brought from its state to the environmental state. To determine the chemical exergy, the environmental state is now to be the initial state and the final state is the dead state. The concept of chemical exergy may be defined as

Chemical exergy is equal to the maximum amount of work obtainable when the substance under consideration is brought from the environmental state to the dead state by processes involving heat transfer and exchange of substances only with the environment (Kotas, 2013).

To evaluate chemical exergy, temperature, pressure, and chemical composition of the environment must be determined. Because the environment is not in equilibrium, an exergy reference-environment was reported by (Kotas, 2013) to aid to calculate the chemical exergy of a gaseous substance containing the elements C, O, H, and N Table 3.1.

Table 3.1 – Standard chemical exergy at reference-environment

Chemical element i	Standard chemical exergy, \bar{e}_i^{CH} [kJ/kmol]
CO ₂	20140
H ₂ O	11710
O ₂	3970
N ₂	720

According to (Moran et al., 2010), the chemical exergy of a mixture of pure substances is given by :

$$e_{\text{mixture}} = \sum_i y_i \bar{e}_i^{\text{CH}} + \bar{R}T_0 \sum_i y_i \ln(y_i) \quad (3.6)$$

\bar{e}_i^{CH} and y_i are the standard chemical exergy of chemical pure substance i and the mole fraction of component i , respectively. In the case of mixing real solutions, there would be consider the activity coefficient. To calculate the exergy of others pure substances, organic or inorganic, See (Szargut, 2005).

(Szargut, 2005) also developed methods to calculate the exergy content of commercial fuels, which do not have a known pure substance composition. One special method presented by him is the method to evaluate the exergy content in wood, which is also valid for sugarcane bagasse:

$$\dot{e}_f = (\text{LHV} + M_w h_f) \phi_{\text{dry}} + 9683 w_s + e_{\text{ash}} w_{\text{ash}} + e_w M_w, \quad (3.7)$$

where e_{ash} and e_w are the specific chemical exergy of ash and water, respectively. In this work, ash and water chemical exergy are considered negligible. The ratio chemical exergy to the LHV, ϕ_{dry} , for the sugarcane bagasse, with the mass ratio ($2.67 > w_o/w_c > 0.667$), (Szargut, 2005), (Kotas, 2013) is:

$$\phi_{\text{dry}} = \frac{1.0438 + 0.1882 \left(\frac{w_h}{w_c} \right) - 0.2509 \left[1 + 0.7256 \left(\frac{w_h}{w_c} \right) \right] + 0.0383 \left(\frac{w_N}{w_c} \right)}{1 - 0.3035 \left(\frac{w_o}{w_c} \right)}. \quad (3.8)$$

3.5 Exergetic Efficiency

Exergy analysis is a powerful tool that uses the conservation of mass and combines the First with the Second law of Thermodynamics to design and analyze energy systems. Let's consider E_p as exergy associated as the production of a process and E_f as the consumed fuel. Exergy efficiency can be defined as the ratio of desired effect (exergy associated with the product) over the necessary driving force (consumed fuel) (Kotas, 2013). Note that the following equation must be satisfied

$$\sum_{\text{in}} \dot{E}_f - \sum_{\text{out}} \dot{E}_p = \dot{B}_d \geq 0 \quad (3.9)$$

B_d is the exergy destruction, associated with the irreversibility of the process and by the second law is always greater than or equal to zero. Dividing both sides by $\sum_{\text{in}} E_f$, then

$$1 - \frac{\dot{B}_d}{\sum_{\text{in}} \dot{E}_f} = \frac{\sum_{\text{out}} \dot{E}_p}{\sum_{\text{in}} \dot{E}_f} \quad (3.10)$$

Yet,

$$\epsilon = 1 - \frac{\dot{B}_d}{\sum_{\text{in}} \dot{E}_f}$$

Thus,

$$\epsilon = \frac{\sum_{\text{out}} \dot{E}_p}{\sum_{\text{in}} \dot{E}_f} \leq 1 \quad (3.11)$$

The exergy efficiency is given by Equation 3.11 and for (Kotas, 2013) is called by rational efficiency. In addition, he introduces a second form of rational efficiency, which is

$$1 - \epsilon = \frac{\sum_i \dot{B}_d}{\sum_{\text{in}} \dot{E}_f} \quad (3.12)$$

For (Kotas, 2013), the difference $1 - \epsilon$ is called efficiency defect and states that a fraction of the fuel input is lost through irreversibility associated with the process. Thereby, given the sum of the fractions of fuels input, (Kotas, 2013) defines that its physical meaning is due to irreversibilities associated with various sub-regions in the system.

4 EXERGETIC COST ANALYSIS

This chapter will be presented a brief review on the thermoeconomic analysis. After that, the theory of exergetic cost analysis is presented. The concept of physical structure, product structure are presented. The fuel-product-loss propositions are presented. To close this chapter, the exergetic cost of all control volumes are presented. The entire development of this chapter as well as concepts was based on the theory developed by (Valero *et al.*, 1986), (Lozano; Valero, 1993), (Valero *et al.*, 2017), and (Torres; Valero, 2018),

4.1 Exergetic cost analysis

Thermoeconomic analysis combines exergy analysis with economic analysis for assessing energy system efficiency and estimating product formation cost (Lozano; Valero, 1993).

Modern theories on thermoeconomics started in the 1960s (Evans *et al.*, 1966), to devise thermoeconomic considerations of sea water demineralization. The term *thermoeconomics* was coined to describe factors associated with thermodynamic process performance requirements.

In 1970, (El-Sayed; Evans, 1970) studies the relationship between thermodynamics and economics in complex systems and formulates the concept of *internal economics*. The concept of internal economics allows for exergy economic value assessment and computes financial losses from the the exergy losses in a thermodynamic system.

In 1983, (Gaggioli, 1983) extends the concept of thermoeconomic analysis to all plants and facilities, aiming to avoid bad decisions and make them optimally. Since then, several researchers reported their own fundamental theories on thermoeconomic analysis as shown in Table 4.1.

Table 4.1 – Thermoeconomic theories reported in the literature

Ref	Thermoeconomic method
(Frangopoulos, 1987)	Thermoeconomic Functional Analysis – TFA
(Lozano; Valero, 1993)	Theory of Exergetic Cost – TEC
(Spakovsky; Evans, 1993)	Engineering functional analysis – EFA
(Tsatsaronis <i>et al.</i> , 1993)	Last in first out principle – LIFO
(Tsatsaronis <i>et al.</i> , 1993)	Exergy economic approach – EEA
(Lazzaretto; Tsatsaronis, 1997)	Specific Exergy Costing – SPECO
(Kim <i>et al.</i> , 1998)	Modified productive structure analysis – MOPSA
(Erlach <i>et al.</i> , 1999)	Structural theory of thermoeconomics – STT
(Moran, 1999)	Moran Method
(Rosen; Dincer, 2003)	Exergy-cost-energy-mass – EXCEM

Surveys were published, illustrating the differences between some of the theories outlined at Table 4.1 and key findings from methodologies based in said theories, see (Cerqueira; Nebra, 1999) and references therein.

4.2 Theory of Exergetic Cost - TEC

The theory of exergetic cost was formulated by (Valero et al., 1986) to calculate the exergetic cost of all flows in a system. The *fundamental cost problem* of the was formulated as follows:

Given a system whose limits have been defined and a level of aggregation that specifies the subsystem which constitute it, how to obtain the cost of all the flows that become interrelated in this structure (Lozano; Valero, 1993).

Step 1 (*Aggregations*) Definition of the physical and productive structure. Resources used in the system as energy, raw materials are specified;

Step 2 (*Mass Balance*) To verify the mass conservation;

Step 3 (*Energy Balance*) To verify the energy conservation;

Step 4 (*Exergy Balance*) Exergy efficiency is an indicator of process quality. By the end of **Step 4**, the exergetic efficiency of each aggregation comprising the system is used to allocate the exergy cost at **Step 5**.

Step 5 (*Exergetic Cost Balance*) To calculate the exergetic cost of all flows using exergy as an allocated criterion. The exergy cost of resources is allocated by their products proportionally to its exergy. In addition, the system produces waste and it must be analyzed to make a correct cost allocation.

Execution of **Step 1** → **Step 5** constitutes a tool for assessing prudent exergetic cost of a system; identifying inefficiencies, and determining their exergetic cost allocation; comparing various design alternatives; performing energy audits, and optimizing specific processes (Valero et al., 2017). The Theory of exergetic cost is based on Graph Theory. You can understand in deep about this topic reading about The physical structure using graph theory in Appendix A and Appendix B. Also, you can read about the mass, energy, and exergy balances in matrix form in Appendix C, Appendix D, and Appendix E. Appendix F and Appendix G shows the propositions in matrix form. Appendix H shows the complete system of equations in terms of unit exergy cost. To avoid repeated citations, these appendix were based on (Valero et al., 1986), (Lozano; Valero, 1993), (Valero et al., 2017), and (Torres; Valero, 2018)

4.3 Productive Structure – Fuel-Product-Loss

Every thermodynamic system has a productive structure, which consists on generating one or various products from external resources whilst losing exergy somewhere along the way

Following (Torres; Valero, 2018), consider Definitions 11 – 14.

Definition 11 (Fuel). Denotes external resource getting into the control volume \mathcal{E}_i , i.e., consumed fuel. Specifically refers to the exergy provided by the fuel flow rate, which can either be (i.) exergy needed for a thermodynamic process to be performed or (ii.) exergy associated to an input flow rate that enters the control volume and leaves – with the same flow rate – after losing exergy.

Definition 12 (Product). Denotes internal resource getting out of the control volume \mathcal{E}_i , i.e., product of thermodynamic process. Specifically refers to the exergy associated to product flow rate, which can either be (i) exergy

produced inside the control volume under analysis or (ii) exergy associated to an output flow rate that enters the control volume and leaves – with the same flow rate – after gaining exergy.

Definition 13 (Loss). Denotes exergy that is never used, i.e., exergy lost at the control volume \mathcal{E}_i .

Example 1 (Boiler: fuel and product). **Fuel:** bagasse is the fuel whose combustion increases the water vapor's capacity of producing work. **Product:** the increase in water enthalpy, from compressed liquid at the boiler's input to superheated steam at the boiler's output. **Loss:** Waste energy lost in the exhaust gases.

Example 2 (Turbine: fuel and product). **Fuel:** Consider a control volume \mathcal{E}_b containing a boiler. At the output of \mathcal{E}_b there is a product – a flow \mathbf{e}_v of saturated vapor. Consider a control volume \mathcal{E}_t containing a turbine. The same flow \mathbf{e}_v is consumed as fuel at the input of \mathcal{E}_b . Explicitly, the negative enthalpy variation of \mathbf{e}_v is consumed at \mathcal{E}_t . **Product:** The turbine produces mechanical power, which flows at the output of \mathcal{E}_t .

Definition 14 (Unit Exergy Consumption). Consider exergy efficiency as defined in section 3.5. The inverse reciprocal of exergy efficiency is exergy unit consumption, κ , and its physical meaning is the amount of fuel required for a certain product to be obtained:

$$\kappa = \frac{\mathbf{E}_{\text{Fuel}}}{\mathbf{E}_{\text{Product}}} \geq 1 \quad (4.1)$$

Characterization of the productive structure and of fuel/products flow rates within the system can be expressed by means of incidence matrices.

4.3.1 Fuel Incidence Matrix

Consider an incidence matrix $\mathbf{A}_F \in \mathbb{R}^{n \times m}$ which associates vectors $\boldsymbol{\zeta}$ and $\boldsymbol{\epsilon}$ whenever the j -th flow rate transports fuel from X to Y . An element of \mathbf{A}_F , at the j -th row, i -th column, is written as $a_{F,ij}$, and is computed according to

$$a_{F,ij} = \begin{cases} a_{ij} & , \text{ if } \mathbf{e}_j \in \mathbb{F} \\ 0 & , \text{ otherwise} \end{cases} \quad (4.2)$$

\mathbb{F}_i is the fuel streams in \mathbb{V}_i .

$$\mathbf{A}_F = \begin{array}{c} \boxed{\text{Control Volume 1}} \\ \boxed{\text{Control Volume 2}} \\ \vdots \\ \boxed{\text{Control Volume } n} \end{array} \begin{array}{c} \boxed{\text{Flow 1}} \quad \boxed{\text{Flow 2}} \quad \dots \quad \boxed{\text{Flow } m} \\ \left[\begin{array}{cccc} a_{F,11} & a_{F,12} & \dots & a_{F,1m} \\ a_{F,21} & a_{F,22} & \dots & a_{F,2m} \\ \vdots & \vdots & \ddots & \vdots \\ a_{F,n1} & a_{F,n2} & \dots & a_{F,nm} \end{array} \right] \end{array} \quad (4.3)$$

4.3.2 Vector of Flows of type *Fuel*

Equation 4.2 and Equation 4.5 indicates flows that are fuel and product at each subsystem, respectively. Furthermore, following equations can be introduced:

$$\mathbf{f} = \mathbf{A}_F \boldsymbol{\varepsilon} \quad (4.4)$$

4.3.3 Product Incidence Matrix

Consider an incidence matrix $\mathbf{A}_F \in \mathbb{R}^{n \times m}$ which associates vectors $\boldsymbol{\zeta}$ and $\boldsymbol{\varepsilon}$ whenever the j -th flow rate transports fuel from X to Y . An element of \mathbf{A}_F , at the j -th row, i -th column, is written as $a_{F,ij}$, and is computed according to

The product incidence matrix is:

$$a_{P,ij} = \begin{cases} -a_{ij} & , \text{ if } e_j \in \mathbb{P} \\ 0 & , \text{ otherwise} \end{cases} \quad (4.5)$$

\mathbb{P} is the product streams in in \mathbb{V} .

$$\mathbf{A}_P = \begin{array}{c} \boxed{\text{Control Volume 1}} \\ \boxed{\text{Control Volume 2}} \\ \vdots \\ \boxed{\text{Control Volume n}} \end{array} \begin{array}{c} \boxed{\text{Flow 1}} \quad \boxed{\text{Flow 2}} \quad \dots \quad \boxed{\text{Flow m}} \\ \left[\begin{array}{cccc} a_{P,11} & a_{P,12} & \dots & a_{P,1m} \\ a_{P,21} & a_{P,22} & \dots & a_{P,2m} \\ \vdots & \vdots & \ddots & \vdots \\ a_{P,n1} & a_{P,n2} & \dots & a_{P,nm} \end{array} \right] \end{array} \quad (4.6)$$

4.3.4 Vector of Flows of type *Product*

And,

$$\mathbf{p} = \mathbf{A}_P \boldsymbol{\varepsilon} \quad (4.7)$$

4.3.5 Loss Incidence Matrix

Consider an incidence matrix $\mathbf{A}_F \in \mathbb{R}^{n \times m}$ which associates vectors $\boldsymbol{\zeta}$ and $\boldsymbol{\varepsilon}$ whenever the j -th flow rate transports fuel from X to Y . An element of \mathbf{A}_F , at the j -th row, i -th column, is written as $a_{F,ij}$, and is computed according to

The loss incidence matrix is:

$$a_{L,ij} = \begin{cases} -a_{ij} & , \text{ if } e_j \in \mathbb{L} \\ 0 & , \text{ otherwise} \end{cases} \quad (4.8)$$

\mathbb{L} is the product streams in in \mathbb{V} .

$$\mathbf{A}_L = \begin{array}{c} \boxed{\text{Control Volume 1}} \\ \boxed{\text{Control Volume 2}} \\ \vdots \\ \boxed{\text{Control Volume n}} \end{array} \begin{array}{c} \boxed{\text{Flow 1}} \quad \boxed{\text{Flow 2}} \quad \dots \quad \boxed{\text{Flow m}} \\ \left[\begin{array}{cccc} a_{L,11} & a_{L,12} & \dots & a_{L,1m} \\ a_{L,21} & a_{L,22} & \dots & a_{L,2m} \\ \vdots & \vdots & \ddots & \vdots \\ a_{L,n1} & a_{L,n2} & \dots & a_{L,nm} \end{array} \right] \end{array} \quad (4.9)$$

Remark 13. To verify the fuel, product and loss incidence matrices the following equation must be satisfied:

$$\mathbf{A} = \mathbf{A}_F - \mathbf{A}_P - \mathbf{A}_L \quad (4.10)$$

4.3.6 Vector of Flows of type Loss

$$\mathbf{l} = \mathbf{A}_L \boldsymbol{\varepsilon} \quad (4.11)$$

4.3.7 Exergy Destruction Vector as a function of \mathbf{f} , \mathbf{p} and \mathbf{l}

Also,

$$\boldsymbol{\varepsilon}_d = \mathbf{f} - \mathbf{p} - \mathbf{l} \quad (4.12)$$

4.3.8 Unit Exergy Consumption Matrix

In addition, a diagonal matrix $\mathbf{K}_d \in \{0\} \cup [1, +\infty)^{n \times n}$ contained the exergy unit consumption of each subsystem is given by:

$$\mathbf{f} = \mathbf{K}_d \mathbf{p} \quad (4.13)$$

Also consider a vector

$$\boldsymbol{\kappa}_d = \text{diag}(\mathbf{K}_d) \quad (4.14)$$

The theory of exergetic cost states that to determine the exergetic cost of the systems, the physical structure, and productive structure must be known (Lozano; Valero, 1993).

4.4 Exergy Cost Definition through Propositions

To determine the exergetic cost, (Lozano; Valero, 1993) formulated four propositions¹ as follows:

Proposition 1 ($\mathcal{P}1$). *The exergetic cost of a flow \mathbf{E}_j^* , fuel \mathbf{f}^* or product \mathbf{p}^* is the quantify of exergy needed to produce it. The exergetic cost is a conservative property. This allows us to formulate as many equations of*

¹ The four propositions were copied from the article “Theory of the exergetic cost” written by M. A. Lozano and A. Valero (Lozano; Valero, 1993). Some symbols have been changed to keep the default symbology of this work.

exergetic cost balance as the number of units in the installation. These balances can be expressed, in the absence of an external assessment as $\mathbf{A}_{n \times m} \mathbf{e}_{m \times 1}^* = \mathbf{0}_n$.

$$\sum E_{in}^* - \sum E_{out}^* = 0 \quad (4.15)$$

Remark 14 (Origin of Exergy Cost Unit Conservation).

$$\sum \kappa_{in}^* E_{in} - \sum \kappa_{out}^* E_{out} = 0 \quad (4.16)$$

Proposition 2 (P2). *In the absence of an external assessment, the exergetic cost of the flows entering the plant equals their exergy. This allows us to formulate as many equations, $E_j^* = E_j$, as flows entering the plant*

Proposition 3 (P3). *All costs generated by the productive process must be included in the cost of final products. In the absence of an external assessment, we have to assign a zero value for the cost of the losses of the plant. This allows us to formulate as many equations ($E_j^* = 0$) as existing loss flows. From this proposition, and from the first, we obtain the following corollaries for every unit $L_i^* = 0$ and $F_i^* = P_i^*$.*

Proposition 4 (P4). *Additional propositions were divided as follows:*

Proposition (P4.1). *If an output flow of a unit is a part of the fuel of this unit, then it is understood that its unit exergetic cost is the same as that of the input flow from which it comes*

$$\frac{E_{in}^*}{E_{in}} = \frac{E_{out}^*}{E_{out}} \quad (4.17)$$

$$\kappa_{in}^* = \kappa_{out}^* \quad (4.18)$$

Proposition (P4.2). *If a unit has a product composed of several flows, then the same unit exergetic cost will be assigned to all of them*

$$\frac{E_{product,i}^*}{E_{product,i}} = \frac{E_{product,j}^*}{E_{product,j}} \quad (4.19)$$

$$\kappa_{product,in}^* = \kappa_{product,out}^* \quad (4.20)$$

4.5 Exergetic cost of Control volumes

The exergetic cost of a product must carry the cost of irreversibilities and exergy losses. As previously stated, the same logic can be used to identify the product of a subsystem for purposes of calculating rational efficiency. The exergetic cost of the product, E_p^* , using the Figure 4.1 as example, is:

$$E_p^* = E_3^* + E_4^* \quad (4.21)$$

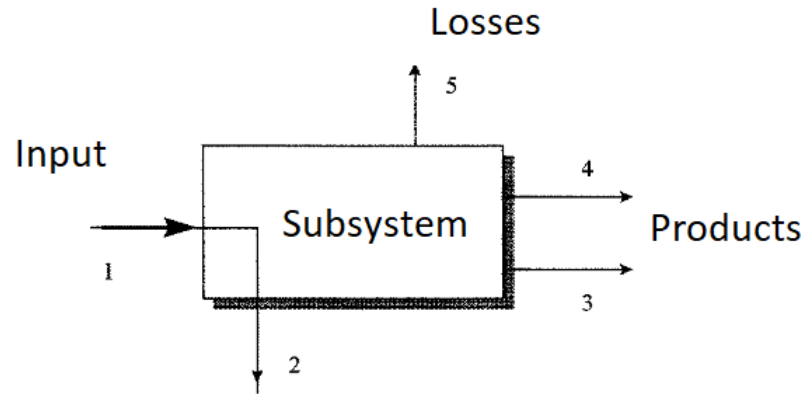


Figure 4.1 – generic subsystem adapted from (Torres, 1999)

The fuel exergetic cost is:

$$E_f^* = E_2^* - E_1^* \quad (4.22)$$

Then, the unit exergetic cost of fuel and products to control volume is:

$$\kappa_f^* = \frac{E_f^*}{E_f} \quad (4.23)$$

To products:

$$\kappa_p^* = \frac{E_p^*}{E_p} \quad (4.24)$$

The values from Equation 4.21 and Equation 4.22 were presented in previous chapters.

In exergetic cost analysis, effective variables are present to evaluating and optimizing a system component. An important variable is the relative cost difference r_k for the k – th component:

$$r_k = \frac{\kappa_{p,k}^* - \kappa_{f,k}^*}{\kappa_{f,k}^*} \quad (4.25)$$

Definition 15 (Relative Cost Difference - (Bejan et al., 1995)). *In a control volume, the relative cost difference expresses the relative increase in the average cost per exergy unit between fuel and product. This variable helps evaluate and optimize a component.*

The relative cost difference determines the inefficient component in the system that has a great influence on the cost of the system. r_k must be greater or equal to zero. The greater r_k more inefficient the control volume is.

5 THERMODYNAMIC & EXERGETIC COST MODELLING

This chapter will be presented the thermodynamic and exergetic cost modelling of the studied system. In this work, a cogeneration cycle fueled with sugarcane bagasse is considered. This facility is located in the midwest of Brazil. The cogeneration system must supply all-electric power needs and thermal power needs, that is, heat(sugar process) and electricity is produced. In this chapter, technical specifications of the system, working conditions of the cogeneration system are presented. Then, the fuel properties, assumptions for energy and exergy analysis are presented. All equations of energy and exergy analysis are also presented. To finish this chapter, all equations of exergetic cost analysis are presented. To help the readers to understand this work, the block diagram in Figure 5.1 was developed .

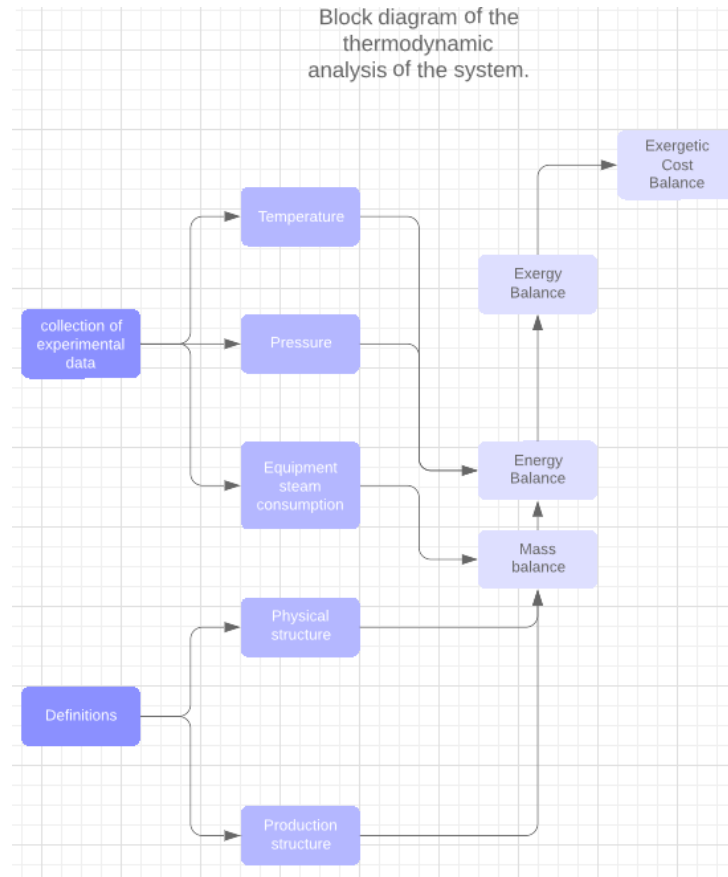


Figure 5.1 – Block diagram of the thermodynamic analysis of the system.

5.1 Description of the cogeneration power plant.

A schematic representation of the analyzed cogeneration system is represented in Figure 5.2. This system is mainly composed of three boilers (B_1 , B_2 , B_3), and seven back pressure steam turbine (BPSP – T_1 to T_7). Boilers B_1 to B_3 are the same model (AZ-353 A).

In this system, the fuel is obtained by processing the sugarcane in the mills, then mixed and burned with heated air in the furnace, producing exhaust gases. These exhaust gases flows to the superheater to produce superheated steam. The maximum steam generation load at nominal conditions are 70 T/h for each boiler and its nominal pressure is at 22 bar and temperature vary from 350-360 °C. In this system, \dot{Q}_{B1} , \dot{Q}_{B2} , and \dot{Q}_{B3} are the energy losses through the boilers. Table 5.1 shows the technical data of the boilers at nominal conditions, provided by the industry.

Table 5.1 – Technical specifications of the boilers at nominal conditions

Parameter	Unit	Value
Nominal steam production	ton/h	70
Operation Pressure	bar	22
Steam temperature	°C	350-360
Water inlet temperature	°C	105
Steam condition	—	Superheated steam
Fuel	—	Bagasse
Fuel consumption	ton/h	97
Excess air	%	30
Water circulation	—	Natural
Water treatment	—	Demineralization
Fabrication year	—	1983

The superheated steam drives the back-pressure steam turbine (BPST). In this system, there are seven turbines. Six of them are responsible to drive machines for the preparation and extraction of sugarcane juice (Turbines \mathbb{T}_1 to \mathbb{T}_6 – machine power) and the last one is to drive electric generator (\mathbb{T}_7). Before the superheated steam goes to the mechanical drive turbines, the flow steam are mixed together through steam pipelines and are represented by virtual thermodynamic equipments(mixing chamber 1 and mixing chamber 2).

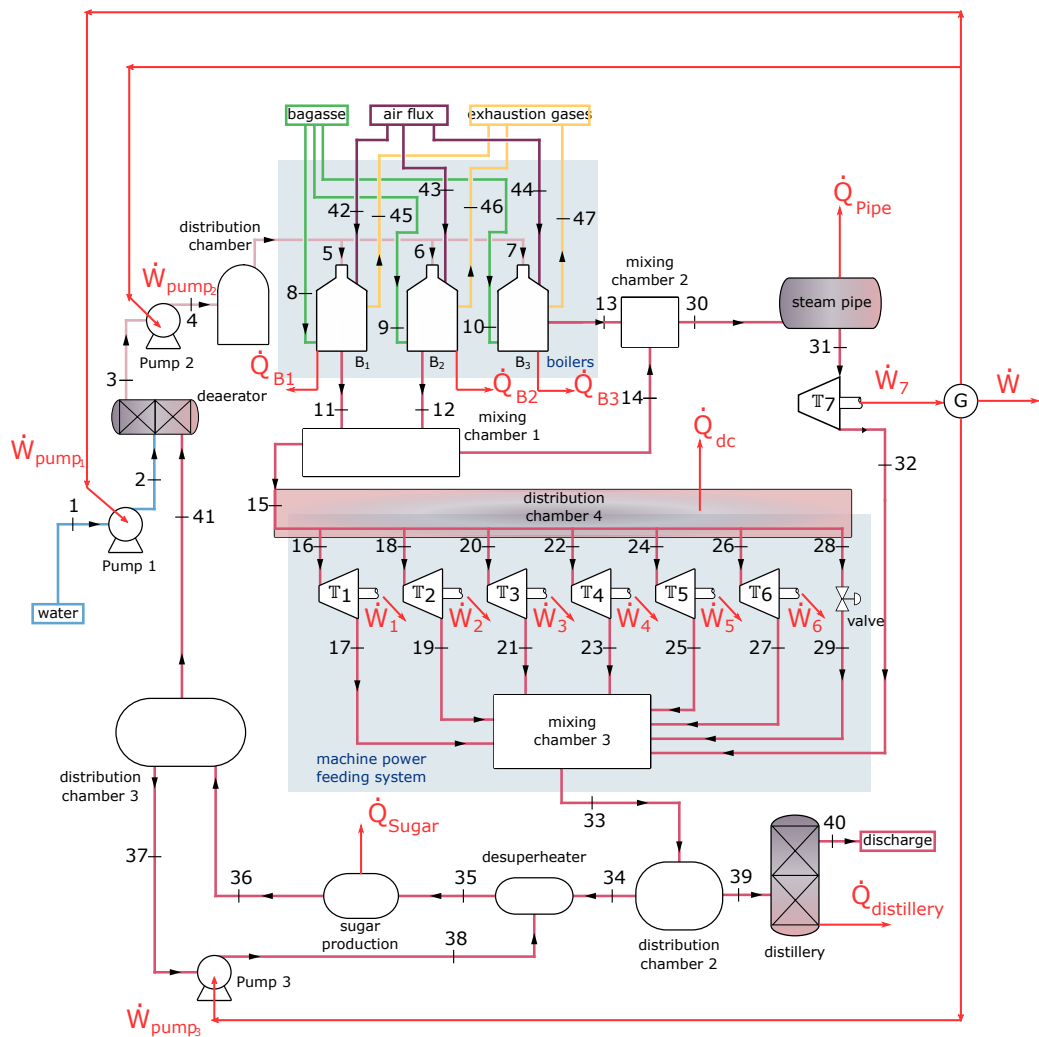


Figure 5.2 – Sugarcane power plant configuration.

These equipment are important to understand the effect of the mixing process on the energy and exergy analysis. The mechanical drive steam turbines system T_1 to T_6 are the same model (TX 2040 ME/20) and T_7 (TXM - 10.000/20) is used to drive electric generators. Table 5.2 and Table 5.3 shows the technical data of TX 2040 ME/20 and TXM - 10.000/20 at nominal conditions, provided by the industry, respectively. The inlet steam pressure and temperature in T_1 to T_7 vary from 21.2 bar to 21.6 bar and 280 °C to 329 °C, respectively. Note that, before flow 30 goes to the turbine, it passes through a giant steam pipe and loses energy to the environment, being represented to \dot{Q}_{pipe} . The nominal mechanical and electric power generation loads are 4000 HP, and 10000 kW, respectively.

After the steam being consumed by the mechanical drive turbines and electric turbine, the output superheated steam will be directly to the mixing chamber 3 to be used as thermal energy. After that, the superheated steam will flow to the distribution chamber 2. The distribution chamber sends steam vapor to (1.) The distillery, where hydrated alcohol and anhydrous alcohol are produced, and (2.) Desuperheater, where its temperature is decreased to a limit temperature for sugar production.

In the distillery process, the superheated steam will change phases, becoming a saturated liquid

Table 5.2 – Technical specifications of the TX-2040ME/20 turbine at nominal conditions

Parameter	Unit	Value
Working power	HP	4000
Rotation	rpm	6000
Steam pressure	bar	22
Outlet pressure	bar	2.5
Steam temperature	°C	300
Turbine consumption	kg/s	11
Stages	—	Single stage
Direction of rotation	—	Counter-clockwise
Fabrication year	—	2008

Table 5.3 – Technical specifications of the TX-10000/20 turbine at nominal conditions

Parameter	Unit	Value
Working power	kW	10000
Rotation	rpm	6000
Steam pressure	bar	22
Outlet pressure	bar	2.5
Steam temperature	°C	350
Turbine consumption	kg/s	31
Stages	—	Triple stage
Direction of rotation	—	Counter-clockwise
Fabrication year	—	2008

Table 5.4 – Working conditions and site data of cogeneration system

Site data obtained in	24/Apr/2019
Fuel type	Bagasse
Lower heat value [(kJ)/(kg)]	7436
Total sugarcane input on harvest [ton]	997395.0
Bagasse produced [(ton/cane)]	0.269
Steam pressure [bar]	22
Steam mass flow rate [ton/h]	175
Fuel mass flow rate [ton/h]	97
Steam bagasse ratio	1.8
Demand mechanical power [kW]	4030
Demand electric power [kW]	6777.0
Nominal electric power [kW]	10000
Operation time [hours]	24
Harvest days [days]	119

and this will be discharged. In the sugar process, the superheated steam flows to a desuperheated to avoid some problems. According to (Hugot, 2014) there is a certain limit temperature above which the sugar in the juice tends

to caramelise, causing at the same time a loss of sucrose and a coloration, which will persist to the final crystal of sugar. To avoid such problem, its temperature must stay between 118 °C to 130 °C.

The condensate from sugar production returns to the deaerator. The loss of condensate due to the distillery process is supplied as liquid water. The water that enters the deaerator is mixed and heated to remove the dissolved oxygen from the water. Then, the output of the liquid is compressed in the pump, then sent to a distribution chamber, and returned to the boilers. The working conditions and site data for the studied system are listed in Table 5.4

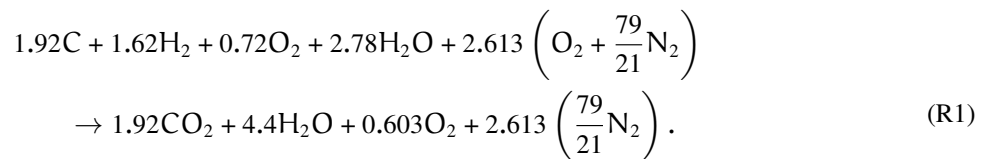
5.2 Fuel properties

Sugarcane bagasse is the feedstock used for this system, delivered at 50 wt.% moisture. The ultimate analysis for fuel is given in Table 5.5.

Table 5.5 – Characteristics of sugarcane bagasse ([Cortes-Rodriguez et al., 2017a](#))

Fuel Ultimate analysis (% wt dry basis)	Sugarcane bagasse
w_c	45.4%
w_h	6.0%
w_n	0.3%
w_{ash}	6.8%
w_s	0.1%
w_o	41.3%

When combustion of bagasse occurs it form carbon dioxide, water in vapor, and other products of combustion. The reaction that describes combustion of the sugarcane bagasse assuming that boiler operates with 30% excess air is given by:



According to ([Ganapathy, 1994](#)), the lower heating value is:

$$LHV_f = HHV - 226.04w_h - 25.82M_w, \tag{5.1}$$

where M_w is the moisture content in the sugarcane bagasse and HHV is the higher heating value, which according to ([Basu, 2006](#)) is:

$$HHV = 338.3w_c + 1443 \left(w_h - \frac{w_o}{8} \right) + 94.2w_s, \tag{5.2}$$

where w_c , w_o , w_h and w_s are the sugarcane bagasse weight percentages of carbon, oxygen, hydrogen, and sulphur respectively.

Remark 15 (Bagasse ultimate analysis and properties – (Cortes-Rodriguez et al., 2017a)). They realized an experimental ultimate analysis of sugarcane bagasse by collecting samples of bagasse near the boiler feeding point. Ashes were collected into various boiler points as below the grate, cyclone discharge, and bottom of the drum. The samples were preserved in a suitable container and sent to the laboratory to make the ultimate analysis. In their work, they collected 6 samples of sugarcane bagasse. For the didactic purposes, the characteristics of sugarcane bagasse shown in Table 5.5 will be the sample mean. Also, they evaluated the Low Heat Value, however, in this work, it was assumed the value as reported in Table 5.4, provided by industry.

5.3 Assumptions for energy and exergy analysis

To evaluate the energy and exergy analysis, mass, energy, and exergy balances must be performed then define thermodynamics efficiencies of each component on energy and exergy based, and its exergy destruction.

For didactic purposes, the transient phases that occur until the plant starts its operation, halts during harvest, or any time variation are disregarded - i.e, this work will study only the steady-state operation. Therefore, the system is considered under steady-state conditions. The adopted assumptions for each control volume are:

1. Potential and kinetic energy changes in all devices are neglect;
2. Boilers do not use work and exhaust gases were considered to be ideal;
3. Complete combustion is supposed;
4. Turbines and pumps are considered to be adiabatic;
5. Steam-bagasse ratio was considered to be 1.8¹

Energy and exergy balances for each control volume will be presented next.

5.3.1 Energy Analysis

In this subsection, energy analysis of the system is presented. The First Law of Thermodynamics, which exhibit energy conservation in any process, is the fundamental theory of energy analysis. The energy balance is employed for modeling the system considering each component being a control volume. The general expression for the First Law of Thermodynamics applied to control volume under steady-state is:

$$0 = \dot{Q}_{cv} - \dot{W}_{cv} + \sum_{in} \left(h + \frac{v^2}{2} + gz \right) \dot{m}_{in} - \sum_{out} \left(h + \frac{v^2}{2} + gz \right) \dot{m}_{out} \quad (5.3)$$

where g is the gravitational acceleration, h is specific enthalpy, \dot{m} is mass flow rate, \dot{Q} is the heat rate at control volume, v is the mass flow rate velocity at control volume, \dot{W} power rate at control volume and z is the height where mass flow rate at control volume occur in relation to a reference line.

For each component, under the assumptions as shown in section 5.3 the energy balance is listed in Table 5.6

¹ According to (Ometto et al., 2009) 2 tons of steam are produced by 1 ton of bagasse.

Table 5.6 – Energy balance for each component

Component	Equation
B ₁	$\dot{m}_5 h_5 + \dot{m}_8 \text{PCI} = \dot{m}_{11} h_{11} + \dot{Q}_{\text{all},1} + \dot{Q}_{\text{eg},1}$
B ₂	$\dot{m}_6 h_6 + \dot{m}_9 \text{PCI} = \dot{m}_{12} h_{12} + \dot{Q}_{\text{all},2} + \dot{Q}_{\text{eg},2}$
B ₃	$\dot{m}_7 h_7 + \dot{m}_{10} \text{PCI} = \dot{m}_{13} h_{13} + \dot{Q}_{\text{all},3} + \dot{Q}_{\text{eg},3}$
Deaerator	$\dot{m}_2 h_2 + \dot{m}_{41} h_{41} = \dot{m}_3 h_3$
Desuperheater	$\dot{m}_{34} h_{34} + \dot{m}_{38} h_{38} = \dot{m}_{35} h_{35}$
Distillery	$\dot{Q}_{\text{dis}} = \dot{m}_{39} (h_{40} - h_{39})$
Distribution chamber 1	$\dot{m}_4 h_4 = \dot{m}_5 h_5 + \dot{m}_6 h_6 + \dot{m}_7 h_7$
Distribution chamber 2	$\dot{m}_{15} h_{15} = \dot{m}_{16} h_{16} + \dot{m}_{18} h_{18} + \dot{m}_{20} h_{20} + \dot{m}_{22} h_{22} + \dot{m}_{24} h_{24} + \dot{m}_{26} h_{26} + \dot{m}_{28} h_{28}$
Distribution chamber 3	$\dot{m}_{36} h_{36} = \dot{m}_{37} h_{37} + \dot{m}_{41} h_{41}$
Expansion Valve	$h_{28} = h_{29}$
Mixing chamber ₁	$\dot{m}_{11} h_{11} + \dot{m}_{12} h_{12} = \dot{m}_{14} h_{14} + \dot{m}_{15} h_{15}$
Mixing chamber ₂	$\dot{m}_{13} h_{13} + \dot{m}_{14} h_{14} = \dot{m}_{30} h_{30}$
Mixing chamber ₃	$\dot{m}_{17} h_{17} + \dot{m}_{19} h_{19} + \dot{m}_{21} h_{21} + \dot{m}_{23} h_{23} + \dot{m}_{25} h_{25} + \dot{m}_{27} h_{27} + \dot{m}_{29} h_{29} + \dot{m}_{32} h_{32} = \dot{m}_{33} h_{33}$
Pump ₁	$\dot{W}_{p,1} = \dot{m}_1 (h_1 - h_2)$
Pump ₂	$\dot{W}_{p,2} = \dot{m}_3 (h_3 - h_4)$
Pump ₃	$\dot{W}_{p,3} = \dot{m}_{37} (h_{37} - h_{38})$
Steam pipe	$\dot{Q}_{\text{pipe}} = \dot{m}_{30} (h_{31} - h_{30})$
Sugar Production	$\dot{Q}_{\text{sugar}} = \dot{m}_{35} (h_{36} - h_{35})$
T ₁	$\dot{W}_{T,1} = \dot{m}_{16} (h_{16} - h_{17})$
T ₂	$\dot{W}_{T,2} = \dot{m}_{18} (h_{18} - h_{19})$
T ₃	$\dot{W}_{T,3} = \dot{m}_{20} (h_{20} - h_{21})$
T ₄	$\dot{W}_{T,4} = \dot{m}_{22} (h_{22} - h_{23})$
T ₅	$\dot{W}_{T,5} = \dot{m}_{24} (h_{24} - h_{25})$
T ₆	$\dot{W}_{T,6} = \dot{m}_{26} (h_{26} - h_{27})$
T ₇	$\dot{W}_{T,7} = \dot{m}_{31} (h_{31} - h_{32})$

The energy loss due to exhaust gas is

$$\dot{Q}_{\text{eg},i} = \dot{m}_{\text{eg}} (h_{\text{out}} - h_0) \quad (5.4)$$

where h_0 is the specific enthalpy at the environmental state. The energy loss due to moisture in the fuel, heat transfer phenomena such as convection and radiation from the surface of the boiler is

$$\dot{Q}_{\text{all},i} = \dot{m}_f \text{PCI} - \dot{m}_{\text{in}} (h_{\text{out}} - h_{\text{in}}) - \dot{Q}_{\text{eg},i} \quad (5.5)$$

$$= \dot{H}_{f,i} - \dot{H}_{b,i} - \dot{Q}_{\text{eg},i} \quad (5.6)$$

Where \dot{H}_f is the useful enthalpic flow supplied by the fuel in the boilers and $\dot{H}_{b,i}$ is the useful enthalpic flow in the boilers to carry out the phase change of water into superheated steam.

The mechanical power is:

$$\dot{W}_{mec} = \sum_{i=1}^6 \dot{W}_{T,i}. \quad (5.7)$$

The net electric power is:

$$\dot{W}_{net} = \dot{W}_{T_7} - \sum_{i=1}^3 \dot{W}_{p,i}. \quad (5.8)$$

5.4 Exergy Analysis

In this subsection the exergy analysis will be presented. The exergy destruction rate of a control volume at steady state is:

$$\dot{E}_d = \sum_j \left(1 - \frac{T_0}{T_j}\right) \dot{Q}_j - \dot{W}_{CV} + \sum_{in} \dot{m}_{in} e_{in} - \sum_{out} \dot{m}_{out} e_{out}, \quad (5.9)$$

where:

- e : Specific flow exergy;
- \dot{E}_d : Exergy destruction rate;
- $\left(1 - \frac{T_0}{T_j}\right) \dot{Q}_j$: is the exergy transfer rate by heat at the location on the boundary at temperature T_j ;
- T_0 : Temperature of dead state;

The total specific flow exergy rate is:

$$e_{total} = e^{PH} + e^{CH}, \quad (5.10)$$

e^{PH} and e^{CH} are physical and chemical exergy, respectively. The specific physical exergy, and chemical exergy are, respectively:

$$e^{PH} = (h - h_0) - T_0 (s - s_0), \quad (5.11)$$

$$e^{CH} = \left(\sum_i y_i \bar{e}_i^{CH} + \bar{R} T_0 \sum_i y_i \ln(y_i) \right) \left(\frac{1}{MM_{ap}} \right), \quad (5.12)$$

\bar{e}_i^{CH} and (MM_{ap}) denotes, respectively, standard chemical exergy of chemical element i , which is reported by (Szargut, 1983) as shown in Table 5.7 and apparent molecular mass of the mixture which is

$$MM_{ap} = \sum_i y_i M_i, \quad (5.13)$$

where M_i is the molecular mass of chemical element i . The chemical exergy of the bagasse was evaluated as previously shown in Equation 3.7

The net exergy transfer by heat in a control volume is:

$$\dot{E}_{q,CV} = \dot{Q}_{CV} \left[1 - \left(\frac{T_0}{T_j} \right) \right]. \quad (5.14)$$

For each component, under the assumptions as shown in section 5.3 the exergy destruction rate is listed in Table 5.8.

Table 5.7 – Standard chemical exergy at reference-environment

Chemical element i	Standard chemical exergy, \bar{e}_i^{CH} [kJ/kmol]
CO ₂	20140
H ₂ O	11710
O ₂	3970
N ₂	720

Table 5.8 – Exergy destruction rate for control volume

Component	Equation
Boiler	$\dot{E}_d = \dot{E}_f - \dot{E}_{\text{steam}} - \dot{E}_{q,\text{all}} - \dot{E}_{\text{eg}}$
Deaerator	$\dot{E}_d = \sum_{\text{in}} \dot{E}_{\text{in}} - \sum_{\text{out}} \dot{E}_{\text{out}}$
Desuperheater	$\dot{E}_d = \sum_{\text{in}} \dot{E}_{\text{in}} - \sum_{\text{out}} \dot{E}_{\text{out}}$
Distillery	$\dot{E}_d = \dot{E}_{\text{in}} - \dot{E}_{\text{out}} - \dot{E}_{q,\text{dis}}$
Distribution chamber	$\dot{E}_d = \sum_{\text{in}} \dot{E}_{\text{in}} - \sum_{\text{out}} \dot{E}_{\text{out}}$
Expansion Valve	$\dot{E}_d = \dot{E}_{\text{in}} - \dot{E}_{\text{out}}$
Mixing chamber	$\dot{E}_d = \sum_{\text{in}} \dot{E}_{\text{in}} - \sum_{\text{out}} \dot{E}_{\text{out}}$
Pump	$\dot{E}_d = \dot{E}_{\text{in}} - \dot{E}_{\text{out}} - \dot{W}_p$
Steam pipe	$\dot{E}_d = \dot{E}_{\text{in}} - \dot{E}_{\text{out}}$
Sugar Production	$\dot{E}_d = \dot{E}_{\text{in}} - \dot{E}_{\text{out}} - \dot{E}_{q,\text{sugar}}$
Turbine	$\dot{E}_d = \dot{E}_{\text{in}} - \dot{E}_{\text{out}} - \dot{W}_{\text{T}}$

5.5 Energy and Exergy Efficiencies

Energy and exergy efficiencies are presented in this section. The equipment efficiencies were determined from the operating information given by the industry. The boiler performance can be measured by its efficiency, which is given by the ratio of energy output to input. In energy analysis, η denotes efficiency. The energy efficiency of boiler is:

$$\eta_B = \frac{\dot{m}_{\text{H}_2\text{O}} (h_{\text{out}} - h_{\text{in}})}{\dot{m}_f \text{LHV}_f} = \frac{\dot{H}_b}{\dot{H}_f}, \quad (5.15)$$

The isentropic efficiency of turbine is:

$$\eta_{\text{iso}} = \frac{h_{\text{in}} - h_{\text{out}}}{h_{\text{in}} - h_{\text{iso}}}, \quad (5.16)$$

The net electrical efficiency is given by the ratio of net electrical energy to the energy input

$$\eta_{\text{el}} = \frac{\dot{W}_{\text{net}}}{\dot{H}_f}. \quad (5.17)$$

For a cogeneration system that produces electricity and heat, its efficiency η_{cog} , is given by the ratio of useful energy output to the energy input:

$$\eta_{\text{cog}} = \frac{\dot{W}_{\text{net}} + \dot{W}_{\text{mec}} + \dot{Q}_{\text{dis}} + \dot{Q}_{\text{sugar}}}{\dot{H}_f}. \quad (5.18)$$

The energy efficiencies do not consider of the energy quality, i.e. work is more valuable than heat. Therefore, if work and heat has different qualities, it is inappropriate to compare their relative energy efficiencies.

This problem can be solved by defining the efficiency based on the second law of thermodynamics, using the exergy concept. The exergy efficiency of boiler is:

$$\epsilon_b = \frac{\dot{E}_{out} - \dot{E}_{in}}{\dot{E}_f}, \quad (5.19)$$

The exergy efficiency of turbines is:

$$\epsilon_T = \frac{\dot{W}_T}{\dot{E}_{in} - \dot{E}_{out}}. \quad (5.20)$$

The net electrical efficiency using exergy base is given by the ratio of net electrical energy to the exergy input:

$$\epsilon_{el} = \frac{\dot{W}_{net}}{\dot{E}_f}, \quad (5.21)$$

The cogeneration efficiency using exergy basis is given by the ratio of useful exergy output to the exergy input:

$$\epsilon_{cog} = \frac{\dot{W}_{net} + \dot{W}_{mec} + \dot{E}_{q,dis} + \dot{E}_{q,sugar}}{\dot{E}_f + \dot{E}_{water}}. \quad (5.22)$$

5.6 Exergetic cost analysis

The exergetic cost analysis can be expressed using the definition of fuel-product and loss as reported by (Lozano; Valero, 1993). They define fuel as the required resources to obtain a determined product, the desired output is the product, and losses are the difference between the fuel and product. The Fuel-Product definitions for the cogeneration system are given in Table 5.9.

To calculate the exergetic cost, the applications of Equation 4.16 applied to all device results in a set of linear equations, as can be seen in Table 5.6. However, the numbers of variables are higher than the set of equations. The missing equations are obtained by using the four propositions related by (Lozano; Valero, 1993). The four propositions were previously stated in section 4.4.

The unitary exergetic cost of demineralized water, bagasse, and air are to be assigned as one, and therefore:

$$\kappa_1^* = \kappa_8^* = \kappa_9^* = \kappa_{10}^* = \kappa_{42}^* = \kappa_{43}^* = \kappa_{44}^* = 1 \quad (5.23)$$

In the distribution chamber 1, 2, 3, and 4 the unitary exergetic cost of entering and leaving is the same. Therefore:

$$\kappa_5^* = \kappa_6^* = \kappa_7^* \quad (5.24)$$

$$\kappa_{15}^* = \kappa_{16}^* = \kappa_{18}^* = \kappa_{20}^* = \kappa_{22}^* = \kappa_{24}^* = \kappa_{26}^* \quad (5.25)$$

$$\kappa_{34}^* = \kappa_{39}^* \quad (5.26)$$

$$\kappa_{37}^* = \kappa_{41}^* \quad (5.27)$$

Table 5.9 – Fuel and product exergy definitions of the cogeneration system

k	Component	Efficiency		
		Fuel (F)	Product (P)	Losses(L)
1	Pump ₁	\dot{W}_{pump1}^a	2-1	
2	Deaerator	2+41	3	
3	Pump ₂	\dot{W}_{pump2}^a	4-3	
4	Distribution Chamber	4	5+6+7	
5	B ₁	8+42	11-5	$45+\dot{Q}_{\text{all},1}^b$
6	B ₂	9+43	12-6	$46+\dot{Q}_{\text{all},2}^b$
7	B ₃	10+44	13-7	$47+\dot{Q}_{\text{all},3}^b$
8	Mixing Chamber ₁	11+12	14+15	
9	Mixing Chamber ₂	13+14	30	
10	Steam Pipe	30	31	\dot{Q}_{pipe}^c
11	T ₁	16-17	\dot{W}_1^d	
12	T ₂	18-19	\dot{W}_2^d	
13	T ₃	20-21	\dot{W}_3^d	
14	T ₄	22-23	\dot{W}_4^d	
15	T ₅	24-25	\dot{W}_5^d	
16	T ₆	26-27	\dot{W}_6^d	
17	T ₇	31-32	\dot{W}_7^d	
18	Valve	28	29	
19	Mixing Chamber ₃	17+19+21+23+25+27+29+32	33	
20	Distribution Chamber ₂	33	34+39	
21	Distillery	39-40	\dot{Q}_{dis}^e	
22	Desuperheater	34+38	35	
23	Sugar Production	35-36	\dot{Q}_{sugar}^f	
24	Distribution Chamber ₃	36	37+41	
25	Pump ₃	\dot{W}_{pump3}^a	38-37	
26	Distribution chamber ₄	15	16+18+20+22+24+26+28	
27	Generator	\dot{W}_7^d	$\dot{W}_{\text{pump1}}+\dot{W}_{\text{pump2}}+\dot{W}_{\text{pump3}}+\dot{W}_{64}$	

In incidence matrix are — $\dot{W}_{\text{pump},j}^a$ Points 55 to 57 — $\dot{Q}_{\text{all},i}^b$ Points 59 to 61 — \dot{Q}_{pipe}^c Point 58 — \dot{W}_j^d Points 48 to 54 — \dot{Q}_{dis}^e Point 62 — \dot{Q}_{sugar}^f Point 63

In the mix chambers 1 and generator the product proposition is applied, respectively. Then:

$$\kappa_{14}^* = \kappa_{15}^* \quad (5.28)$$

$$\kappa_{55}^* = \kappa_{56}^* = \kappa_{57}^* = \kappa_{64}^* \quad (5.29)$$

For turbines T₁ to T₇, sugar production, and distillery the fuel proposition is applied, respectively. Then:

$$\kappa_{16}^* = \kappa_{17}^* \quad (5.30)$$

$$\kappa_{18}^* = \kappa_{19}^* \quad (5.31)$$

Table 5.10 – Equations for exergetic cost balance of the cogeneration system

k	Component	$\sum \kappa_{in}^* E_{in}$	$\sum \kappa_{out}^* E_{out}$
1	Pump ₁	$\kappa_1^* E_1 - \kappa_{55}^* \dot{W}_{pump1}$	$\kappa_2^* E_2$
2	Deaerator	$\kappa_2^* E_2 + \kappa_{41}^* E_{41}$	$\kappa_3^* E_3$
3	Pump ₂	$\kappa_3^* E_3 - \kappa_{56}^* \dot{W}_{pump2}$	$\kappa_4^* E_4$
4	Distribution Chamber	$\kappa_4^* E_4$	$\kappa_5^* E_5 + \kappa_6^* E_6 + \kappa_7^* E_7$
5	B ₁	$\kappa_5^* E_5 + \kappa_8^* E_8 + \kappa_{42}^* E_{42}$	$\kappa_{11}^* E_{11} + \kappa_{45}^* E_{45} + \kappa_{59}^* E_{59}$
6	B ₂	$\kappa_6^* E_6 + \kappa_9^* E_9 + \kappa_{43}^* E_{43}$	$\kappa_{12}^* E_{12} + \kappa_{46}^* E_{46} + \kappa_{60}^* E_{60}$
7	B ₃	$\kappa_7^* E_7 + \kappa_{10}^* E_{10} + \kappa_{44}^* E_{44}$	$\kappa_{13}^* E_{13} + \kappa_{47}^* E_{47} + \kappa_{61}^* E_{61}$
8	Mixing Chamber ₁	$\kappa_{11}^* E_{11} + \kappa_{12}^* E_{12}$	$\kappa_{14}^* E_{14} + \kappa_{15}^* E_{15}$
9	Mixing Chamber ₂	$\kappa_{13}^* E_{13} + \kappa_{14}^* E_{14}$	$\kappa_{30}^* E_{30}$
10	Steam Pipe	$\kappa_{30}^* E_{30}$	$\kappa_{31}^* E_{31} + \kappa_{58}^* E_{58}$
11	T ₁	$\kappa_{16}^* E_{16}$	$\kappa_{17}^* E_{17} + \kappa_{48}^* \dot{W}_{T_1}$
12	T ₂	$\kappa_{18}^* E_{18}$	$\kappa_{19}^* E_{19} + \kappa_{49}^* \dot{W}_{T_2}$
13	T ₃	$\kappa_{20}^* E_{20}$	$\kappa_{21}^* E_{21} + \kappa_{50}^* \dot{W}_{T_3}$
14	T ₄	$\kappa_{22}^* E_{22}$	$\kappa_{23}^* E_{23} + \kappa_{51}^* \dot{W}_{T_4}$
15	T ₅	$\kappa_{24}^* E_{24}$	$\kappa_{25}^* E_{25} + \kappa_{52}^* \dot{W}_{T_5}$
16	T ₆	$\kappa_{26}^* E_{26}$	$\kappa_{27}^* E_{27} + \kappa_{53}^* \dot{W}_{T_6}$
17	T ₇	$\kappa_{31}^* E_{31}$	$\kappa_{32}^* E_{32} + \kappa_{54}^* \dot{W}_{T_7}$
18	Valve	$\kappa_{28}^* E_{28}$	$\kappa_{29}^* E_{29}$
19	Mixing Chamber ₃	$\kappa_{17}^* E_{17} + \kappa_{19}^* E_{19} + \kappa_{21}^* E_{21} + \kappa_{23}^* E_{23} + \kappa_{25}^* E_{25} + \kappa_{27}^* E_{27} + \kappa_{29}^* E_{29} + \kappa_{32}^* E_{32}$	$\kappa_{33}^* E_{33}$
20	Distribution Chamber ₂	$\kappa_{33}^* E_{33}$	$\kappa_{34}^* E_{34} + \kappa_{39}^* E_{39}$
21	Distillery	$\kappa_{39}^* E_{39}$	$\kappa_{40}^* E_{40} + \kappa_{62}^* E_{62}$
22	Desuperheater	$\kappa_{34}^* E_{34} + \kappa_{38}^* E_{38}$	$\kappa_{35}^* E_{35}$
23	Sugar Production	$\kappa_{35}^* E_{35} + \kappa_{63}^* E_{63}$	$\kappa_{36}^* E_{36}$
24	Distribution Chamber ₃	$\kappa_{36}^* E_{36}$	$\kappa_{37}^* E_{37} + \kappa_{41}^* E_{41}$
25	Pump ₃	$\kappa_{37}^* E_{37} - \kappa_{57}^* \dot{W}_{pump3}$	$\kappa_{38}^* E_{38}$
26	Distribution chamber ₂	$\kappa_{15}^* E_{15}$	$\kappa_{16}^* E_{16} + \kappa_{18}^* E_{18} + \kappa_{20}^* E_{20} + \kappa_{22}^* E_{22} + \kappa_{24}^* E_{24} + \kappa_{26}^* E_{26} + \kappa_{28}^* E_{28}$
27	Generator	$\kappa_{54}^* \dot{W}_{T_7}$	$\kappa_{55}^* \dot{W}_{pump1} + \kappa_{56}^* \dot{W}_{pump2} + \kappa_{57}^* \dot{W}_{pump3} + \kappa_{54}^* \dot{W}_{64}$

$$\kappa_{20}^* = \kappa_{21}^* \quad (5.32)$$

$$\kappa_{22}^* = \kappa_{23}^* \quad (5.33)$$

$$\kappa_{24}^* = \kappa_{25}^* \quad (5.34)$$

$$\kappa_{26}^* = \kappa_{27}^* \quad (5.35)$$

$$\kappa_{31}^* = \kappa_{32}^* \quad (5.36)$$

$$\kappa_{35}^* = \kappa_{36}^* \quad (5.37)$$

$$\kappa_{39}^* = \kappa_{40}^* \quad (5.38)$$

The unitary exergetic cost of the losses are to be null, and therefore:

$$\kappa_{45}^* = 0, \kappa_{46}^* = 0, \kappa_{47}^* = 0, \kappa_{58}^* = 0, \kappa_{59}^* = 0, \kappa_{60}^* = 0, \kappa_{61}^* = 0 \quad (5.39)$$

6 RESULTS AND DISCUSSION

This chapter will be presented the results and discussion of the studied system, which were presented in the previous chapter. First, the flow identification and thermodynamics properties are presented. Then, the consistency of energy, as well as the exergy balance, are verified. The discussion of energy and exergy analysis is presented. Second, the exergetic cost analysis is presented. In this part, the exergy, exergetic cost, and unitary exergetic cost of each flow are presented and discussed. In this part, results obtained for unit exergetic cost considering power generation as a product are compared to works found out in the literature. Then, the unit exergetic cost and relative cost difference of each control volume are presented to find out the component with the highest priority to be improved. Third, proposed modifications based on the results obtained using these methods are presented. In this part, the exergy and exergetic cost analyses of the proposed modifications are evaluated and discussed. To finish this chapter, the main results comparing the base case with the proposed modification are discussed.

6.1 Performance of the sugarcane power plant

The performance of the sugarcane power plant system is examined through different parameters as: energy and exergy efficiencies, electric to heating ratios, exergy destruction, and exergetic cost. The thermodynamic properties for the schematic system are shown in Table 6.1 and Table 6.2. These properties were obtained from a commercially available software, Engineering Equation Solver ([Klein; Alvarado, 2020](#)). You can find the calculation procedure in Appendix I.

Table 6.1 – Flow identification and thermodynamic properties.

Flow	T [°C]	P[bar]	\dot{m} [(kg)/(s)]	h [(kJ)/(kg)]	s [(kJ)/(kg·K)]	e [(kJ)/(kg)]
1	25	1.01	9.722	104.9	0.3672	0
2	27.43	2.5	9.722	115.2	0.4011	0.1905
3	81.53	2.5	48.61	341.6	1.094	20.11
4	82.69	32	48.61	348.8	1.105	23.81
5	82.69	22	7.78	348	1.106	22.82
6	82.69	22	19.44	348	1.106	22.82
7	82.69	22	21.39	348	1.106	22.82
8	—	—	4.322	—	—	8536.833
9	—	—	10.8	—	—	8536.833
10	—	—	11.88	—	—	8536.833
11	294	22	7.778	3004	6.692	1014
12	295	22	19.44	3007	6.696	1015
13	333	22	21.39	3095	6.846	1058
14	294.7	22	2.419	3006	6.695	1014
15	294.7	22	24.8	3006	6.695	1014
16	294.5	21.5	5.061	3007	6.707	1012
17	190	2.5	5.061	2848	7.358	658.8
18	290	21.2	6.481	2997	6.695	1005
19	160	2.6	6.481	2785	7.2	643.2
20	280	21.6	2.764	2972	6.642	996.1
21	168	2.7	2.764	2801	7.22	653.4
22	282	21.5	2.222	2977	6.653	997.9
23	152	2.6	2.222	2769	7.161	638.1
24	282	21.5	2.478	2977	6.653	997.9
25	153	2.5	2.478	2772	7.186	633.7
26	281	21.5	2.889	2975	6.649	996.8
27	183	2.7	2.889	2833	7.289	663.8
28	294.7	22	2.908	3006	6.695	1014
29	268	2.5	2.908	3006	7.673	722.8
30	329	22	23.81	3086	6.831	1054
31	314	21.5	23.81	3052	6.786	1034
32	152	2.7	23.81	2768	7.142	642.9
33	166.1	2.5	48.61	2799	7.249	642.1
34	166.1	2.5	38.89	2799	7.249	642.1
35	128	2.5	40.25	2718	7.056	618.7
36	95	2.5	40.25	398.2	1.25	30.01
37	95	2.5	1.362	398.2	1.25	30.01

38	96.73	3	1.362	405.6	1.27	31.49
39	166.1	2.5	9.722	2799	7.249	642.1
40	127.4	2.5	9.722	535.3	1.607	60.71
41	95	2.5	38.89	398.2	1.25	30.01
42	25	1.01	15.64	338.9	9.525	0
43	25	1.01	39.10	338.9	9.525	0
44	25	1.01	43.02	338.9	9.525	0
45	170	1.01	19.96	519.1	10.01	273.2
46	170	1.01	49.91	519.1	10.01	273.2
47	170	1.01	54.9	519.1	10.01	273.2

Table 6.2 – Non-Material flow identification

Flow	Type	Value [kW]
48	\dot{W}_1	804.4
49	\dot{W}_2	1372
50	\dot{W}_3	470.8
51	\dot{W}_4	463
52	\dot{W}_5	509.1
53	\dot{W}_6	410.4
54	\dot{W}_7	6777
55	$\dot{W}_{\text{pump},1}$	1.5
56	$\dot{W}_{\text{pump},2}$	350
57	$\dot{W}_{\text{pump},3}$	1.5
58	\dot{Q}_{pipe}	-793.6
59	$\dot{Q}_{B,1}$	-3599
60	$\dot{Q}_{B,2}$	-8997
61	$\dot{Q}_{B,3}$	-9897
62	$\dot{Q}_{\text{distillery}}$	22005
63	\dot{Q}_{sugar}	93356
64	\dot{W}	6424

These parameters are examined to identify the sub-system that presents the worst thermodynamic performance. This study is important from an economic point of view since the present study was applied to an existing system and new operation strategies can arise.

The consistency of mass conservation was verified, taking into account the accuracy of the measuring devices. The energy and exergy balance and its efficiency for boilers are shown in Table 6.3. The second and third columns represents the helpful enthalpic flow to carry out the phase change of water into superheated steam and the enthalpic flow supplied by the fuel, respectively. The energy balance suggest that the most responsible of the lost fuel energy in B_1 , B_2 , and B_3 are due to moisture in the fuel, convection, and radiation losses from the boilers surface. These factors together accounts for 47219 kW of energy losses, i.e., 23.51% of the combustion energy of fuel (third column). The exhaust gases (fifth column) takes a significant portion in the energy losses and it accounts for 22492 kW, i.e., 11.20% of the combustion energy of fuel, which is lost to the atmosphere. (Singh, 2019) reported a cogeneration system of sugarcane and found that 6.34% of fuel energy is lost to the atmosphere through the exhaust gases. (Kamate; Gangavati, 2009) evaluated an exergy analysis of a heat-matched bagassed cogeneration plant and found that 3.80% of fuel energy is lost through the exhaust gases. As a result of these losses, and comparing to the design point value (86%), the energy efficiency of B_1 , B_2 , and B_3 are found to be quiet low 64.3%, 64.4% and 66.5%, respectively.

Energy losses and efficiencies based on energy do not provide a real measure of the performance of analyzed boilers. The second law efficiency, with lower values, shows the effects of the combustion and internal heat transfer with finite temperature differences irreversibilities.

Table 6.3 – Energy and exergy balance for the boilers and efficiency on energy and exergy base.

sub-system	\dot{H}_b [kW]	\dot{H}_f [kW]	\dot{Q}_{all} [kW]	\dot{Q}_{eg} [kW]	\dot{E}_f [kW]	\dot{E}_{steam} [kW]	η [%]	ϵ [%]
B_1	20665	32140	7875	3600	36898	7709.39	64.3	20.9
B_2	51682	80309	19632	8995	92198	19287.97	64.4	20.9
B_3	58755	88365	19712	9897	101446	22142.50	66.5	21.8
Total	131102	200814	47222	22492	230542	49139.86	—	—

Table 6.4 shows the energy and exergy balance for turbines. The power values is not referring the nominal conditions of turbine, but part load condition instead. Turbines T_1 to T_6 are TX2040 ME/20 model turbine with 4000 HP nominal power and T_7 is a TXM 10.000/20 model turbine with 10.000 kW nominal power. The total power generation (the sum of values in the third column) is 10806.7 kW, a load of 38.7% of the nominal value. The exergy variation of the steam flow is presented in the fourth column. Isentropic efficiency and the second-law efficiencies are presented in columns five and six, respectively. Exergy efficiencies of BPST are lower than those reported by (Kamate; Gangavati, 2009), which vary from 83% to 89%.

The exergy destruction in each components of the analysed cogeneration system expressed as percent of fuel exergy input is given in Table 6.5 which can be used to guide system performance improvement. Note that the largest exergy destruction occurs in the boilers, 58.57% of the fuel exergy is destroyed due to combustion and internal heat transfer irreversibilities.

The results show that 14.59% of the fuel exergy is lost to the environment due to high exhaust gas temperature. The exergy destruction due exhaust gases is viewed as an external irreversibility. This part of exergy

Table 6.4 – energy and exergy balance for turbines and efficiency on energy and exergy base.

sub-system	\dot{W}_{iso} [kW]	\dot{W}_{real} [kW]	$\Delta \dot{E}$ [kW]	η_{iso} [%]	ϵ [%]
T_1	2171	804.4	1787	37.0	45.0
T_2	2703	1372	2347	50.7	58.4
T_3	1125	470.8	947.1	41.9	49.7
T_4	919.7	463	799.5	50.3	57.9
T_5	1042	509.1	902.4	48.9	56.4
T_6	1175	410.4	961.8	34.9	42.7
T_7	10231	6777	9777	71.5	77.4

Table 6.5 – Exergy balance of the analyzed cogeneration system and the percentage ratio of exergy to fuel exergy input

	[kW]	%
Fuel Exergy input	230542.00	100.00
Exergy destruction in the boiler furnace	135017.00	58.57
Exergy destruction through exhaust gases	33644.00	14.59
Exergy destruction in the turbines	6248.90	2.71
Exergy destruction in the mixing chambers	2865.87	1.25
Exergy destruction in the expansion valve	848.10	0.36
Exergy destruction in the Desuperheater	112.20	0.04
Exergy destruction in other components	12310.83	5.34
Exergy utilization in sugarcane production	23604.00	10.24
Exergy utilization in Destillery	5626.00	2.44
Net power output	10265.10	4.46

destruction can be reduced by reducing the exhaust temperature, also by reducing the heat transfer temperature difference. So, the exergy associated with the exhaust gases could be used for increase the water temperature that is sent to the boilers. The exergy destruction in the mixing chambers represent 1.24% of the fuel exergy. This part of exergy destruction can be reduced by reducing the temperature difference of working fluid at each equipment.

The exergy destruction at desuperheater represent 0.04% of the fuel exergy. This exergy destruction could be reduced if the heat transfer temperature of the working fluid could be reduced further, but results shows that the energy loss associated with the desuperheater is thermodynamically insignificant, once its work producing potential is very low. The exergy destruction in the expansion valve represent 0.36%. In this manner, the expansion valve is a purely dissipative device and its exergy destruction could be reduced by sending its working fluid to T_7 . Hence, the exergy destruction in turbines could be reduced due to an increase in the turbine efficiencies.

The exergy utilization in sugarcane process and net power output was reported by (Singh, 2019) as to be 8.67% and 12.40%, respectively. Comparing results obtained herein, it is suggested that the sugar production process herein is more efficiently, but net power output is not.

The net electrical efficiency using exergy base and cogeneration exergy efficiency of the analysed system is estimated to be 2.7% and 17.14% respectively. Cogeneration exergy efficiency obtained herein was lower

that those reported by (Taner; Sivrioglu, 2015) (37.4%), (Kamate; Gangavati, 2009) (21.1%), (Singh, 2019)(21%), (Cavalcanti et al., 2020)(18.76%) and higher than (Cavalcanti et al., 2019) (16.89%).

These low values obtained from exergy analysis indicate that a high scope available for improving the cogeneration system. Thus, to determine the exergy needed to produce each flow and product, an exergetic cost analysis is realized.

6.2 Exergetic cost analysis

As previously evaluated, the exergy analysis allowed to identify irreversibility and efficiency of plant components and the entire system. However, exergetic cost analysis will go further by estimating the exergy needed to produce each flow and product. All the flows and properties are given in Table 6.6. Detailed results of exergetic cost E^* of each flow and unit exergetic cost κ^* are presented in Table 6.7.

Table 6.6 – Flow identification and thermodynamic properties.

Flow	T [°C]	P[bar]	\dot{m} [(kg)/(s)]	h [(kJ)/(kg)]	s [(kJ)/(kg·K)]	e [(kJ)/(kg)]	E^* [kW]
1	25	1.01	9.722	104.9	0.3672	0	—
2	27.43	2.5	9.722	115.2	0.4011	0.1905	9.787
3	81.53	2.5	48.61	341.6	1.094	20.11	5893
4	82.69	32	48.61	348.8	1.105	23.81	8173
5	82.69	22	7.78	348	1.106	22.82	1308
6	82.69	22	19.44	348	1.106	22.82	3270
7	82.69	22	21.39	348	1.106	22.82	3598
8	—	—	4.322	—	—	8536.833	36888
9	—	—	10.8	—	—	8536.833	92219
10	—	—	11.88	—	—	8536.833	101441
11	294	22	7.778	3004	6.692	1014	38196
12	295	22	19.44	3007	6.696	1015	95489
13	333	22	21.39	3095	6.846	1058	105038
14	294.7	22	2.419	3006	6.695	1014	11882
15	294.7	22	24.8	3006	6.695	1014	121804
16	294.5	21.5	5.061	3007	6.707	1012	25042
17	190	2.5	5.061	2848	7.358	658.8	16304
18	290	21.2	6.481	2997	6.695	1005	31861
19	160	2.6	6.481	2785	7.2	643.2	20383
20	280	21.6	2.764	2972	6.642	996.1	13462
21	168	2.7	2.764	2801	7.22	653.4	8831
22	282	21.5	2.222	2977	6.653	997.9	10843
23	152	2.6	2.222	2769	7.161	638.1	6934
24	282	21.5	2.478	2977	6.653	997.9	12090
25	153	2.5	2.478	2772	7.186	633.7	7677

26	281	21.5	2.889	2975	6.649	996.8	14080
27	183	2.7	2.889	2833	7.289	663.8	9377
28	294.7	22	2.908	3006	6.695	1014	14426
29	268	2.5	2.908	3006	7.673	722.8	14426
30	329	22	23.81	3086	6.831	1054	116920
31	314	21.5	23.81	3052	6.786	1034	116920
32	152	2.7	23.81	2768	7.142	642.9	72704
33	166.1	2.5	48.61	2799	7.249	642.1	156635
34	166.1	2.5	38.89	2799	7.249	642.1	125308
35	128	2.5	40.25	2718	7.056	618.7	125524
36	95	2.5	40.25	398.2	1.25	30.01	6088
37	95	2.5	1.362	398.2	1.25	30.01	205.4
38	96.73	3	1.362	405.6	1.27	31.49	215.2
39	166.1	2.5	9.722	2799	7.249	642.1	31327
40	127.4	2.5	9.722	535.3	1.607	60.71	2962
41	95	2.5	38.89	398.2	1.25	30.01	5883
42	25	1.01	15.64	338.9	9.525	0	—
43	25	1.01	39.10	338.9	9.525	0	—
44	25	1.01	43.02	338.9	9.525	0	—
45	170	1.01	19.96	519.1	10.01	273.2	—
46	170	1.01	49.91	519.1	10.01	273.2	—
47	170	1.01	54.9	519.1	10.01	273.2	—

Table 6.7 – Exergy, exergetic cost and unitary exergetic cost of each flow

Flow	E [kW]	E* [kW]	$\kappa^* \frac{[\text{kW}]}{[\text{kW}]}$	Flow	E [kW]	E* [kW]	$\kappa^* \frac{[\text{kW}]}{[\text{kW}]}$
1	—	—	1	33	31215	156635	5.018
2	1.453	9.787	6.736	34	24972	125308	5.018
3	961.7	5893	6.127	35	24901	125524	5.041
4	1142	8176	7.162	36	1208	6088	5.041
5	182.7	1308	7.162	37	40.75	205.4	5.041
6	456.6	3270	7.162	38	41.1	215.2	5.237
7	502.3	3598	7.162	39	6243	31327	5.018
8	36888	36888	1	40	590.2	2962	5.018
9	92219	92219	1	41	1167	5883	5.041
10	101441	101441	1	42	—	—	1
11	7884	38196	4.845	43	—	—	1
12	19731	95489	4.84	44	—	—	1
13	22633	105038	4.641	45	—	—	0

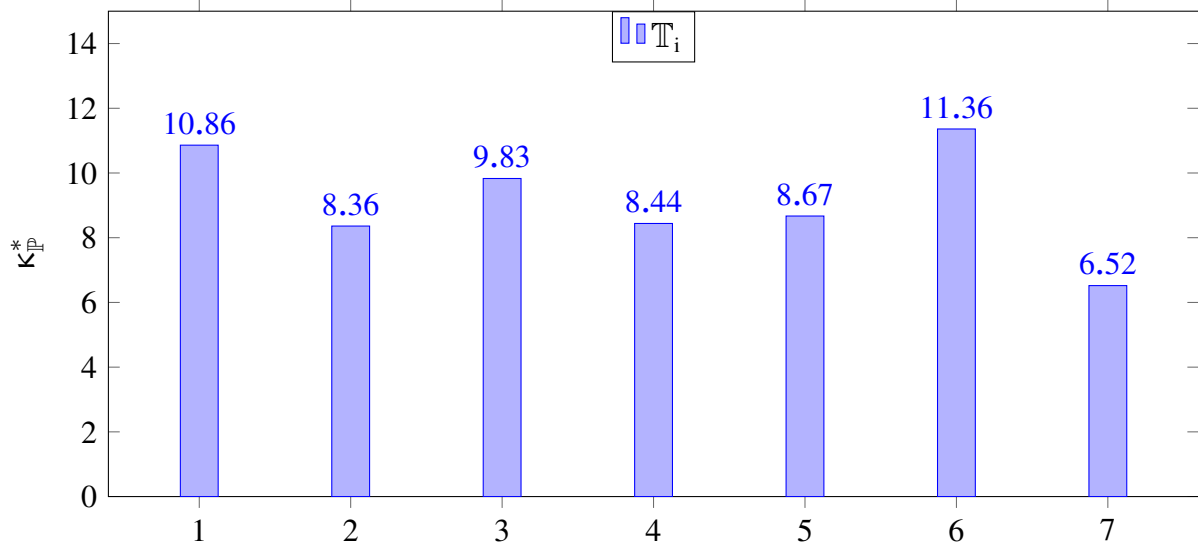
14	2454	11882	4.841	46	—	—	0
15	25160	121804	4.841	47	—	—	0
16	5121	25042	4.89	48	804.4	8738	10.86
17	3334	16304	4.89	49	1372	11479	8.368
18	6516	31861	4.89	50	470.8	4631	9.837
19	4168	20383	4.89	51	463	3909	8.444
20	2753	13462	4.89	52	509.1	4413	8.667
21	1806	8831	4.89	53	410.4	4703	11.36
22	2218	10843	4.89	54	6777	44216	6.525
23	1418	6934	4.89	55	1.5	9.787	6.525
24	2473	12090	4.89	56	350	2284	6.525
25	1570	7677	4.89	57	1.5	9.787	6.525
26	2880	14080	4.89	58	—	—	0
27	1918	9377	4.89	59	—	—	0
28	2950	14426	4.89	60	—	—	0
29	2102	14426	6.863	61	—	—	0
30	25084	116920	4.661	62	23603	119435	5.06
31	24617	116920	4.75	63	5626	28365	5.042
32	15307	72704	4.75	64	6424	41913	6.525

The unit exergetic cost of input resources such as water, bagasse, and air is 1 (point 1, 8, 9, 10, 42, 43, and, 44) because the cost of the resources entering the plant must be equivalent to their exergy (see Proposition 2).

To reach a better distribution of product-fuel costs, the use of virtual devices (distribution chambers and mixing chambers) can help to allocate the exergetic cost of each flow. Note that the exergetic cost of distribution chambers is the same because no irreversibility is associated with them. In the mixing chamber 3, due to mixing effects, the exergetic cost of each flow will suffer a small variation, increasing by 2.4%. In the expansion valve (points 28 — 29) the unit exergetic cost of the outlet flow increased by 40% because the expansion valve is a purely dissipative device. These results suggest that the more exergy is destroyed to produce the flow, the more expensive is the unit exergetic cost.

The exergetic parameters for each turbine of the cogeneration system can be seen in Figure 6.1. Unit exergetic cost considering mechanical power as a product takes the highest value equals to $\kappa_{53}^* = 11.36$ in \mathbb{T}_6 . This high value indicates that this equipment is the least efficient in the mechanical power feeding system. The high exergetic cost of this product can be explained for some reasons: (1.) Because this turbine is operating under partial load conditions, about 73% below the nominal conditions, (2.) This turbine is a single-stage, i.e, old technology and, (3.) This turbine is operating with a low-efficiency cogeneration system based on a steam cycle with superheated steam at 22 bar and temperature around 285 °. The results of this turbine are in accordance with the exergy analysis evaluation presented in chapter 6. Also, (Ensinas et al., 2007) and (Macedo, 2001) corroborate

Figure 6.1 – Unit exergetic cost considering power generation as a product



that turbines operating at these load conditions have low efficiency.

Unit exergetic cost considering electrical power as a product takes $\kappa_p^* = 6.52$ as can be seen in Figure 6.1. Note that this turbine is operating at partial-load conditions and low-pressure-temperature conditions. Previous studies evaluated unit exergetic cost considering electrical power as to be $\kappa_p^* = 2.427$ (Modesto; Nebra, 2006). Highlights some important facts of the (Modesto; Nebra, 2006) works: (1.) They evaluated a Rankine regenerative system using blast furnace gas and coke oven gas with turbines operating at 87 bar and 510° in the steel industry, (2.) They evaluated the exergetic cost of turbines in condensing steam using the extraction model. The results presented in this work suggest that the high exergetic cost of these devices is caused by inappropriate devices use and old technologies, comparing with the results obtained by (Modesto; Nebra, 2006). These suggestions are in accordance with papers presented by (Macedo, 2001) and (Ensinas et al., 2007). Then, in case the industry wants to sell electric energy to the grid, this work suggests investing in better technologies in this cogeneration systems, especially those operating with superheated steam higher than 60 bar.

As expected, the exergetic cost is increasing through the system to the final products. The generator products (points 55 to 57) are several flows and, then, according to the Proposition 4, the same unit exergetic cost must be assigned to all of them. Because of that, the unit exergetic cost of pumps takes the same value being $\kappa_{pumps}^* = 6.52$. As previously stated, from Proposition 2 exergetic cost of input resources as water will be assigned as one. In this manner, point 1 has an exergetic cost as to be one. However, this work considers the pump as adiabatic, then, all exergetic costs associated with inputs and generation are allocated to the output. Because of that, a remarkable increase in exergetic cost increase in point 2 is obtained. Note that, the return flow, point 41 has a unit exergetic cost less than point 2, but the deaerator product (point 3) will have a high exergetic cost unit. However, this effect is beneficial, because increases the inlet water temperature.

Table 6.8 presents the unit exergetic cost and relative cost difference of each control volume. E_f^* and E_p^* are the exergetic cost of fuel and product, respectively. κ_f^* , κ_p^* and, r_k are unit exergetic cost of fuel, product, and the relative cost difference, respectively. The ranking of the components according to their exergy destruction, exergetic cost, and relative cost difference shows which components should have priority in enhancement measures

to increase the efficiency of the whole system.

The component with the highest priority if found to be the boilers B_1 , B_2 , and B_3 with relative cost difference as to be 3.79, 3.79, and 3.58, respectively (see Figure 6.2). This high value of the relative cost difference is due to various irreversible factors such as the combustion process, convection, radiation losses, exergy destruction, and exhaust gases. In this particular system, to reduce the relative cost difference, the exhaust gases could be used to heat the water inlet temperature. Note that the unit exergetic cost of fuel is to be one because the exergetic cost of fuel is equal to the exergy of the fuel. These results are in accordance with the exergy analysis as previously presented.

Table 6.8 – Unit exergetic cost and relative cost difference of each control volumes

Control Volume	Names	E_f^*	E_p^*	κ_f^*	κ_p^*	r_k
—	—	kW		kW/kW		kW/kW
1	Pump ₁	9.8	9.8	6.525	6.736	0.032
2	Deaerator	5893	5893	5.043	6.127	0.215
3	Pump ₂	2284	2284	6.525	12.69	0.945
4	Distribution Chamber	8176	8176	7.162	7.162	0
5	B_1	36888	36888	1	4.79	3.79
6	B_2	92219	92219	1	4.785	3.79
7	B_3	101441	101441	1	4.584	3.58
8	Mixing Chamber ₁	133685	133685	4.841	4.841	0
9	Mixing Chamber ₂	116920	116920	4.661	4.661	0
10	Steam pipe	116920	116920	4.661	4.75	0.0190
11	T_1	8738	8738	4.89	10.86	1.222
12	T_2	11479	11479	4.89	8.368	0.711
13	T_3	4631	4631	4.89	9.837	1.012
14	T_4	3909	3909	4.89	8.444	0.727
15	T_5	4413	4413	4.89	8.667	0.773
16	T_6	4703	4703	4.89	11.46	1.344
17	T_7	44216	44216	4.75	6.525	0.374
18	Valve	14426	14426	4.89	6.863	0.404
19	Mixing Chamber ₃	156635	156635	4.953	5.018	0.013
20	Distribution Chamber ₂	156635	156635	5.018	5.018	0
21	Distillery	28365	28365	4.543	5.042	0.110
22	Desuperheater	125524	125524	5.018	5.041	0.005
23	Sugar Production	119435	119435	5.041	5.06	0.003
24	Distribution Chamber ₃	6.1	6088	5.041	5.041	0
25	Pump ₃	9.8	9.8	6.525	28.55	3.376
26	Distribution chamber ₄	121804	121804	4.841	4.89	0.010

27	Generator	44216	44216	6.525	6.525	0
----	-----------	-------	-------	-------	-------	---

The next component to improvement priority is Pump₃. The Pump₃ presents high values of relative cost difference because: (1.) This equipment is powered by a flow of electrical energy generated by the system itself; (2.) As previously stated, the exergetic cost is increasing through the system.

The others top-ranked components are the turbines of the system. As expected, \mathbb{T}_6 is the most inefficient component followed by \mathbb{T}_1 with relative cost difference as to be 1.344 and 1.222, respectively. These results are in accordance with the exergy analysis and exergetic cost analysis.

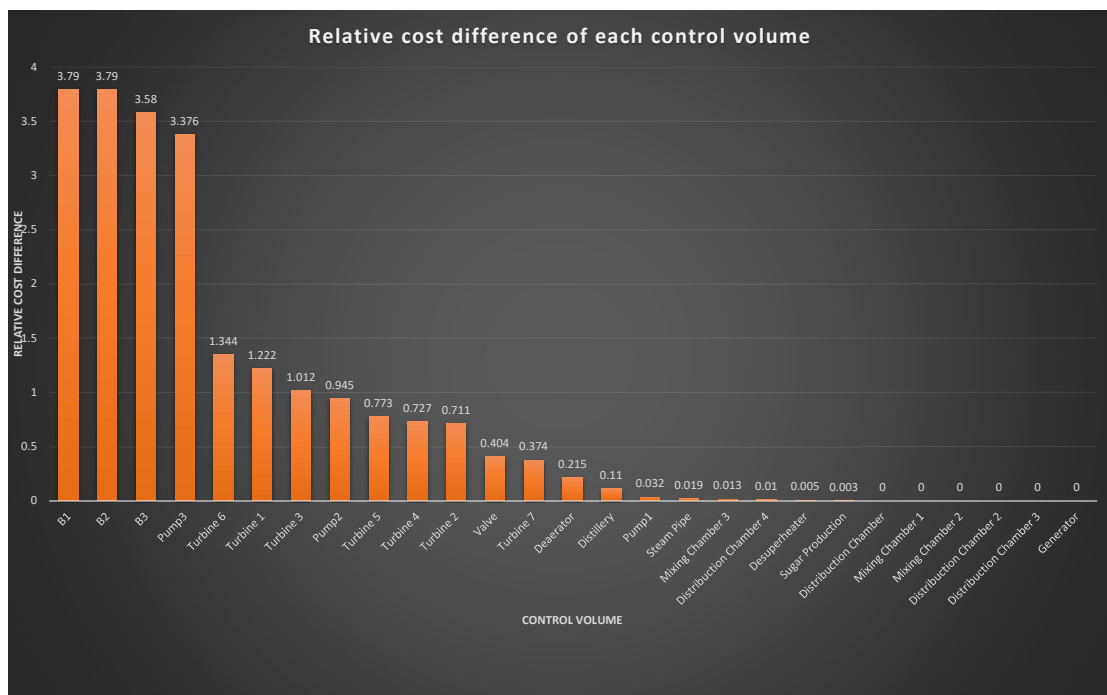


Figure 6.2 – Top-ranked Relative Cost Differences at each control volume in the system

Looking now to the expansion valve, although this component presents a low relative cost difference (0.404), it is purely dissipative and is suggested to be deactivated whenever is possible. As previously presented, the distribution chamber is a virtual device and its relative cost difference is zero because no changes in temperature and pressure are associated with this component, i.e., no irreversibility is associated with it. Thus, further modifications could be considered to enhance system efficiency.

6.3 Proposed modifications based on exergy and exergetic cost analyses

The major drawback of the system that can be changed with the minor investment are:

- I** In the exergy analysis, \mathbb{T}_6 presented the worst efficiency. As previously stated, this low efficiency is caused because this turbine is operating under partial-load conditions, single-stage operation, and old technologies. By the exergetic cost analysis, the product obtained by this turbine was found to be the highest.
- II** The expansion valve is a purely dissipative device and whenever possible it must be deactivated.
- III** In the exergetic cost analysis, \mathbb{T}_7 has a high unit exergetic cost considering electrical power as a product. Note that \mathbb{T}_7 is working at partial load conditions.

Based on the results obtained, this work proposes to analyze a new configuration with some modifications as:

- Change I** The replacement of \mathbb{T}_6 by an electric motor. It will be required a minor investment comparing to change operation conditions such as increasing boiler pressure and temperature. In this case, it would be necessary to change all turbines operating conditions, and a higher investment would be needed.
- Change II** Disable the expansion valve.
- Change III** As previously stated, the turbine \mathbb{T}_7 is operating at partial load conditions. With the changes proposed in **Change I** and **Change II**, this turbine has the ability to receive the working fluid from the \mathbb{T}_6 and the expansion Valve. With such modification \mathbb{T}_7 will be operating near at its nominal capacity. It is expected to generate more power and increase global cogeneration efficiency with these changes. With this measure, apart from the increase of efficiency, the system could sell the electric power surplus to the grid, increasing the competitiveness and profitability of the sugarcane power plant analyzed.

Increasing old technology efficiency systems is important to increase the competitiveness and profitability of the sugarcane power plant analyzed in this work. A new mass, energy, exergy, and exergetic cost balance were made to the proposed case.

6.4 Exergy and exergetic cost analyses of the proposed modifications

The properties for the proposed system are shown in Table 6.9. The consistency of mass, energy, exergy, and exergetic cost balance were verified. To perform these balance, further considerations were done:

1. \mathbb{T}_6 and valve were disabled.
2. Inlet flow rate of \mathbb{T}_6 and valve were sent to the mixing chamber₂ to be sent to the Turbine.
3. Inlet and outlet temperature at sugar production was considered the same.

Table 6.9 – Flow identification and thermodynamic properties of the proposed case

Flow	T [°C]	P[bar]	\dot{m} [(kg)/(s)]	h [(kJ)/(kg)]	s [(kJ)/(kg·K)]	e [(kJ)/(kg)]
1	25	1.01	9.722	104.9	0.3672	0
2	25	2.5	9.722	105.1	0.3672	0.1494
3	81.05	2.5	48.61	339.6	1.088	19.78
4	82.21	32	48.61	346.8	1.1	23.48
5	82.21	32	7.778	346.8	1.1	23.48
6	82.21	32	19.44	346.8	1.1	23.48
7	82.21	32	21.39	346.8	1.1	23.48
8	—	—	4.321	—	—	—
9	—	—	10.8	—	—	—
10	—	—	11.88	—	—	—
11	294	22	7.778	3004	6.692	1014
12	295	22	19.44	3007	6.696	1015
13	333	22	21.39	3095	6.846	1058
14	294.7	22	2.42	3006	6.695	1014
15	294.7	22	24.8	3006	6.695	1014
16	294.5	21.5	5.061	3007	6.707	1012
17	190	2.5	5.061	2848	7.358	658.8
18	290	21.2	6.481	2997	6.695	1005
19	160	2.6	6.481	2785	7.2	643.2
20	280	21.6	2.764	2972	6.642	996.1
21	168	2.7	2.764	2801	7.22	653.4
22	282	21.5	2.222	2977	6.653	997.9
23	152	2.6	2.222	2769	7.161	638.1
24	282	21.5	2.478	2977	6.653	997.9
25	153	2.5	2.478	2772	7.186	633.7
26	281	21.5	2.889	2975	6.649	996.8
27	—	—	—	—	—	—
28	294.7	22	2.908	3006	6.695	1014
29	—	—	—	—	—	—
30	320.9	22	29.61	3067	6.8	1044
31	314	21.5	29.61	3052	6.786	1034
32	152	2.7	29.61	2768	7.142	642.9
33	157.4	2.5	48.61	2781	7.207	636.5
34	157.4	2.5	38.89	2781	7.207	636.5
35	128	2.5	39.94	2718	7.056	618.7
36	95	2.5	39.94	398.2	1.25	30.01
37	95	2.5	1.055	398.2	1.25	30.01
38	95.33	3	1.055	399.6	1.254	30.32
39	157.4	2.5	9.722	2781	7.207	636.5
40	127.4	2.5	9.722	535.3	1.607	60.71
41	95	2.5	38.89	398.2	1.25	30.01

The schematic proposed modification case can be seen in Figure 6.3

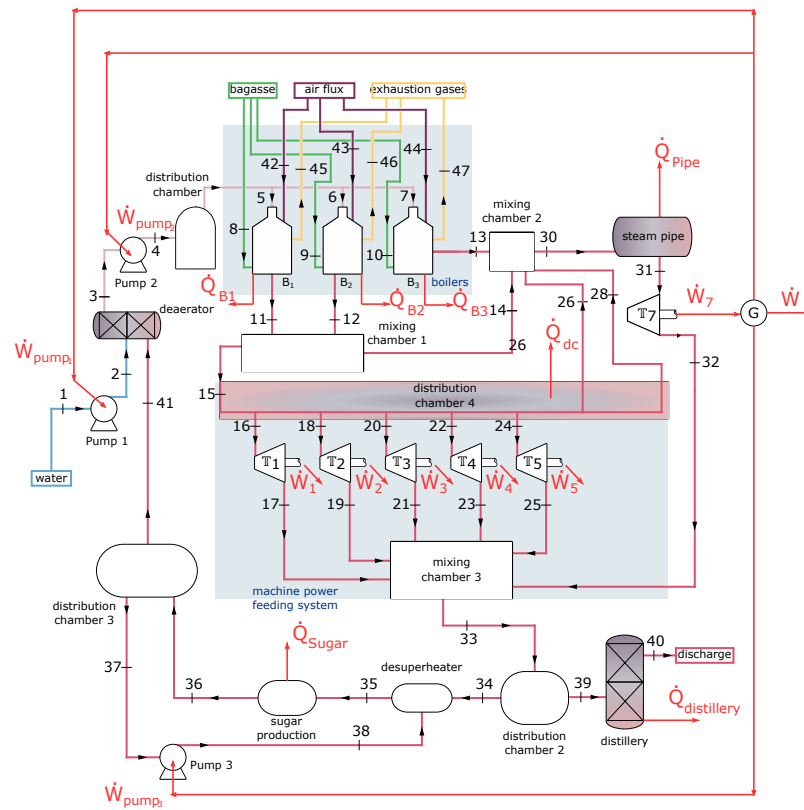


Figure 6.3 – Proposed modification plant

A comparison between the real case exergy destruction and proposed case is presented at Table 6.10.

Table 6.10 – A comparison between the exergy destruction on the analysed cogeneration system and the proposed case.

Equipment	Real Case		Proposed Case	
	\dot{E}_D [kW]	\dot{E}_D [%]	\dot{E}_D [kW]	\dot{E}_D [%]
B ₁	30890	15.32	30890	15.40
B ₂	77217	38.30	77217	38.50
B ₃	84628	41.98	84628	42.20
T ₁	982.6	0.48	982.6	0.48
T ₂	975.7	0.48	975.7	0.48
T ₃	476.3	0.23	476.3	0.23
T ₄	336.5	0.16	336.5	0.16
T ₅	393.3	0.19	393.3	0.19
T ₆	551.5	0.27	—	—
T ₇	2533	1.25	3149	1.57
Expansion Valve	848.10	0.42	—	—
In other components	1737	0.86	1503	0.75
Total	201569	100	200551	100

The results has revealed that 1018 kW of exergy destruction was reduced in the proposed case. Table 6.11 shows the effect of proposed case in net power output and efficiencies on energy and exergy base. The

Table 6.11 – Effect of proposed changes on net power output, net electrical efficiency on energy and exergy based and cogeneration efficiency on energy and exergy based.

	Real Case	Proposed Case	
Net Power output	10265.50	11363.9	[kW]
Surplus Energy	—	1098.4	[kW]
η_{el}	3.10	3.82	[%]
ϵ_{el}	2.70	3.32	[%]
η_{cog}	62.56	62.63	[%]
ϵ_{cog}	17.14	17.47	[%]

calculated electrical efficiency on energy and exergy base for both analyzed system case is presented in Table 6.11. The energy and exergy electrical efficiency present very similar values (3.10% versus 2.70% to the real case — 3.82% versus 3.32% to the proposed case). This happen because only electric power production is considered. Considering heat, mechanical and electric power, substantially different values emerge (62.56% versus 17.14% to the real case — 62.63% versus 17.47% to the proposed case). When comparing the real case and proposed case, slightly higher values of these factors are achieved for the proposed case. This shows that the modifications proposed here makes the system more efficient, since more electric energy is generated and less exergy is destruc-

ted. Results shows that positive results were obtained with the proposed changes since there is a surplus energy 1098.4kW, which is 10.69% greater than the power output of the real case, which can be sold to the grid.

The exergetic cost were evaluated to the new proposed case and compared to the reference case. Detailed results of exergetic cost E^* of each flow and unit exergetic cost κ^* are presented in Table 6.12. The results presented in the exergetic cost analysis is interesting to observe details of the system behavior.

Table 6.12 – Exergy, exergetic cost, and unitary exergetic cost of each flow for the proposed case

Flow	E [kW]	E* [kW]	$\kappa^* \frac{[\text{kW}]}{[\text{kW}]}$	Flow	E [kW]	E* [kW]	$\kappa^* \frac{[\text{kW}]}{[\text{kW}]}$
1	—	—	1	33	30939	150513	4.865
2	1.453	10.29	7.081	34	24751	120410	4.865
3	961.726	5704	5.931	35	24713	120575	4.879
4	1142	8105	7.099	36	1199	5848	4.879
5	182.702	1297	7.099	37	31.66	154.4	4.879
6	456.684	3242	7.099	38	31.99	164.7	5.15
7	502.324	3566	7.099	39	6188	30103	4.865
8	36888	36888	1	40	590.134	2871	4.865
9	92219	92219	1	41	1167	5694	4.879
10	101441	101441	1	42	—	—	1
11	7884	38184	4.844	43	—	—	1
12	19731	95461	4.838	44	—	—	1
13	22633	105007	4.64	45	—	—	0
14	2454	11879	4.84	46	—	—	0
15	25160	121766	4.84	47	—	—	0
16	5121	25035	4.888	48	804.327	8735	10.86
17	3334	16299	4.888	49	1372	11475	8.365
18	6516	31852	4.888	50	470.8	4630	9.834
19	4168	20377	4.888	51	463	3908	8.441
20	2753	13458	4.888	52	509.060	4411	8.665
21	1806	8828	4.888	53	—	—	—
22	2218	10840	4.888	54	8427	54979	6.524
23	1418	6932	4.888	55	1.500	10.29	6.858
24	2473	12086	4.888	56	350	2400	6.858
25	1570	7675	4.888	57	1.500	10.29	6.858
26	2880	14076	4.888	58	—	—	0
27	—	—	—	59	—	—	0
28	2950	14420	4.888	60	—	—	0
29	—	—	—	61	—	—	0
30	30914	145381	4.703	62	23423	114727	4.898
31	30610	145381	4.749	63	5581	27231	4.879
32	19034	90402	4.749	64	7663	55373	6.858

The values of unit exergetic cost of input resources as water, bagasse, and air are to be 1 because the cost of the resources entering the plant must be equivalent to their exergy. The most remarkable reduce can be seen in:

- Superheated steam from $\kappa_{27}^* (\mathbb{C}_0) = 4.89$ to $\kappa_{27}^* (\mathbb{C}_1) = 0$
- Superheated steam from $\kappa_{29}^* (\mathbb{C}_0) = 6.863$ to $\kappa_{29}^* (\mathbb{C}_1) = 0$
- Work $\kappa_{53}^* (\mathbb{C}_0) = 11.5$ to $\kappa_{53}^* (\mathbb{C}_1) = 0$

In the new system, as previously stated, the expansion valve and \mathbb{T}_6 were disabled. The exergetic cost of the boilers was the same as the base case because no changes were done to these devices. The proposed changes reduced the cost formation through the system, decreasing about 8.54% comparing to the reference case (see Table 6.13). In this system, the only point where the unit cost was slightly high was in κ_{30}^* . This happened because the exergy destruction in the proposed at this device were slightly high comparing to the reference device. Note that the only point where the unit exergetic cost was slightly high in the proposed case was in This happen because the exergy destruction in the proposed case at this device were slightly high comparing to the reference device.

Table 6.13 – A comparison between the unit exergetic cost of the reference system and the proposed case.

Flow	κ_a^*	κ_b^*	$\Delta \kappa^*$	Flow	κ_a^*	κ_b^*	$\Delta \kappa^*$
1	1	1	0	33	5.018	4.862	-0.156
2	6.736	6.733	-0.003	34	5.018	4.862	-0.156
3	6.127	5.928	-0.199	35	5.041	4.877	-0.164
4	7.162	6.993	-0.169	36	5.041	4.877	-0.164
5	7.162	6.993	-0.169	37	5.041	4.877	-0.164
6	7.162	6.993	-0.169	38	5.237	5.132	-0.105
7	7.162	6.993	-0.169	39	5.018	4.862	-0.156
8	1	1	0	40	5.018	4.862	-0.156
9	1	1	0	41	5.041	4.877	-0.164
10	1	1	0	42	1	1	0
11	4.845	4.841	-0.004	43	1	1	0
12	4.84	4.836	-0.004	44	1	1	0
13	4.641	4.637	-0.004	45	0	0	0
14	4.841	4.837	-0.004	46	0	0	0
15	4.841	4.837	-0.004	47	0	0	0
16	4.89	4.886	-0.004	48	10.86	10.85	-0.01
17	4.89	4.886	-0.004	49	8.368	8.361	-0.007
18	4.89	4.886	-0.004	50	9.837	9.829	-0.008
19	4.89	4.886	-0.004	51	8.444	8.437	-0.007
20	4.89	4.886	-0.004	52	8.667	8.66	-0.007

21	4.89	4.886	-0.004	53	11.5	—	-11.46
22	4.89	4.886	-0.004	54	6.525	6.521	-0.004
23	4.89	4.886	-0.004	55	6.525	6.521	-0.004
24	4.89	4.886	-0.004	56	6.525	6.521	-0.004
25	4.89	4.886	-0.004	57	6.525	6.521	-0.004
26	4.89	4.886	-0.004	58	0	0	0
27	4.89	—	-4.89	59	0	0	0
28	4.89	4.886	-0.004	60	0	0	0
29	6.863	—	-6.863	61	0	0	0
30	4.661	4.7	0.039	62	5.06	4.895	-0.165
31	4.75	4.747	-0.003	63	5.042	4.877	-0.165
32	4.75	4.747	-0.003	64	6.525	6.521	-0.004
$ \Delta \kappa_{\text{total}}^* = 25.9$							

κ_a^* is the unit exergetic cost at the reference system

κ_b^* is the unit exergetic cost at proposed case

$|\Delta \kappa_{\text{total}}^*|$ is module of $\sum_{j=1}^{j=64} \kappa_b^* - \sum_{j=1}^{j=64} \kappa_a^*$

Table 6.14 presents the unit exergetic cost and relative cost difference of each control volume. E_f^* and E_p^* are the exergetic cost of fuel and product, respectively. κ_f^* , κ_p^* and, r_k are unit exergetic cost of fuel, product, and the relative cost difference, respectively.

Table 6.14 – Unit exergetic cost and relative cost difference of all control volumes from the proposed case

Control Volume	Names	E_f^*	E_p^*	κ_f^*	κ_p^*	r_k
—	—	kW		kW/kW		kW/kW
1	Pump ₁	9.8	9.8	6.521	6.733	0.032
2	Deaerator	5701	5701	4.879	5.928	0.215
3	Pump ₂	2282	2282	6.521	12.69	0.945
4	Distribution Chamber	7983	7983	6.993	6.993	0
5	B ₁	36888	36888	1	4.79	3.79
6	B ₂	92219	92219	1	4.785	3.79
7	B ₃	101441	101441	1	4.584	3.58
8	Mixing Chamber ₁	133577	133577	4.837	4.837	0
9	Mixing Chamber ₂	145307	145307	4.7	4.7	0
10	Steam pipe	145307	145307	4.7	4.747	0.009
11	T ₁	8731	8731	4.886	10.85	1.222
12	T ₂	11469	11469	4.886	8.361	0.711
13	T ₃	4627	4627	4.886	9.829	1.012
14	T ₄	3906	3906	4.886	8.437	0.727

15	T_5	4409	4409	4.886	8.66	0.773
16	T_6	—	—	—	—	—
17	T_7	54951	54951	4.747	6.521	0.373
18	Valve	—	—	—	—	—
19	Mixing Chamber ₃	150437	150437	4.801	4.862	0.013
20	Distribution Chamber ₂	150437	150437	4.862	4.862	0
21	Distillery	27217	27217	4.399	4.877	0.109
22	Desuperheater	120513	120513	4.863	4.877	0.003
23	Sugar Production	114668	114668	4.877	4.895	0.004
24	Distribution Chamber ₃	5845	5845	4.877	4.877	0
25	Pump ₃	9.8	9.8	6.521	29.63	3.544
26	Distribution chamber ₄	121705	121705	4.837	4.886	0.011
27	Generator	54951	54951	6.521	6.521	0

As previously stated, the ranking of the components according to their exergy destruction, exergetic cost, and relative cost difference shows which components should have priority in enhancement measures to increase the efficiency of the whole system.

The components with the highest relative cost difference are still the boilers, with relative cost differences as to be 3.79, 3.79, and 3.58, respectively. The reasons for that high relative cost difference were previously presented. The next component to improvement priority is Pump₃. Note that in the proposed case, the relative cost difference of the Pump₃ was slightly higher than the base case. This happened because of an increase in the exergy destruction.

The other top-ranked components are the turbines of the system. These devices are operating at partial load conditions. Also, these devices by the exergy and exergetic cost analysis have to be proved to be inefficient.

As a result of this study, exergy and exergetic cost analysis were performed. According to the results obtained, the base case is presented, then, the proposed improvement is presented. This system has been proved to be inefficient. Although the modifications proposed here, the increase in global efficiency was low. Thus, further modifications could be considered to enhance system efficiency. Based on previous works, to increase the global efficiency of the system, it is suggested that the boilers could operate with better technologies, such as those producing super-heated steam pressure higher than 60 bar and work with an extraction controlled steam turbine to supply heat to sugar and alcohol production process.

7 CONCLUSION AND FUTURE STUDIES

Energy, exergy, and exergetic cost analyses for a sugarcane power plant fueled with sugarcane bagasse, which produce 10,265.50 kW of net mechanical and electric power output were carried out. The boilers presented an exergy destruction rate of 168,661.00 kW, representing 73.17% of the fuel exergy. These destruction are associated to moisture in the fuel, energy transfer by convection and radiation from the boilers surface and exhaust gases.

The exergy destruction rate through exhaust gases is 33,644.00 kW representing 14.59% of the fuel exergy. It could be reduced by decreasing the exhaust gases temperature and also it could be used for increasing the water temperature that is sent to the boilers. As results of these losses the energy efficiency of the B_1 to B_3 is found to be quite low due to partial load 64.3%, 64.4% and 66.5% respectively, when compared to the nominal conditions which is 86.0%.

The results has also shown that destruction of the fuel exergy was: Exergy destruction in the turbines 2.71%, exergy destruction in the mixing chambers 1.25%, exergy destruction in the expansion valve 0.36%, exergy destruction in the desuperheater 0.04% and the exergy destruction in other componets 5.34%. These destructions could be reduced, for example, by bringing down the temperature difference of the working fluid at each mix chamber, in the dessuperheater could be decreased if the energy transfer temperature of the working fluid could be reduced further. The exergy utilization in sugarcane production, distillery and, net power output are 10.24%, 2.44%, and 4.49%, respectively. The results shows also that the expansion valve is a purely dissipative device and its exergy destruction could be reduced by sending its working fluid to T_7 .

The exergy analysis has shown that the cogeneration system is operating at 17.14% of global exergy efficiencies. This efficiency is found to be low because this system is operating with old technology as well as low pressure and temperature conditions (see Table 6.1). Cogeneration systems using better technologies are being operated with superheated steam pressure higher than 60 bars.

The exergetic cost analysis allows estimating the exergy needed to produce each flow. The unit exergetic cost of fuel, such as water and bagasse, is to be 1. The results show that the cost formation through the system to the final product is increasing. Because of its old technology and inefficiency, unit exergetic cost considering electrical power a product is almost 3 times higher than others cogeneration system using better technologies.

The exergetic cost can rank the top components, according to their exergy destruction, which should have priority in enhancement measures to increase the efficiency of the whole system. The top components with the highest priority were the boilers. These results were expected because of various factors such as the combustion process, convection, radiation losses, and losses of exergy in the exhaust gases. These results are in accordance with the exergy analysis. The other top-ranked components are the turbines of the system, special attention must be given to the most inefficient device, which was the T_6 . This result was expected since from the exergy analysis this turbine has been proved to be the most inefficient. The expansion valve present low relative cost difference; however, is a purely dissipative device and whenever is possible it is suggest to be deactivated.

Therefore, modifications could be considered to enhance system efficiency, based on the results obtained by the exergy and exergetic cost analysis. These modifications was: (1.) Disabling the expansion valve

and (2.) The replacement of T_6 by an electric motor. With such modifications, the working fluid of both (1.) and (2.) was sent to T_7 .

When the proposed system was simulated the results revealed that a reduction of 3,216 kW in the exergy destruction and a surplus energy of 1098.4 kW was obtained, which is 10.69% greater than the power output of the real case. This surplus energy is considered environmentally friendly since the emissions to the air are the same as the real case. The results have also shown that the global exergy efficiency has increased 1.92% with these modifications.

The theory of exergetic cost analysis shows the effect of cost formation through the systems. With the proposed system, the cost formation through the cogeneration plant has decreased by 8.54% comparing to the base case.

The modifications proposed here have been proved to be effective from a thermodynamics point of view and can be implemented to make the surplus energy available for sale to the grid as a future project. These modifications are based only on the change of operating conditions and do not require high investments to change all cogeneration system configuration i.e., new boilers and new turbines which operate at increased pressure and temperature working conditions.

Recommendations for future work are:

1. Carry out a feasibility study of replacing boilers operating with pressure higher than 60 bar and replacing the back pressure steam turbines that are responsible for driving mechanical equipment by electric motors. In addition, the replacement of the back pressure steam turbine coupled to the generator by a controlled extraction steam turbine.
2. Realize an economic and exergoeconomic analysis of all scenarios to obtain information such as the product cost rate, the Levelized cost of the products, annual operating costs, the cost to be paid for the grid electricity, and payback ratio.
3. Based on the important parameters, building a computer program to evaluate all parameters obtained by the exergetic and exergoeconomic analysis in the cogeneration systems in the sugarcane sector to monitor their plant to increase their system efficiency.
4. Suggest the industry realize an exergetic and exergoeconomic analysis of the sugarcane and alcohol production.
5. Evaluate an exergoenvironmental analysis to identify the location, the magnitude and the causes of environmental impact of all scenarios.
6. The use of optimization methods to identify the conditions that given maximum or minimum values of the thermodynamic system.

BIBLIOGRAPHY

- Aghbashlo, M.; Mandegari, M.; Tabatabaei, M.; Farzad, S.; Soufiyan, M. M.; Görgens, J. F. Exergy analysis of a lignocellulosic-based biorefinery annexed to a sugarcane mill for simultaneous lactic acid and electricity production. **Energy**, v. 149, p. 623–638, 2018.
- Aghbashlo, M.; Tabatabaei, M.; Hosseini, S. S.; Dashti, B. B.; Soufiyan, M. M. Performance assessment of a wind power plant using standard exergy and extended exergy accounting (eea) approaches. **Journal of Cleaner Production**, v. 171, p. 127–136, 2018.
- Arnao, J. H. S. **Caldeiras aquatubulares de bagaço—estudo do sistema de recuperação de energia**. Tese (Doutorado) — Tese de Doutorado em Engenharia Mecânica, Universidade Estadual de Campinas, 2007.
- Basu, P. **Combustion and gasification in fluidized beds**. [S.l.]: CRC press, 2006.
- Battle, E. A. O.; Palacio, J. C. E.; Lora, E. E. S.; Bortoni, E. D. C.; Nogueira, L. A. H.; Caballero, G. E. C.; Julio, A. A. V.; Escorcia, Y. C. Energy, economic, and environmental assessment of the integrated production of palm oil biodiesel and sugarcane ethanol. **Journal of Cleaner Production**, v. 311, p. 127638, 2021.
- Bejan, A.; Tsatsaronis, G.; Moran, M. J. **Thermal design and optimization**. [S.l.]: John Wiley & Sons, 1995.
- Biggs, N.; Lloyd, E. K.; Wilson, R. J. **Graph Theory, 1736-1936**. [S.l.]: Oxford University Press, 1986.
- Bizzo, W. A.; Lenço, P. C.; Carvalho, D. J.; Veiga, J. P. S. The generation of residual biomass during the production of bio-ethanol from sugarcane, its characterization and its use in energy production. **Renewable and Sustainable Energy Reviews**, v. 29, p. 589–603, 2014.
- Callen, H. B. **Thermodynamics and an Introduction to Thermostatistics**. [S.l.]: American Association of Physics Teachers, 1998.
- Camargo, J. M.; Gallego-Rios, J. M.; Neto, A. M. P.; Antonio, G. C.; Modesto, M.; Leite, J. T. Characterization of sugarcane straw and bagasse from dry cleaning system of sugarcane for cogeneration system. **Renewable Energy**, v. 158, p. 500–508, 2020.
- Cavalcanti, E. J.; Carvalho, M.; Azevedo, J. L. Exergoenvironmental results of a eucalyptus biomass-fired power plant. **Energy**, v. 189, p. 116188, 2019.
- Cavalcanti, E. J.; Carvalho, M.; Silva, D. R. da. Energy, exergy and exergoenvironmental analyses of a sugarcane bagasse power cogeneration system. **Energy conversion and management**, v. 222, p. 113232, 2020.
- Center, B. P. Annual energy outlook 2020. **Energy Information Administration, Washington, DC**, 2020.
- Gama Cerqueira, S. A. A. da; Nebra, S. A. Cost attribution methodologies in cogeneration systems. **Energy Conversion and Management**, v. 40, n. 15-16, p. 1587–1597, 1999.
- Chum, H. L.; Warner, E.; Seabra, J. E.; Macedo, I. C. A comparison of commercial ethanol production systems from brazilian sugarcane and us corn. **Biofuels, bioproducts and biorefining**, v. 8, n. 2, p. 205–223, 2014.
- CONAB. Acompanhamento da safra brasileira de cana-de-acucar. **Terceiro Levantamento**, n. 1, p. 62, 2020.
- Cortes-Rodriguez, E. F.; Nebra, S. A.; Sosa-Arnao, J. H. Experimental efficiency analysis of sugarcane bagasse boilers based on the first law of thermodynamics. **Journal of the Brazilian Society of Mechanical Sciences and Engineering**, v. 39, n. 3, p. 1033–1044, 2017.
- Cortes-Rodriguez, E. F.; Nebra, S. A.; Sosa-Arnao Juan Harold, P. B. R. Experimental efficiency analysis of sugarcane bagasse boilers based on the first and second law of thermodynamics. **Efficiency, cost optimization, simulation and environmental impact of energy systems**, v. 39, n. 3, p. 1033–1044, 2017.
- Dadak, A.; Aghbashlo, M.; Tabatabaei, M.; Najafpour, G.; Younesi, H. Sustainability assessment of photobiological hydrogen production using anaerobic bacteria (*rhodospirillum rubrum*) via exergy concept: Effect of substrate concentrations. **Environmental Progress & Sustainable Energy**, v. 35, n. 4, p. 1166–1176, 2016.

- Dantas, D. N. **Uso da biomassa de cana-de-açúcar para geração de energia elétrica: análise energética, exergetica e ambiental de sistemas de cogeração em sucroalcooleiras do interior paulista**. Tese (Doutorado) — Universidade de São Paulo, 2010.
- Dincer, I. Exergy as a potential tool for sustainable drying systems. **Sustainable Cities and Society**, v. 1, n. 2, p. 91–96, 2011.
- Dincer, I.; Abu-Rayash, A. Chapter 5 - community energy systems. In: Dincer, I.; Abu-Rayash, A. (Ed.). **Energy Sustainability**. Academic Press, 2020. p. 101–118. ISBN 978-0-12-819556-7. Disponível em: <<https://www.sciencedirect.com/science/article/pii/B978012819556700005X>>.
- Dincer, I.; Rosen, M. A. Thermodynamic aspects of renewables and sustainable development. **Renewable and Sustainable Energy Reviews**, v. 9, n. 2, p. 169–189, 2005.
- Directive, E. E. Eu energy efficiency directive 2012/27/eu. **Journal reference**, v. 50, n. 315, p. 1–56, 2012.
- Dogbe, E. S.; Mandegari, M. A.; Görgens, J. F. Exergetic diagnosis and performance analysis of a typical sugar mill based on aspen plus® simulation of the process. **Energy**, v. 145, p. 614–625, 2018.
- El-Sayed, Y.; Evans, R. Thermoeconomics and the design of heat systems. 1970.
- El-Sayed, Y. M. **The thermoeconomics of energy conversions**. [S.l.]: Elsevier, 2013.
- Enrico, S.; Wall, G. A brief commented history of exergy from the beginnings to 2004. **International Journal of Thermodynamics**, v. 10, 03 2007.
- Ensinas, A. V.; Nebra, S. A.; Lozano, M. A.; Serra, L. M. Analysis of process steam demand reduction and electricity generation in sugar and ethanol production from sugarcane. **Energy Conversion and Management**, v. 48, n. 11, p. 2978–2987, 2007.
- EPE. Análise de conjuntura dos biocombustíveis. **Empresa de Pesquisa Energetica**, v. 15, 2015.
- EPE. Analysis of biofuels current outlook. **Ministry of Mines and Energy**, v. 19, n. 19, p. 1–80, 2019.
- EPE. **Empresa de Pesquisa Energética. Balanço Energético Nacional (BEN)**. 2019. Available at <<https://www.epe.gov.br/pt>>.
- EPE, B. E. Balanço energético nacional. **EPE**, 2021.
- Erdem, H. H.; Akkaya, A. V.; Cetin, B.; Dagdas, A.; Sevilgen, S. H.; Sahin, B.; Teke, I.; Gungor, C.; Atas, S. Comparative energetic and exergetic performance analyses for coal-fired thermal power plants in turkey. **International Journal of Thermal Sciences**, v. 48, n. 11, p. 2179–2186, 2009.
- Erlach, B.; Serra, L.; Valero, A. Structural theory as standard for thermoeconomics. **Energy Conversion and Management**, v. 40, n. 15-16, p. 1627–1649, 1999.
- Evans, R. B.; Crellin, G. L.; Tribus, M. Thermoeconomic considerations of sea water demineralization. In: **Principles of desalination**. [S.l.]: Academic Press New York and London, 1966. p. 21–75.
- Ferreira, L.; Otto, R.; Silva, F.; De Souza, S.; De Souza, S.; Junior, O. A. Review of the energy potential of the residual biomass for the distributed generation in brazil. **Renewable and Sustainable Energy Reviews**, v. 94, p. 440–455, 2018.
- Frangopoulos, C. A. Thermo-economic functional analysis and optimization. **Energy**, v. 12, n. 7, p. 563–571, 1987.
- Frías, M.; Villar, E.; Savastano, H. Brazilian sugar cane bagasse ashes from the cogeneration industry as active pozzolans for cement manufacture. **Cement and concrete composites**, v. 33, n. 4, p. 490–496, 2011.
- Fukushima, N. A.; Palacios-Bereche, M. C.; Palacios-Bereche, R.; Nebra, S. A. Energy analysis of the ethanol industry considering vinasse concentration and incineration. **Renewable Energy**, v. 142, p. 96–109, 2019.
- Gaggioli, R. A. Second law analysis for process and energy engineering. 1983.
- Ganapathy, V. **Steam plant calculations manual**. [S.l.: s.n.], 1994.

Gholamian, E.; Mahmoudi, S.; Zare, V. Proposal, exergy analysis and optimization of a new biomass-based cogeneration system. **Applied Thermal Engineering**, v. 93, p. 223–235, 2016.

Hugot, E. **Handbook of cane sugar engineering**. [S.l.]: Elsevier, 2014.

IEA. **World Energy Outlook**. 2018. Available at <<https://www.iea.org/data-and-statistics/charts?energy=electricity&type=pie>>.

IEA. **World Energy Outlook**. 2019. Available at <<https://www.iea.org/reports/world-energy-outlook-2019>>.

ISO. The sugar market. **International Sugar Organization**, n. 1, p. 1, 2022.

Kamate, S.; Gangavati, P. Exergy analysis of cogeneration power plants in sugar industries. **Applied Thermal Engineering**, v. 29, n. 5-6, p. 1187–1194, 2009.

Karimi, M. H.; Chitgar, N.; Emadi, M. A.; Ahmadi, P.; Rosen, M. A. Performance assessment and optimization of a biomass-based solid oxide fuel cell and micro gas turbine system integrated with an organic rankine cycle. **International Journal of Hydrogen Energy**, v. 45, n. 11, p. 6262–6277, 2020.

Khatriwada, D.; Seabra, J.; Silveira, S.; Walter, A. Power generation from sugarcane biomass—a complementary option to hydroelectricity in nepal and brazil. **Energy**, v. 48, n. 1, p. 241–254, 2012.

Kim, S.-M.; Oh, S.-D.; Kwon, Y.-H.; Kwak, H.-Y. Exergoeconomic analysis of thermal systems. **Energy**, v. 23, n. 5, p. 393–406, 1998.

Klein, S.; Alvarado, F. Ees - engineering equation solver. **Academic Version**, v. 1446, 2020.

Kotas, T. J. **The exergy method of thermal plant analysis**. [S.l.]: Elsevier, 2013.

Kumar, R. A critical review on energy, exergy, exergoeconomic and economic (4-e) analysis of thermal power plants. **Engineering Science and Technology, an International Journal**, v. 20, n. 1, p. 283–292, 2017.

Lazzaretto, A.; Tsatsaronis, G. On the quest for objective equations in exergy costing. In: AES. **Proceedings of the ASME advanced energy systems division**. [S.l.], 1997. v. 37, p. 197–210.

Leal, M. R. L.; Galdos, M. V.; Scarpere, F. V.; Seabra, J. E.; Walter, A.; Oliveira, C. O. Sugarcane straw availability, quality, recovery and energy use: a literature review. **Biomass and Bioenergy**, v. 53, p. 11–19, 2013.

Lira, J. D.; Gallo, W. L. R. Exergy analysis of an operating biomass thermal power plant. **34th international conference on efficiency, cost, optimization, simulation and environmental impact of energy system ECOS**, 2021.

López, J. C.; Escobar, A.; Cárdenas, D. A.; Restrepo, Á. Parabolic trough or linear fresnel solar collectors? an exergy comparison of a solar-assisted sugarcane cogeneration power plant. **Renewable Energy**, v. 165, p. 139–150, 2021.

López, J. C.; Restrepo, Á.; Bazzo, E. Exergy analysis of the annual operation of a sugarcane cogeneration power plant assisted by linear fresnel solar collectors. **Journal of Solar Energy Engineering**, v. 140, n. 6, 2018.

Lozano, M.; Valero, A. Theory of the exergetic cost. **Energy**, v. 18, n. 9, p. 939–960, 1993.

Macedo, I. d. C. Sugar cane residues for power generation in the sugar/ethanol mill in brazil. **Energy for Sustainable Development**, n. 1, p. 77–82, 2001.

Mauricio, T. Energia termelétrica, gás natural, biomassa, carvão, nuclear. **Tolmasquim(coord) - EPE**, 2016.

Milão, R. d. F. D.; Carminati, H. B.; Queiroz, F. A. Ofélia de; Medeiros, J. L. de. Thermodynamic, financial and resource assessments of a large-scale sugarcane-biorefinery: prelude of full bioenergy carbon capture and storage scenario. **Renewable and Sustainable Energy Reviews**, v. 113, p. 109251, 2019.

Modesto, M.; Nebra, S. Analysis of a repowering proposal to the power generation system of a steel mill plant through the exergetic cost method. **Energy**, v. 31, n. 15, p. 3261–3277, 2006.

Moran, M. J. Fundamentals of exergy analysis and exergy-aided thermal systems design. In: **Thermodynamic optimization of complex energy systems**. [S.l.]: Springer, 1999. p. 73–92.

Moran, M. J.; Shapiro, H. N.; Boettner, D. D.; Bailey, M. B. **Fundamentals of engineering thermodynamics**. [S.l.]: John Wiley & Sons, 2010.

Neto, J. V. S.; Gallo, W. L. Potential impacts of vinasse biogas replacing fossil oil for power generation, natural gas, and increasing sugarcane energy in brazil. **Renewable and Sustainable Energy Reviews**, v. 135, p. 110281, 2021.

Ometto, A. R.; Hauschild, M. Z.; Roma, W. N. L. Lifecycle assessment of fuel ethanol from sugarcane in brazil. **The international journal of life cycle assessment**, v. 14, n. 3, p. 236–247, 2009.

Ortiz, P. A. S.; Marechal, F.; Oliveira Junior, S. de. Exergy assessment and techno-economic optimization of bioethanol production routes. **Fuel**, v. 279, p. 118327, 2020.

Oyekale, J.; Petrollese, M.; Heberle, F.; Brüggemann, D.; Cau, G. Exergetic and integrated exergoeconomic assessments of a hybrid solar-biomass organic rankine cycle cogeneration plant. **Energy Conversion and Management**, v. 215, p. 112905, 2020.

Palacios-Bereche, M. C.; Palacios-Bereche, R.; Nebra, S. A. Comparison through energy, exergy and economic analyses of two alternatives for the energy exploitation of vinasse. **Energy**, v. 197, p. 117231, 2020.

Palacios-Bereche, R.; Mosqueira-Salazar, K. J.; Modesto, M.; Ensinas, A. V.; Nebra, S. A.; Serra, L. M.; Lozano, M.-A. Exergetic analysis of the integrated first-and second-generation ethanol production from sugarcane. **Energy**, v. 62, p. 46–61, 2013.

Paredes-Sánchez, J. P.; Míguez, J.; Blanco, D.; Rodríguez, M.; Collazo, J. Assessment of micro-cogeneration network in european mining areas: A prototype system. **Energy**, v. 174, p. 350–358, 2019.

Pérez, Á. A. D.; Palacio, J. C. E.; Venturini, O. J.; Reyes, A. M. M.; Orozco, D. J. R.; Lora, E. E. S.; Olmo, O. A. A. del. Thermodynamic and economic evaluation of reheat and regeneration alternatives in cogeneration systems of the brazilian sugarcane and alcohol sector. **Energy**, v. 152, p. 247–262, 2018.

Picoli, J. F.; Seabra, J. E. A.; MATSUURA, M.; Cavalett, O.; Chagas, M. F. Desempenho ambiental da cana-de-açúcar: avaliação regional do ciclo de vida. In: In: CONGRESSO BRASILEIRO DE PLANEJAMENTO ENERGÉTICO, 10., 2016. Gramado **Embrapa Meio Ambiente-Artigo em anais de congresso (ALICE)**. [S.l.], 2016.

Pina, E. A.; Palacios-Bereche, R.; Chavez-Rodriguez, M. F.; Ensinas, A. V.; Modesto, M.; Nebra, S. A. Reduction of process steam demand and water-usage through heat integration in sugar and ethanol production from sugarcane—evaluation of different plant configurations. **Energy**, v. 138, p. 1263–1280, 2017.

Prestipino, M.; Salmeri, F.; Cucinotta, F.; Galvagno, A. Thermodynamic and environmental sustainability analysis of electricity production from an integrated cogeneration system based on residual biomass: A life cycle approach. **Applied Energy**, v. 295, p. 117054, 2021.

Rahman, M. M.; Velayutham, E. Renewable and non-renewable energy consumption-economic growth nexus: new evidence from south asia. **Renewable Energy**, v. 147, p. 399–408, 2020.

Rein, P. et al. **Cane sugar engineering**. [S.l.]: Verlag Dr. Albert Bartens KG, 2016.

Rodriguez, E. F. C. Determinação de eficiência de caldeiras de bagaço de cana de açúcar: identificação de oportunidades de melhoramento. **Universidade Federal do ABC, Dissertação de mestrado**, 2014.

Da Rosa, A. V.; Ordonez, J. C. **Fundamentals of renewable energy processes**. [S.l.]: Academic Press, 2021.

Rosen. Exergy analysis of waste emissions. **International Journal of Energy Research**, v. 23, n. 13, p. 1153–1163, 1999.

Rosen, M.; Dincer, I. Exergy–cost–energy–mass analysis of thermal systems and processes. **Energy Conversion and Management**, v. 44, n. 10, p. 1633–1651, 2003.

Roser, M. Future population growth. **Our World in Data**, 2013, <https://ourworldindata.org/future-population-growth>.

Sciubba, E. Beyond thermoeconomics? the concept of extended exergy accounting and its application to the analysis and design of thermal systems. **Exergy, an international journal**, v. 1, n. 2, p. 68–84, 2001.

- Seabra, J. E.; Macedo, I. C. Comparative analysis for power generation and ethanol production from sugarcane residual biomass in brazil. **Energy Policy**, v. 39, n. 1, p. 421–428, 2011.
- Seabra, J. E.; Macedo, I. C.; Chum, H. L.; Faroni, C. E.; Sarto, C. A. Life cycle assessment of brazilian sugarcane products: Ghg emissions and energy use. **Biofuels, Bioproducts and Biorefining**, v. 5, n. 5, p. 519–532, 2011.
- Seabra, J. E.; Tao, L.; Chum, H. L.; Macedo, I. C. A techno-economic evaluation of the effects of centralized cellulosic ethanol and co-products refinery options with sugarcane mill clustering. **Biomass and Bioenergy**, v. 34, n. 8, p. 1065–1078, 2010.
- Shimelmitz, R.; Kuhn, S. L.; Jelinek, A. J.; Ronen, A.; Clark, A. E.; Weinstein-Evron, M. ‘fire at will’: The emergence of habitual fire use 350,000 years ago. **Journal of Human Evolution**, v. 77, p. 196–203, 2014.
- Singh, O. K. Exergy analysis of a grid-connected bagasse-based cogeneration plant of sugar factory and exhaust heat utilization for running a cold storage. **Renewable energy**, v. 143, p. 149–163, 2019.
- Singh, O. K. Application of kalina cycle for augmenting performance of bagasse-fired cogeneration plant of sugar industry. **Fuel**, v. 267, p. 117176, 2020.
- Smith, P.; Botermans, R. **Advanced Piping Design**. [S.l.]: Elsevier, 2013.
- Soltanian, S.; Aghbashlo, M.; Almasi, F.; Hosseinzadeh-Bandbafha, H.; Nizami, A.-S.; Ok, Y. S.; Lam, S. S.; Tabatabaei, M. A critical review of the effects of pretreatment methods on the exergetic aspects of lignocellulosic biofuels. **Energy Conversion and Management**, v. 212, p. 112792, 2020.
- Soltanian, S.; Aghbashlo, M.; Farzad, S.; Tabatabaei, M.; Mandegari, M.; Görgens, J. F. Exergoeconomic analysis of lactic acid and power cogeneration from sugarcane residues through a biorefinery approach. **Renewable energy**, v. 143, p. 872–889, 2019.
- Souza, S. P.; Nogueira, L. A. H.; Martinez, J.; Cortez, L. A. B. Sugarcane can afford a cleaner energy profile in latin america & caribbean. **Renewable Energy**, v. 121, p. 164–172, 2018.
- Souza, S. P.; Horta Nogueira, L. A.; Watson, H. K.; Lynd, L. R.; Elmissiry, M.; Cortez, L. A. Potential of sugarcane in modern energy development in southern africa. **Frontiers in Energy Research**, v. 4, p. 39, 2016.
- Von Spakovsky, M.; Evans, R. Engineering functional analysis—part i. 1993.
- Szargut, J. **Thermodynamic and Economic Analysis in Power Generation Industry, in polish**. [S.l.]: Wydawnictwa Naukowe - Techniczne, Warsaw, 1983.
- Szargut, J. **Exergy method: technical and ecological applications**. [S.l.]: WIT press, 2005. v. 18.
- Taner, T.; Sivrioglu, M. Energy–exergy analysis and optimisation of a model sugar factory in turkey. **Energy**, v. 93, p. 641–654, 2015.
- Torres, E. Avaliação exergética e termoeconômica de um sistema de cogeração de um pólo petroquímico. **FEM/UNICAMP, tese de doutorado. Campinas-SP**, 1999.
- Torres, C.; Valero, A. A new methodology to compute exergy cost part i: The flow-process table. 2018.
- Tsatsaronis, G. Definitions and nomenclature in exergy analysis and exergoeconomics. **Energy**, v. 32, n. 4, p. 249–253, 2007.
- Tsatsaronis, G.; Lin, L.; Pisa, J. Exergy costing in exergoeconomics. 1993.
- Valero, A.; Lozano, M.; Muñoz, M. A general theory of exergy saving. i. on the exergetic cost. **Computer-aided engineering and energy systems: second law analysis and modelling**, v. 3, p. 1–8, 1986.
- Valero, A.; Usón, S.; Torres, C.; Stanek, W. Theory of exergy cost and thermo-ecological cost. In: **Thermodynamics for sustainable management of natural resources**. [S.l.]: Springer, 2017. p. 167–202.
- Velásquez, H.; De Oliveira, S.; Benjumea, P.; Pellegrini, L. Exergo-environmental evaluation of liquid biofuel production processes. **Energy**, v. 54, p. 97–103, 2013.
- Wetzstein, G.; Lanman, D.; Hirsch, M.; Raskar, R. Tensor Displays: Compressive Light Field Synthesis using Multilayer Displays with Directional Backlighting. **ACM Trans. Graph. (Proc. SIGGRAPH)**, New York, NY, USA, v. 31, n. 4, p. 1–11, 2012.

Appendix

APPENDIX A – THEORY OF EXERGETIC COST - PHYSICAL STRUCTURE

All systems have a physical structure, a concept that abstracts devices and their interconnections. A physical structure may include pumps, deaerators, distribution and mixing chambers, turbines, valves, heat exchangers, *et cetera*.

Although, a graph wasn't the first depiction of a physical structure, see (Lozano; Valero, 1993), several concepts from graph theory are useful when describing of a physical structure. Lately, as in (Valero et al., 2017) and other references, a physical structure is modeled as a graph – the structure from discrete mathematics.

As appendixes to Definition 16, Definitions 17 and Definitions 18 are presented as follows.

Definition 16 (Graph – (Biggs et al., 1986)). *Consider a finite set ζ of n distinct elements. Consider a finite set \mathcal{E} of m elements. Let any j -th element of \mathcal{E} , $1 \leq j \leq m$, be a pair e_j , not necessarily ordered, of the form $e_j = (a, b)$; $a, b \in \zeta$; a not necessarily different from b ; two elements e_i and e_j , $i \neq j$, are not necessarily different pairs. A graph, denoted by $\mathcal{G}(\zeta, \mathcal{E})$, is defined over any two sets ζ and \mathcal{E} .*

Definition 17 (Graph vertex – (Biggs et al., 1986), (Valero et al., 2017)). *“Vertex” is synonym to “node” of a graph. It denotes one of the points on which the graph is defined and which may be connected to other points by means of graph edges, see Definition 18. Other synonyms are “point”, “junction”, and “0-simplex”. The set of all vertices in a graph, denoted by ζ , is as stated in Definition 16.*

Definition 18 (Graph edge – (Biggs et al., 1986), (Valero et al., 2017)). *The i -th edge of a graph, denoted by e_i , is a pair of different nodes, i.e., different elements of ζ , of the form $e_i = (a, b)$, where a and b are any two elements of ζ , a not necessarily different from b . The set of all edges in a graph, denoted by \mathcal{E} , is as stated in Definition 16. Two distinct elements of \mathcal{E} may correspond to the same pair; i.e., two elements e_i and e_j , $i \neq j$, are not necessarily different pairs.*

There are some circular references between Definitions 16, 17, and 18. Not a problem. The union of Definitions 16, 17, and 18 expresses precisely what is meant by a graph within the scope of this text.

Example 3 (Graph, Vertices and Edges – (Lozano; Valero, 1993)). *Let $\mathcal{G}(\zeta, \mathcal{E})$ denote the graph at Figure A.1. From Definitions 16, 17, sets ζ and \mathcal{E} are*

$$\zeta = \{a, b, c, d\}; \quad \mathcal{E} = \{(a, b), (c, d), (a, d), (b, d), (c, d)\} \quad (\text{A.1})$$

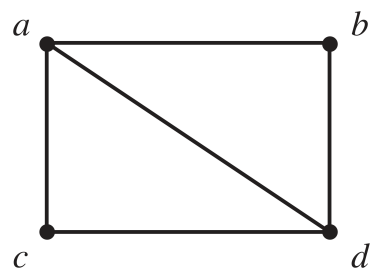


Figure A.1 – An example of a *simple graph*.

APPENDIX B – THEORY OF EXERGETIC COST - PHYSICAL STRUCTURE AS A DIRECTED GRAPH

It immediately follows that any thermal energy plant may be abstracted as by establishing two semantic parallels: (1.) control volumes are similar to vertices and (2.) pipes and electrical/mechanical couplings in thermal plants are similar to edges.

First, there is enough semantic equivalence between a device within the thermal plant and a graph vertex; furthermore, there is enough semantic equivalence between any control volume – which may aggregate any number of equipments within a thermal plant – and a graph vertex. The equivalence stems from the fact that a graph vertex may be connected to any other graph vertex within the same graph. Equivalently, a control volume may be connected to any other control volume within the same thermal plant.

Definition 19 (Aggregation level). *Refers to a certain control volume to which a balance equation has been applied. It may be comprised of one or more devices.*

Second, there is enough semantic equivalence between graph edges and pipes/electric-mechanical couplings in thermal plants. The equivalence stems from the fact that graph nodes are connected to other graph nodes through edges. Equivalently, in a thermal plant, devices(control volumes) receive(pass on) matter and/or energy from(to) other devices(control volumes).

Remark 16 (Adequate notion of vertex). *There are more general notions of graph, where, for instance, graphs are defined so as to allow loops – when a vertex is connected to itself – and multiple edges – when there is more than one edge connecting the same two vertices. Throughout the literature, a graph that doesn't allow loops or multiple edges is named “simple graph”. This text deals exclusively with simple graphs. Within a thermal plant, any control volume is never connected to itself, i.e., at Definition 16, $a \neq b$.*

Remark 17 (Adequate notion of edge). *Within a thermal plant, the flow going from device a to device b is not the same as the flow from b to a . For instance, compressed liquid may flow from a pump to a boiler, but never from a boiler to a pump. In graph theory terms, it's as if edge (a, b) is not the same as edge (b, a) . An edge directed from node a to node b is denoted as (\vec{a}, b) or, simply, “ordered pair (a, b) ”, notated as e_j , in contrast to the non-ordered pair $e_j = (a, b)$, see Definition 18.*

Considering Remarks 16 and 17, an adequate data structure to represent the physical structure of a thermal plant is given by a directed simple graph.

Definition 20 (Directed simple graph). *Let $\zeta = \{v_0, v_1, \dots, v_n\}$ be a set of distinct graph nodes. Let $\mathcal{E} = \{e_1, \dots, e_m\}$ be a set of graph edges. Let any j -th element of \mathcal{E} , $1 \leq j \leq m$, be an ordered pair of the form $e_j = (a, b)$; $a, b \in \zeta$; $a \neq b$; $e_i \neq e_j$ for $i \neq j$. Any two sets ζ and \mathcal{E} define a directed simple graph $\mathcal{G}(\zeta, \mathcal{E})$.*

Example 4 (Directed graph). *Let $\mathcal{G}(\zeta, \mathcal{E})$ denote the graph at Figure B.1. From Definitions 16, 17, sets ζ and \mathcal{E}*

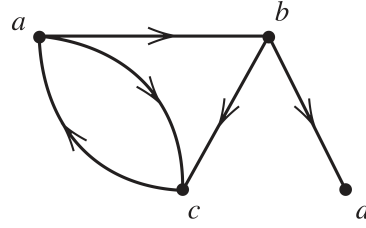


Figure B.1 – An example of a directed graph.

are

$$\zeta = \{a, b, c, d\}; \quad \mathcal{E} = \{(a \vec{b}), (b \vec{d}), (b \vec{c}), (a \vec{c}), (c \vec{a})\} \quad (\text{B.1})$$

Do note that $\mathcal{G}(\zeta, \mathcal{E})$ is a directed graph, but not simple, since the pair (a, c) associates to 2 edges.

Definition 21 (Incidence Matrix of a Directed Graph). An incidence matrix, synonym to “incidence relation”, denotes a logical matrix that denotes a relationship between two sets. Let ζ and \mathcal{E} , from Definition 20, be these two sets. Let ζ and \mathcal{E} be related by the incidence matrix $\mathbf{A} \in \{-1, 0, 1\}^{n \times m}$. Let a_{ij} denote the element of matrix \mathbf{A} at the i -th row, $1 \leq i \leq n$, and j -th column, $1 \leq j \leq m$. Thus,

$$a_{ij} = \begin{cases} -1, & \text{if edge } \mathbf{e}_j \text{ is directed to the } i\text{-th vertex} \\ 1, & \text{if edge } \mathbf{e}_j \text{ is directed from the } i\text{-th vertex} \\ 0, & \text{otherwise} \end{cases} \quad (\text{B.2})$$

Example 5 (Incidence Matrix). Let $\mathcal{G}(\zeta, \mathcal{E})$ denote the graph at Figure B.1. From Definitions 16, 17, sets ζ and

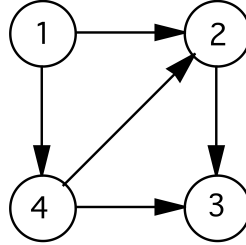


Figure B.2 – Another example of a directed graph.

\mathcal{E} are

$$\zeta = \{1, 2, 3, 4\}; \quad \mathcal{E} = \{(1 \vec{2}), (1 \vec{4}), (2 \vec{3}), (4 \vec{2}), (4 \vec{3})\}. \quad (\text{B.3})$$

Finally, the incidence matrix $\mathbf{A} \in \{0, 1, -1\}^{4 \times 5}$ is:

$$\mathbf{A} = \begin{array}{c} \begin{array}{|c|} \hline \text{Node 1} \\ \hline \end{array} \\ \begin{array}{|c|} \hline \text{Node 2} \\ \hline \end{array} \\ \begin{array}{|c|} \hline \text{Node 3} \\ \hline \end{array} \\ \begin{array}{|c|} \hline \text{Node 4} \\ \hline \end{array} \end{array} \begin{bmatrix} \boxed{e_1} & \boxed{e_2} & \boxed{e_3} & \boxed{e_4} & \boxed{e_5} \\ 1 & 1 & 1 & 0 & 0 \\ -1 & 0 & 1 & -1 & 0 \\ -1 & 0 & 1 & -1 & 0 \\ 0 & 0 & -1 & 0 & -1 \end{bmatrix} \quad (\text{B.4})$$

The next three paragraphs conclude the modeling of a thermal plant as a directed simple graph.

Consider a set $\mathcal{Z} = \{v_0, v_1, \dots, v_n\}$ to represent the n devices or processes in a thermodynamic system whose aggregation levels are fully defined. Element v_0 represents the system's surrounding environment and each equipment v_i , $i = 1, \dots, n$, is described by a set of parameters. This set may include name of equipment and types of thermodynamic processes.

Consider a set $\mathcal{E} = \{e_1, \dots, e_m\}$ to represent the m flows in the thermodynamic system. Each j -th flow e_j , $j = 1, \dots, m$, is defined by the pair of devices (v_p, v_q) , $p \neq q$, $1 \leq p \leq n$, $1 \leq q \leq n$, that it links. Furthermore, attributes such as type of flow – *e.g.*, mass, heat, work, waste – may be annexed to an i -th flow e_j .

Consider an incidence matrix $\mathbf{A} \in \{-1, 0, 1\}^{n \times m}$ describing interconnections amongst devices v_i and flows e_i . An element a_{ij} from matrix \mathbf{A} takes the value +1 if the flow e_m gets into a device v_i or -1 if it gets out of it, and 0 if there is no connection. Thus,

$$a_{ij} = \begin{cases} +1, & \text{if} \\ -1, & \text{if} \\ 0, & \text{otherwise} \end{cases} \quad (\text{B.5})$$

Matrix \mathbf{A} is of the form:

$$\mathbf{A} = \begin{array}{c} \boxed{\text{Device 1}} \\ \boxed{\text{Device 2}} \\ \vdots \\ \boxed{\text{Device } n} \end{array} \left[\begin{array}{cccc} \boxed{\text{Flow 1}} & \boxed{\text{Flow 2}} & \dots & \boxed{\text{Flow } m} \\ a_{11} & a_{12} & \dots & a_{1m} \\ a_{21} & a_{22} & \dots & a_{2m} \\ \vdots & \vdots & \ddots & \vdots \\ a_{n1} & a_{n2} & \dots & a_{nm} \end{array} \right] \quad (\text{B.6})$$

APPENDIX C – THEORY OF EXERGETIC COST - MASS BALANCE OVER ALL AGGREGATION LEVELS IN MATRIX FORM

Consider an incidence matrix $\mathbf{A} \in \{-1, 0, 1\}^{n \times m}$. Consider a column-vector $\mathbf{m} = \begin{bmatrix} M_1 & M_2 & \dots & M_m \end{bmatrix}^T \in \mathbb{R}_+^m$, whose j -th entry $M_j \geq 0$ denotes the mass flow rate associated to the j -th flow in kg/s. In steady state conditions, the mass balance, in matrix form, is:

$$\mathbf{A}\mathbf{m} = \mathbf{0}_m \quad (\text{C.1})$$

The same equation is written in terms of scalar variables as:

$$\begin{bmatrix} a_{11} & a_{12} & \dots & a_{1n} \\ a_{21} & a_{22} & \dots & a_{2n} \\ \vdots & \vdots & \ddots & \vdots \\ a_{m1} & a_{m2} & \dots & a_{mn} \end{bmatrix} \begin{bmatrix} M_1 \\ M_2 \\ \vdots \\ M_m \end{bmatrix} = \begin{bmatrix} 0 \\ 0 \\ \vdots \\ 0 \end{bmatrix} \quad (\text{C.2})$$

The vector M correspond to the mass flow rate in kg/s. If the j -th element of \mathbf{m} denotes either flow of heat or work, then $M_i = 0$. The linear transformation, explicitly, is given by the algebraic linear system of equations:

$$\begin{array}{ccccccc} a_{11}M_1 & + & a_{12}M_2 & + & \dots & + & a_{1n}M_m & = & 0 \\ a_{21}M_1 & + & a_{22}M_2 & + & \dots & + & a_{2n}M_m & = & 0 \\ \vdots & & \vdots & & \ddots & & \vdots & & \vdots \\ a_{m1}M_1 & + & a_{m2}M_2 & + & \dots & + & a_{mn}M_m & = & 0 \end{array} \quad (\text{C.3})$$

Remark 18 (Equation C.3). *In practice, this equation helps in verifying whether the incidence matrix obtained from a set of control volumes is correct given that all mass flow rates M_1, \dots, M_m are already known. Since thermoeconomic analysis starts at an investigation stage where \mathbf{m} is already known, this current remark is always valid.*

APPENDIX D – THEORY OF EXERGETIC COST - ENERGY BALANCE OVER ALL AGGREGATION LEVELS IN MATRIX FORM

Consider an incidence matrix $\mathbf{A} \in \{-1, 0, 1\}^{n \times m}$. Consider a column-vector $\mathbf{e} = [E_1 \ E_2 \ \dots \ E_m]^T \in \mathbb{R}^m$, whose j -th entry $E_j > 0$ denotes the energy flow rate associated to the j -th flow, in kW. In steady state conditions, the energy balance, in matrix form, is:

$$\mathbf{A}\mathbf{e} = \mathbf{0}_m \quad (\text{D.1})$$

The same equation is written in terms of scalar variables as:

$$\begin{bmatrix} a_{11} & a_{12} & \dots & a_{1n} \\ a_{21} & a_{22} & \dots & a_{2n} \\ \vdots & \vdots & \ddots & \vdots \\ a_{m1} & a_{m2} & \dots & a_{mn} \end{bmatrix} \begin{bmatrix} E_1 \\ E_2 \\ \vdots \\ E_m \end{bmatrix} = \begin{bmatrix} 0 \\ 0 \\ \vdots \\ 0 \end{bmatrix} \quad (\text{D.2})$$

The j -th element of \mathbf{e} , i.e., E_j , corresponds to either heat or work, thus:

$$E_j = Q_j \quad \vee \quad E_j = W_j. \quad (\text{D.3})$$

The linear transformation, in explicit form, is given by the algebraic linear system of equations:

$$\begin{array}{cccccc} a_{11}E_1 & + & a_{12}E_2 & + & \dots & + & a_{1n}E_m & = & 0 \\ a_{21}E_1 & + & a_{22}E_2 & + & \dots & + & a_{2n}E_m & = & 0 \\ \vdots & & \vdots & & \ddots & & \vdots & & \vdots \\ a_{m1}E_1 & + & a_{m2}E_2 & + & \dots & + & a_{mn}E_m & = & 0 \end{array} \quad (\text{D.4})$$

Remark 19 (Equation D.4). *This linear system of algebraic equations is never meant to be solved! It is only a block of a larger linear system of algebraic equations assembled, at the end of the current chapter, as a formulation of the exergetic cost balance. Although there is a possibility of solving Equation D.4 by means of the Moore–Penrose generalized inverse, said possibility is of no interest whatsoever within the context of this current chapter.*

Remark 20 (Equation H.14). *In practice, this equation helps in verifying whether the incidence matrix obtained from a set of control volumes is correct given that all energy flow rates E_1, \dots, E_m are already known. Since thermoeconomic analysis starts at an investigation stage where \mathbf{e} is already known, this current remark is always valid.*

APPENDIX E – THEORY OF EXERGETIC COST - EXERGY BALANCE OVER ALL AGGREGATION LEVELS IN MATRIX FORM

Consider an incidence matrix $\mathbf{A} \in \{-1, 0, 1\}^{n \times m}$. Consider a column-vector $\boldsymbol{\varepsilon} = [\mathbf{E}_1 \ \mathbf{E}_2 \ \dots \ \mathbf{E}_m]^\top \in \mathbb{R}^m$, whose j -th entry $\mathbf{E}_j \geq 0$ denotes the exergy flow rate associated to the j -th flow, in kW.

Remark 21 (Case $\mathbf{E}_j = 0$). *It means the j -th flow is at the dead state.*

Consider a column-vector $\boldsymbol{\varepsilon}_d = [\mathbf{E}_{d,1} \ \mathbf{E}_{d,2} \ \dots \ \mathbf{E}_{d,m}]^\top \in \mathbb{R}^m$, whose j -th entry $\mathbf{E}_{d,j} \geq 0$ denotes the exergy destruction flow rate associated to the j -th flow, in kW.

Remark 22 (Case $\mathbf{E}_{d,j} = 0$). *It means the j -th flow is completely ideal¹.*

In steady state conditions, the exergy balance, in matrix form, is:

$$\mathbf{A}\boldsymbol{\varepsilon} = \boldsymbol{\varepsilon}_d \quad (\text{E.1})$$

The same equation is written in terms of scalar variables as:

$$\begin{bmatrix} a_{11} & a_{12} & \dots & a_{1n} \\ a_{21} & a_{22} & \dots & a_{2n} \\ \vdots & \vdots & \ddots & \vdots \\ a_{n1} & a_{n2} & \dots & a_{nm} \end{bmatrix} \begin{bmatrix} \mathbf{E}_1 \\ \mathbf{E}_2 \\ \vdots \\ \mathbf{E}_m \end{bmatrix} = \begin{bmatrix} \mathbf{E}_{d,1} \\ \mathbf{E}_{d,2} \\ \vdots \\ \mathbf{E}_{d,n} \end{bmatrix} \quad (\text{E.2})$$

When the j -th element of $\boldsymbol{\varepsilon}$, *i.e.*, \mathbf{E}_j , denotes either heat or work, then

$$\mathbf{E}_j = Q_j \left(1 - \frac{T_0}{T_j} \right) \quad \vee \quad \mathbf{E}_j = W_j, \quad (\text{E.3})$$

where T_0 is the average surrounding environment temperature, in K. The linear transformation between vectors $\boldsymbol{\varepsilon}$ and $\boldsymbol{\varepsilon}_d$, in explicit form, is given by the algebraic linear system of equations:

$$\begin{aligned} a_{11}\mathbf{E}_1 + a_{12}\mathbf{E}_2 + \dots + a_{1n}\mathbf{E}_m &= \mathbf{E}_{d,1} \\ a_{21}\mathbf{E}_1 + a_{22}\mathbf{E}_2 + \dots + a_{2n}\mathbf{E}_m &= \mathbf{E}_{d,2} \\ \vdots & \quad \quad \quad \vdots \\ a_{n1}\mathbf{E}_1 + a_{n2}\mathbf{E}_2 + \dots + a_{nm}\mathbf{E}_m &= \mathbf{E}_{d,n} \end{aligned} \quad (\text{E.4})$$

Remark 23 (Equation H.14). *In practice, this equation helps in verifying whether the incidence matrix obtained from a set of control volumes is correct given that all exergy flow rates $\mathbf{E}_1, \dots, \mathbf{E}_m$ and destroyed exergy flow rates $\mathbf{E}_{d,1}, \mathbf{E}_{d,2}, \dots, \mathbf{E}_{d,m}$ are already known. Since thermoeconomic analysis starts at an investigation stage where $\boldsymbol{\varepsilon}$ and $\boldsymbol{\varepsilon}_d$ are already known, this current remark is always valid.*

¹ In fluid mechanics terminology, an ideal flow refers to the flow of ideal fluids, *i.e.*, inviscid fluids with zero viscosity. In thermodynamics, the j -th flow being ideal may refer to fluid flow with zero friction loss or to electro-mechanical power flow.

APPENDIX F – THEORY OF EXERGETIC COST -EXERGETIC COST BALANCE PER PROPOSITION P1

Consider an incidence matrix $\mathbf{A} \in \{-1, 0, 1\}^{n \times m}$. Consider a column-vector $\mathbf{\epsilon}^* = [\mathbf{E}_1^* \quad \mathbf{E}_2^* \quad \dots \quad \mathbf{E}_m^*]^\top \in \mathbb{R}^m$, whose j -th entry $\mathbf{E}_j^* \geq 0$ denotes the exergy cost flow rate associated to the j -th flow, in kW.

Remark 24 (Case $\mathbf{E}_j^* = 0$). *It means the j -th flow is readily available such that no energy is spent in sustaining it.*

Consider a column-vector $\mathbf{\epsilon}_d^* = [\mathbf{E}_{d,1}^* \quad \mathbf{E}_{d,2}^* \quad \dots \quad \mathbf{E}_{d,m}^*]^\top \in \mathbb{R}^m$, whose j -th entry $\mathbf{E}_{d,j}^* = 0$ denotes the exergy destruction cost flow rate associated to the j -th flow, in kW.

Remark 25 (Case $\mathbf{E}_{d,j}^* = 0$). *It means the exergy lost at the j -th flow comes at zero exergy cost.*

In steady state conditions, the exergy cost balance, in matrix form, per Proposition P1 is:

$$\mathbf{A}_{n \times m} \mathbf{\epsilon}_{m \times 1}^* = \mathbf{0}_{n \times 1} \quad (\text{F.1})$$

The same equation is written in terms of scalar variables as:

$$\begin{bmatrix} a_{11} & a_{12} & \dots & a_{1n} \\ a_{21} & a_{22} & \dots & a_{2n} \\ \vdots & \vdots & \ddots & \vdots \\ a_{n1} & a_{n2} & \dots & a_{nm} \end{bmatrix}_{n \times m} \begin{bmatrix} \mathbf{E}_1^* \\ \mathbf{E}_2^* \\ \vdots \\ \mathbf{E}_m^* \end{bmatrix}_{m \times 1} = \begin{bmatrix} 0 \\ 0 \\ \vdots \\ 0 \end{bmatrix} \quad (\text{F.2})$$

When the j -th element of $\mathbf{\epsilon}$, *i.e.*, \mathbf{E}_j , denotes either heat or work, then

$$\mathbf{E}_j^* = \mathbf{E}_j \quad \vee \quad \mathbf{E}_j = \text{unknown}, \quad (\text{F.3})$$

The linear transformation between vectors $\mathbf{\epsilon}$ and $\mathbf{\epsilon}_d$, in explicit form, is given by the algebraic linear system of equations:

$$\begin{aligned} a_{11}\mathbf{E}_1^* + a_{12}\mathbf{E}_2^* + \dots + a_{1n}\mathbf{E}_m^* &= 0 \\ a_{21}\mathbf{E}_1^* + a_{22}\mathbf{E}_2^* + \dots + a_{2n}\mathbf{E}_m^* &= 0 \\ \vdots & \\ a_{n1}\mathbf{E}_1^* + a_{n2}\mathbf{E}_2^* + \dots + a_{nm}\mathbf{E}_m^* &= 0 \end{aligned} \quad (\text{F.4})$$

Note that the numbers of flow is higher ($m - n$).

APPENDIX G – THEORY OF EXERGETIC COST – APPENDING (N-M) EQUATIONS USING PROPOSITIONS

Therefore, auxiliary equations will be determined using the four propositions and a new matrix α will be needed, then, concatenate the four propositions amount to the following system of equations:

$$\left[\begin{array}{c} \mathcal{P}1_{n \times m} \\ \mathcal{P}2_{f \times m} \\ \mathcal{P}3_{(p+l) \times m} \\ (\mathcal{P}4.1 \wedge \mathcal{P}4.2)_{b \times m} \end{array} \right]_{m \times m} \left[\begin{array}{c} \boldsymbol{\epsilon}_{\mathcal{P}1, n \times 1}^* \\ \boldsymbol{\epsilon}_{\mathcal{P}2, f \times 1}^* \\ \boldsymbol{\epsilon}_{\mathcal{P}3, (p+l) \times 1}^* \\ \boldsymbol{\epsilon}_{\mathcal{P}4, b \times 1}^* \end{array} \right]_{m \times 1} = \left[\begin{array}{c} \mathbf{0}_n \\ \mathbf{0}_f \\ \boldsymbol{\epsilon}_{p+l} \\ \mathbf{0}_b \end{array} \right]_{m \times 1} \quad (\text{G.1})$$

Note that:

$$n + f + p + l + b = m \quad (\text{G.2})$$

Let there be a vector $\boldsymbol{\delta} \in \mathbb{R}^m$ given by:

$$\boldsymbol{\delta} = \left[\mathbf{0}_n^\top \quad \mathbf{0}_f^\top \quad \mathbf{0}_f^\top \quad \boldsymbol{\epsilon}_{p+l}^\top \quad \mathbf{0}_b^\top \right]^\top \quad (\text{G.3})$$

In terms of matrices, the same can be written as:

$$\mathbf{P}_{m \times m} \boldsymbol{\epsilon}_{m \times 1}^* = \boldsymbol{\delta}_{m \times 1} \quad (\text{G.4})$$

APPENDIX H – THEORY OF EXERGETIC COST - COMPLETE SYSTEM OF EQUATIONS IN TERMS OF UNIT EXERGY COST κ^*

In steady state conditions, the exergy cost equation, in matrix form, per Propositions $\mathcal{P}_1, \mathcal{P}_2, \mathcal{P}_3$ and \mathcal{P}_4 is:

$$\mathbf{P}_{m \times m} \boldsymbol{\varepsilon}_{m \times 1}^* = \boldsymbol{\delta}_{m \times 1} \quad (\text{H.1})$$

The vector κ^* is obtained from $\boldsymbol{\varepsilon}^*$ by performing the Hadamard division

$$\boldsymbol{\kappa}^* = \boldsymbol{\varepsilon}^* \oslash \boldsymbol{\varepsilon} \quad (\text{H.2})$$

$$= \begin{bmatrix} \mathbf{E}_1^* / \mathbf{E}_1 & \mathbf{E}_2^* / \mathbf{E}_2 & \dots & \mathbf{E}_m^* / \mathbf{E}_m \end{bmatrix}^\top \quad (\text{H.3})$$

$$= \begin{bmatrix} \boxed{\mathbf{E}_1^{-1}} & 0 & \dots & 0 \\ 0 & \boxed{\mathbf{E}_2^{-1}} & \dots & 0 \\ \vdots & \vdots & \ddots & \vdots \\ 0 & 0 & \dots & \boxed{\mathbf{E}_m^{-1}} \end{bmatrix} \begin{bmatrix} \mathbf{E}_1^* \\ \mathbf{E}_2^* \\ \vdots \\ \mathbf{E}_m^* \end{bmatrix} \quad (\text{H.4})$$

$$= \text{blkdiag}(\mathbf{E}_1^{-1}, \dots, \mathbf{E}_m^{-1}) \begin{bmatrix} \mathbf{E}_1^* & \mathbf{E}_2^* & \dots & \mathbf{E}_m^* \end{bmatrix}^\top \quad (\text{H.5})$$

Definition 22 (Hadamard Division of Two Matrices ([Wetzstein et al., 2012](#))). *Let there be matrices A, B and C of same size. Assume, just within this current chapter on thermoeconomics, all matrices are real-valued, i.e., $A, B, C \in \mathbb{R}^{p \times q}$. Then, “C equals A Hadamard-divided by B” is notated by $C = A \oslash B$ meaning that $C_{ij} = \frac{A_{ij}}{B_{ij}}$, $B_{ij} \neq 0$, over all $1 \leq i \leq p$ and $1 \leq j \leq q$.*

We now proceed to a variable change in equation

$$\mathbf{P}_{m \times m} \boldsymbol{\varepsilon}_{m \times 1}^* = \boldsymbol{\delta}_{m \times 1} \quad (\text{H.6})$$

$$\mathbf{P}_{m \times m}^{-1} \mathbf{P}_{m \times m} \boldsymbol{\varepsilon}_{m \times 1}^* = \mathbf{P}_{m \times m}^{-1} \boldsymbol{\delta}_{m \times 1} \quad (\text{H.7})$$

$$\boldsymbol{\varepsilon}_{m \times 1}^* = \mathbf{P}_{m \times m}^{-1} \boldsymbol{\delta}_{m \times 1} \quad (\text{H.8})$$

$$\text{blkdiag}(\mathbf{E}_1^{-1}, \dots, \mathbf{E}_m^{-1})_{m \times m} \boldsymbol{\varepsilon}_{m \times 1}^* = \text{blkdiag}(\mathbf{E}_1^{-1}, \dots, \mathbf{E}_m^{-1})_{m \times m} \mathbf{P}_{m \times m}^{-1} \boldsymbol{\delta}_{m \times 1} \quad (\text{H.9})$$

$$\boldsymbol{\kappa}_{m \times 1}^* = \text{blkdiag}(\mathbf{E}_1^{-1}, \dots, \mathbf{E}_m^{-1})_{m \times m} \mathbf{P}_{m \times m}^{-1} \boldsymbol{\delta}_{m \times 1} \quad (\text{H.10})$$

$$\mathbf{P}_{m \times m} \boldsymbol{\kappa}_{m \times 1}^* = \mathbf{P}_{m \times m} \text{blkdiag}(\mathbf{E}_1^{-1}, \dots, \mathbf{E}_m^{-1})_{m \times m} \mathbf{P}_{m \times m}^{-1} \boldsymbol{\delta}_{m \times 1} \quad (\text{H.11})$$

Though it hardly may be of use, Equation H.11 can be presented as a concise formulation for the unit exergy cost problem:

$$\mathbf{P}_{m \times m} \boldsymbol{\kappa}_{m \times 1}^* = \boldsymbol{\gamma}_{m \times 1} \quad (\text{H.12})$$

where $\boldsymbol{\gamma} \triangleq \mathbf{P}_{m \times m} \text{blkdiag}(\mathbf{E}_1^{-1}, \dots, \mathbf{E}_m^{-1})_{m \times m} \mathbf{P}_{m \times m}^{-1} \boldsymbol{\delta}_{m \times 1}$.

The same equation is written in terms of scalar variables as:

$$\begin{bmatrix}
 p_{11} & p_{12} & \cdots & p_{1m} \\
 \vdots & \vdots & \ddots & \vdots \\
 p_{n1} & p_{n2} & \cdots & p_{nm} \\
 \hline
 p_{(n+1),1} & p_{(n+1),2} & \cdots & p_{(n+1),m} \\
 \vdots & \vdots & \ddots & \vdots \\
 p_{(n+f),1} & p_{(n+f),2} & \cdots & p_{(n+f),m} \\
 \hline
 p_{(n+f+1),1} & p_{(n+f+1),2} & \cdots & p_{(n+f+1),m} \\
 \vdots & \vdots & \ddots & \vdots \\
 p_{(n+f+p),1} & p_{(n+f+p),2} & \cdots & p_{(n+f+p),m} \\
 \hline
 p_{(n+f+p+1),1} & p_{(n+f+p+1),2} & \cdots & p_{(n+f+p+1),m} \\
 \vdots & \vdots & \ddots & \vdots \\
 p_{(n+f+p+l),1} & p_{(n+f+p+l),2} & \cdots & p_{(n+f+p+l),m} \\
 \hline
 p_{(n+f+p+l+1),1} & p_{(n+f+p+l+1),2} & \cdots & p_{(n+f+p+l+1),m} \\
 \vdots & \vdots & \ddots & \vdots \\
 p_{m1} & p_{m2} & \cdots & p_{mm}
 \end{bmatrix}_{m \times m}
 \begin{bmatrix}
 \kappa_1^* \\
 \vdots \\
 \kappa_n^* \\
 \hline
 \kappa_{n+1}^* \\
 \vdots \\
 \kappa_{n+f}^* \\
 \hline
 \kappa_{n+f+1}^* \\
 \vdots \\
 \kappa_{n+f+p}^* \\
 \hline
 \kappa_{n+f+p+1}^* \\
 \vdots \\
 \kappa_{n+f+p+l}^* \\
 \hline
 \kappa_{n+f+p+l+1}^* \\
 \vdots \\
 \kappa_m^*
 \end{bmatrix}_{m \times 1}
 =
 \begin{bmatrix}
 \gamma_1 \\
 \vdots \\
 \gamma_n \\
 \hline
 \gamma_{n+1} \\
 \vdots \\
 \gamma_{n+f} \\
 \hline
 \gamma_{n+f+1} \\
 \vdots \\
 \gamma_{n+f+p} \\
 \hline
 \gamma_{n+f+p+1} \\
 \vdots \\
 \gamma_{n+f+p+l} \\
 \hline
 \gamma_{n+f+p+l+1} \\
 \vdots \\
 \gamma_m
 \end{bmatrix}_{m \times 1}
 \quad (H.13)$$

In explicit form:

$$\begin{aligned}
 p_{11} \kappa_1^* + a_{12} \kappa_2^* + \dots + a_{1n} \kappa_m^* &= \gamma_1 \\
 p_{21} \kappa_1^* + a_{22} \kappa_2^* + \dots + a_{2n} \kappa_m^* &= \gamma_2 \\
 \vdots & \\
 p_{n1} \kappa_1^* + a_{n2} \kappa_2^* + \dots + a_{nm} \kappa_m^* &= \gamma_n \\
 \vdots &
 \end{aligned}
 \quad (H.14)$$

APPENDIX I – EES SOURCE CODE

```

1 {mass balance}
2 mass[1] = m[1]-m[2]
3 mass[2] = m[2]+m[41]-m[3]
4 mass[3] = m[3]-m[4]
5 mass[4] = m[4]-m[5]-m[6]-m[7]
6 mass[5] = m[5]+m[8]-m[11]+m[42]-m[45]
7 mass[6]=m[6]+m[9]-m[12]+m[43]-m[46]
8 mass[7] = m[7]+m[10]-m[13]+m[44]-m[47]
9 mass[8] = m[11]+m[12]-m[14]-m[15]
10 mass[9]=m[13]+m[14]-m[30]
11 mass[10]=m[30]-m[31]
12 mass[11] = m[16]-m[17]
13 mass[12] = m[18]-m[19]
14 mass[13] = m[20]-m[21]
15 mass[14] = m[22]-m[23]
16 mass[15] = m[24]-m[25]
17 mass[16] = m[26]-m[27]
18 mass[17] = m[31]-m[32]
19 mass[18] = m[28]-m[29]
20 mass[19] = m[17]+m[19]+m[21]+m[23]+m[25]+m[27]+m[29]
    ]+m[32]-m[33]
21 mass[20]=m[33]-m[34]-m[39]
22 mass[21]=m[39]-m[40]
23 mass[22]=m[34]+m[38]-m[35]
24 mass[23]=m[35]-m[36]
25 mass[24]=m[36]-m[37]-m[41]
26 mass[25]=m[37]-m[38]
27 mass[26]=m[15]-m[16]-m[18]-m[20]-m[22]-m[24]-m[26]-
    m[28]
28
29 {energy balance}
30
31
32 energy[1] = m[1]*(h[1]-h[2])-W_pump1
33 energy[2] = m[2]*h[2]+m[41]*h[41]-m[3]*h[3]
34 energy[3]=m[3]*h[3]-W_pump2-m[4]*h[4]
35 energy[4] = m[4]*h[4]-m[5]*h[5]-m[6]*h[6]-m[7]*h[7]
36 energy[5] = m[5]*h[5]+m[8]*PCI_bagaco-m[11]*h[11]-
    Q_perdido_paredel-Q_perdido_gases_1
37 energy[6]= m[6]*h[6]+m[9]*PCI_bagaco-m[12]*h[12]-
    Q_perdido_paredel2-Q_perdido_gases_2
38 energy[7]= m[7]*h[7]+m[10]*PCI_bagaco-m[13]*h[13]-
    Q_perdido_paredel3-Q_perdido_gases_3

```

```

39 energy[8]= m[11]*h[11]+m[12]*h[12]-m[14]*h[14]-m[15
    ]*h[15]
40 energy[9]=m[13]*h[13]+m[14]*h[14]-m[30]*h[30]
41 energy[10] = m[30]*h[30]-m[31]*h[31]+Q_p_steampipe
42 energy[11]= m[16]*h[16]-m[17]*h[17]-W_T1
43 energy[12]= m[18]*h[18]-m[19]*h[19]-W_T2
44 energy[13]= m[20]*h[20]-m[21]*h[21]-W_T3
45 energy[14]= m[22]*h[22]-m[23]*h[23]-W_T4
46 energy[15]= m[24]*h[24]-m[25]*h[25]-W_T5
47 energy[16]= m[26]*h[26]-m[27]*h[27]-W_T6
48 energy[17]= m[31]*h[31]-m[32]*h[32]-W_T7
49 energy[18]=m[28]*h[28]-m[29]*h[29]
50 energy[19] = m[17]*h[17]+m[19]*h[19]+m[21]*h[21]+m[
    23]*h[23]+m[25]*h[25]+m[27]*h[27]+m[29]*h[29]+m[
    32]*h[32]-m[33]*h[33]
51 energy[20] = m[33]*h[33]-m[34]*h[34]-m[39]*h[39]
52 energy[21] = m[39]*h[39]-m[40]*h[40]-Q_destilaria
53 energy[22]= m[34]*h[34]+m[38]*h[38]-m[35]*h[35]
54 energy[23]= m[35]*h[35]-m[36]*h[36]-Q_sugar
55 energy[24]=m[36]*h[36]-m[41]*h[41]-m[37]*h[37]
56 energy[25] = m[37]*(h[37]-W_pump3-h[38])
57 energy[26] = m[15]*h[15]-(m[16]*h[16]+m[18]*h[18]+m
    [20]*h[20]+m[22]*h[22]+m[24]*h[24]+m[26]*h[26]+m[
    28]*h[28]+Q_distribution_turbines)
58 energy[27] = W[64]-W[54]+W[57]+W[56]+W[55]
59
60
61 {exergy destruction balance}
62
63 exergyDestruction[01] = B_destruído_pump1
64 exergyDestruction[02] = B_destruído_desaerador
65 exergyDestruction[03] = B_destruído_pump2
66 exergyDestruction[04] = B_destruído_camara1
67 exergyDestruction[05] = B_destruído_caldeira_1+
    gases_b1*e_ch_total
68 exergyDestruction[06] = B_destruído_caldeira_2
69 exergyDestruction[07] = B_destruído_caldeira_3
70 exergyDestruction[08] = B_destruído_mix1
71 exergyDestruction[09] = B_destruído_mix2
72 exergyDestruction[10] = B_destruído_heat_losses
73 exergyDestruction[11] = W_destruídoT1
74 exergyDestruction[12] = W_destruídoT2
75 exergyDestruction[13] = W_destruídoT3
76 exergyDestruction[14] = W_destruídoT4
77 exergyDestruction[15] = W_destruídoT5
78 exergyDestruction[16] = W_destruídoT6
79 exergyDestruction[17] = W_destruídoT7

```

```

80 exergyDestruction[18] = B_destruido_valvula
81 exergyDestruction[19] = B_destruido_mix3
82 exergyDestruction[20] = B_destruido_camara2
83 exergyDestruction[21] = B_destruido_destilaria
84 exergyDestruction[22] =
    B_destruido_dessuperaquecedor
85 exergyDestruction[23] =
    B_destruido_sugar_production
86 exergyDestruction[24] = B_destruido_camara3
87 exergyDestruction[25] = B_destruido_pump3
88 exergyDestruction[26] = B_destruido_destrubuction
89 exergyDestruction[27] = W[64]-W[54]+W[57]+W[56]+W[
    55]
90
91
92
93
94
95 {exergetic cost balance}
96
97 custo[1] = B[1]+B[55]-B[2]
98 custo[2] = B[2]+B[41]-B[3]
99 custo[3] = B[3]+B[56]-B[4]
100 custo[4] = B[4]-B[5]-B[6]-B[7]
101 custo[5] = B[5]+B[8]-B[11]
102 custo[6] = B[6]+B[9]-B[12]
103 custo[7] = B[7]+B[10]-B[13]
104 custo[8] = B[11]+B[12]-B[14]-B[15]
105 custo[9] = B[13]+B[14]-B[30]
106 custo[10] = B[30]-B[31]
107 custo[11] = B[16]-B[17]-B[48]
108 custo[12] = B[18]-B[19]-B[49]
109 custo[13] = B[20]-B[21]-B[50]
110 custo[14] = B[22]-B[23]-B[51]
111 custo[15] = B[24]-B[25]-B[52]
112 custo[16] = B[26]-B[27]-B[53]
113 custo[17] = B[31]-B[32]-B[54]
114 custo[18] = B[28]-B[29]
115 custo[19] = B[17]+B[19]+B[21]+B[23]+B[25]+B[27]+B[
    29]+B[32]-B[33]
116 custo[20] = B[33]-B[34]-B[39]
117 custo[21] = B[39]-B[63]-B[40]
118 custo[22] = B[34]+B[38] - B[35]
119 custo[23] = B[35]-B[62]-B[36]
120 custo[24] = B[36] - B[37] - B[41]
121 custo[25] = B[37]+B[57]-B[38]
122 custo[26] = B[15] - B[16]-B[18]-B[20]-B[22]-B[24]-B

```

```

    [26]-B[28]
123 custo[27] = B[54] - B[55]-B[56]-B[57] -B[64]
124
125 {exergetic cost of control volume -- Fuel}
126
127
128 fuelCost[1] = B[55]
129 fuelCost[2] = B[2]+B[41]
130 fuelCost[3] = B[56]
131 fuelCost[4] = B[4]
132
133
134
135 fuelCost[5] = B[8]
136 fuelCost[6] = B[9]
137 fuelCost[7] = B[10]
138 fuelCost[8] = B[11]+B[12]
139 fuelCost[9] = B[13]+B[14]
140 fuelCost[10] = B[30]
141 fuelCost[11] = B[16]-B[17]
142 fuelCost[12] = B[18]-B[19]
143 fuelCost[13] = B[20]-B[21]
144 fuelCost[14] = B[22]-B[23]
145 fuelCost[15] = B[24]-B[25]
146 fuelCost[16] = B[26]-B[27]
147 fuelCost[17] = B[31]-B[32]
148
149 fuelCost[18] = B[28]
150 fuelCost[19] = B[17]+B[19]+B[21]+B[23]+B[25]+B[27]+
    B[29]+B[32]
151 fuelCost[20] = B[33]
152 fuelCost[21] = B[39]-B[40]
153 fuelCost[22] = B[34]+ B[38]
154 fuelCost[23] = B[35]-B[36]
155 fuelCost[24] = B[36]
156 fuelCost[25] = B[57]
157 fuelCost[26] = B[15]
158 fuelCost[27] = B[54]
159
160
161 {exergetic cost of control volume -- Product}
162 productCost[1] = B[2]-B[1]
163 productCost[2] = B[3]
164 productCost[3] = B[4]-B[3]
165 productCost[4] = B[5]+B[6]+B[7]
166
167 productCost[5] = B[11]-B[5]

```

```

168 productCost[6] = B[12]-B[6]
169 productCost[7] = B[13]-B[7]
170 productCost[8] = B[14]+B[15]
171 productCost[9] = B[30]
172 productCost[10] = B[31]
173 productCost[11] = B[48]
174 productCost[12] = B[49]
175 productCost[13] = B[50]
176 productCost[14] = B[51]
177 productCost[15] = B[52]
178 productCost[16] = B[53]
179 productCost[17] = B[54]
180
181
182 productCost[18] = B[29]
183
184 productCost[19] = B[33]
185 productCost[20] = B[34]+ B[39]
186 productCost[21] = B[63]
187 productCost[22] = B[35]
188 productCost[23] = B[62]
189 productCost[24] = B[37]+B[41]
190 productCost[25] = B[38]-B[37]
191 productCost[26] = B[16]+B[18]+B[20]+B[22]+B[24]+B[
    26]+B[28]
192 productCost[27] = B[55]+B[56]+B[57]+B[64]
193
194
195 {unit exergetic cost of control volume -- Fuel}
196 kFuel[1] = fuelCost[1]/exergia[55]
197 kFuel[2] = fuelCost[2]/(exergia[2]+exergia[41])
198 kFuel[3] = fuelCost[3]/exergia[56]
199 kFuel[4] = fuelCost[4]/exergia[4]
200
201 kFuel[5] = fuelCost[5]/exergia[8]
202 kFuel[6] = fuelCost[6]/exergia[9]
203 kFuel[7] = fuelCost[7]/exergia[10]
204 kFuel[8] = fuelCost[8]/(exergia[11]+exergia[12])
205 kFuel[9] = fuelCost[9]/(exergia[13]+exergia[14])
206 kFuel[10] = fuelCost[10]/exergia[30]
207
208
209 kFuel[11] = fuelCost[11]/(exergia[16]-exergia[17])
210 kFuel[12] = fuelCost[12]/(exergia[18]-exergia[19])
211 kFuel[13] = fuelCost[13]/(exergia[20]-exergia[21])
212 kFuel[14] = fuelCost[14]/(exergia[22]-exergia[23])
213 kFuel[15] = fuelCost[15]/(exergia[24]-exergia[25])

```

```

214 kFuel[16] = fuelCost[16]/(exergia[26]-exergia[27])
215 kFuel[17] = fuelCost[17]/(exergia[31]-exergia[32])
216
217 kFuel[18] = fuelCost[18]/exergia[28]
218
219
220 kFuel[19] = fuelCost[19]/(exergia[17]+exergia[19]+
    exergia[21]+exergia[23]+exergia[25]+exergia[27]+
    exergia[29]+exergia[32])
221 kFuel[20] = fuelCost[20]/exergia[33]
222 kFuel[21] = fuelCost[21]/exergia[39]
223 kFuel[22] = fuelCost[22]/(exergia[38]+exergia[34])
224 kFuel[23] = fuelCost[23]/(exergia[35]-exergia[36])
225 kFuel[24] = fuelCost[24]/exergia[36]
226 kFuel[25] = fuelCost[25]/exergia[57]
227 kFuel[26] = fuelCost[26]/exergia[15]
228 kFuel[27] = fuelCost[27]/exergia[54]
229
230 {unit exergetic cost of control volume -- Product}
231 kProdut[1] = productCost[1]/(exergia[2]-exergia[1])
232 kProdut[2] = productCost[2]/(exergia[3])
233 kProdut[3] = productCost[3]/(exergia[4]-exergia[3])
234 kProdut[4] = productCost[4]/(exergia[5]+exergia[6]+
    exergia[7])
235
236 kProdut[5] = productCost[5]/(exergia[11]-exergia[5]
    )
237 kProdut[6] = productCost[6]/(exergia[12]-exergia[6]
    )
238 kProdut[7] = productCost[7]/(exergia[13]-exergia[7]
    )
239 kProdut[8] = productCost[8]/(exergia[14]+exergia[15]
    )
240 kProdut[9] = productCost[9]/exergia[30]
241
242 kProdut[10] = productCost[10]/exergia[31]
243
244 kProdut[11] = productCost[11]/exergia[48]
245 kProdut[12] = productCost[12]/exergia[49]
246 kProdut[13] = productCost[13]/exergia[50]
247 kProdut[14] = productCost[14]/exergia[51]
248 kProdut[15] = productCost[15]/exergia[52]
249 kProdut[16] = productCost[16]/exergia[53]
250 kProdut[17] = productCost[17]/exergia[54]
251
252 kProdut[18] = productCost[18]/exergia[29]
253

```



```

254
255 kProdut[19] = productCost[19]/exergia[33]
256 kProdut[20] = productCost[20]/(exergia[34]+exergia[
    39])
257
258
259 kProdut[21] = productCost[21]/(exergia[63])
260
261 kProdut[22] = productCost[22]/(exergia[35])
262 kProdut[23] = productCost[23]/(exergia[62])
263
264 kProdut[24] = productCost[24]/(exergia[37]+exergia[
    41])
265 kProdut[25] = productCost[25]/(exergia[38]-exergia[
    37])
266 kProdut[26] = productCost[26]/(exergia[16]+exergia[
    18]+exergia[20]+exergia[22]+exergia[24]+exergia[
    26]+exergia[28])
267
268 kProdut[27] = productCost[27]/exergia[54]
269
270
271
272
273 {unit exergetic cost ratio}
274 razaoFuelProduct[1] = (kProdut[1] - kFuel[1])/kFuel
    [1]
275 razaoFuelProduct[2] = (kProdut[2] - kFuel[2])/kFuel
    [2]
276 razaoFuelProduct[3] = (kProdut[3] - kFuel[3])/kFuel
    [3]
277 razaoFuelProduct[4] = (kProdut[4] - kFuel[4])/kFuel
    [4]
278
279
280 razaoFuelProduct[5] = (kProdut[5] - kFuel[5])/kFuel
    [5]
281 razaoFuelProduct[6] = (kProdut[6] - kFuel[6])/kFuel
    [6]
282 razaoFuelProduct[7] = (kProdut[7] - kFuel[7])/kFuel
    [7]
283 razaoFuelProduct[8] = (kProdut[8] - kFuel[8])/kFuel
    [8]
284 razaoFuelProduct[9] = (kProdut[9] - kFuel[9])/kFuel
    [9]
285 razaoFuelProduct[10] = (kProdut[10] - kFuel[10])/
    kFuel[10]

```

```

286
287
288
289
290 razaoFuelProduct [11] = (kProdut [11] - kFuel [11]) /
    kFuel [11]
291 razaoFuelProduct [12] = (kProdut [12] - kFuel [12]) /
    kFuel [12]
292 razaoFuelProduct [13] = (kProdut [13] - kFuel [13]) /
    kFuel [13]
293 razaoFuelProduct [14] = (kProdut [14] - kFuel [14]) /
    kFuel [14]
294 razaoFuelProduct [15] = (kProdut [15] - kFuel [15]) /
    kFuel [15]
295 razaoFuelProduct [16] = (kProdut [16] - kFuel [16]) /
    kFuel [16]
296 razaoFuelProduct [17] = (kProdut [17] - kFuel [17]) /
    kFuel [17]
297
298
299 razaoFuelProduct [18] = (kProdut [18] - kFuel [18]) /
    kFuel [18]
300 razaoFuelProduct [19] = (kProdut [19] - kFuel [19]) /
    kFuel [19]
301 razaoFuelProduct [20] = (kProdut [20] - kFuel [20]) /
    kFuel [20]
302 razaoFuelProduct [21] = (kProdut [21] - kFuel [21]) /
    kFuel [21]
303 razaoFuelProduct [22] = (kProdut [22] - kFuel [22]) /
    kFuel [22]
304 razaoFuelProduct [23] = (kProdut [23] - kFuel [23]) /
    kFuel [23]
305 razaoFuelProduct [24] = (kProdut [24] - kFuel [24]) /
    kFuel [24]
306 razaoFuelProduct [25] = (kProdut [25] - kFuel [25]) /
    kFuel [25]
307 razaoFuelProduct [26] = (kProdut [26] - kFuel [26]) /
    kFuel [26]
308 razaoFuelProduct [27] = (kProdut [27] - kFuel [27]) /
    kFuel [27]
309
310
311 //
    //////////////////////////////////////
    Balanço de massa, energia, exergia e custo
    exergético
    //////////////////////////////////////

```

```

312
313
314
315   T[0] = 25 [°C]
316   P[0] = 1,01 [bar]
317   h[0]=enthalpy(Steam;T=T[0];P=P[0])
318   s[0]=entropy(Steam;T=T[0];P=P[0])
319   T_0 = 25+273,15
320
321   //
          //////////////////////////////////////
          Equipamento 1 ---- Bomba 1
          //////////////////////////////////////

322
323   /// Dados de entrada da bomba -- Bomba eleva
          pressão ambiente até 2.5 bar
324   T[1] = 25
325   P[1] = 1,01
326   P[2] = 2,5
327   eta_pump1 = 0,70
328
329
330   W_pump1 = -1,5
331
332   /// balanço de massa
333
334   W_pump1 = m[1]*(h[1]-h[2])
335
336   T[2] = temperature(Steam;P=P[2];h=h[2])
337
338
339
340
341
342   h[1]=enthalpy(Steam;T=T[1];P=P[1])
343   s[1]=entropy(Steam;T=T[1];P=P[1])
344   h2_iso = enthalpy(Steam;P=P[2];s=s[1])
345   v[1]=volume(Water;T=T[1];P=P[1])
346   s[2]=entropy(Steam;T=T[2];P=P[2])
347
348   m[1] = m[2]
349
350   m[1] = m[40]
351
352

```

```

353
354 /// calculo das propriedades termodinâmicas
355
356
357
358 /// calculo de h[2]
359
360 {
361 eta_pump1 = (h[1]-h2_iso)/(h[1]-h[2])
362 T[2]=temperature(Water,P=P[2],h=h[2])
363
364
365 W_pump1 = (v[1]*(P[1]-P[2])*100)/eta_pump1 }
366
367 W[55] = -W_pump1
368
369 B_destruido_pump1 = W[55] + m[1]*(e[1]-e[2])
370
371
372
373
374
375 //
    //////////////////////////////////////
    Equipamento 3 ---- Bomba 2
    //////////////////////////////////////

376
377 /// Informações da bomba fornecida pela empresa
378
379 W_pump2 = -350
380 P[4] = 32
381
382 /// Balanço de massa
383
384 m[4]=m[3]
385
386 /// Balanço de energia
387
388
389
390 W_pump2 = m[4]*(h[3]-h[4]) /// Determinando h[4]
391
392 W[56] = -W_pump2
393
394 T[4] = temperature(Steam;P=P[4];h=h[4])
395

```



```

////////////////////////////////////
437
438 P[3] = P[2]
439
440
441
442 /// balanço de massa
443
444 m[3] = m[41]+m[2]
445
446 /// balanço de energia
447
448 m[2]*h[2]+m[41]*h[41]=m[3]*h[3]    /// determinar a
    entalpia do ponto 3 para determinar a temperatura
    e entropia
449
450
451
452 T[3]=temperature(Steam;P=P[3];h=h[3])
453 s[3]=entropy(Steam;T=T[3];P=P[3])
454
455
456 B_destruido_desaerador = m[41]*e[41]+m[2]*e[2]-m[3]
    *e[3]
457
458
459
460
461
462 //
    //////////////////////////////////////
    Equipamento 4 ---- Distribution chamber 1
    //////////////////////////////////////

463
464
465 /// balanço de massa
466
467 m[4]=m[5]+m[6]+m[7]
468
469 /// balanço de energia
470
471 m[4]*h[4]=m[5]*h[5]+m[6]*h[6]+m[7]*h[7]
472 B_destruido_camara1 = m[4]*e[4]-m[5]*e[5]-m[6]*e[6]
    -m[7]*e[7]
473

```

```

474  /// equipamento virtual; propriedades não variam.
475  T[5] = T[4]
476  P[5] = P[4]
477  T[6] = T[4]
478  P[6] = P[4]
479  T[7] = T[4]
480  P[7] = P[4]
481  h[5]=enthalpy(Steam;T=T[5];P=P[5])
482  s[5]=entropy(Steam;T=T[5];P=P[5])
483  h[6]=enthalpy(Steam;T=T[6];P=P[6])
484  s[6]=entropy(Steam;T=T[6];P=P[6])
485  s[7]=entropy(Steam;T=T[7];P=P[7])
486
487
488
489
490
491
492
493
494
495
496  //
    //////////////////////////////////////
    Equipamento 5,6 e 7 ---- Caldeira 1,2 e 3
    //////////////////////////////////////

497
498
499  T_j = 170+273,15  //qual tempeartura usar??  --
    usei a temperatura do gás - saída da caldeira -
500  b_bagaco = 8536,833  //retirado artigo de monica
501  PCI_bagaco = 7436  /// retirado da tabela da
    industria
502
503
504
505  ///Consumo de vapor das caldeiras em toneladas por
    horas fornecido pela industria
506  consumo_cald_1 = 28
507  consumo_cald_2 = 70
508  consumo_cald_3 = 77
509
510  /// Converter para kg/s
511
512  conv = 0,277778  /// Fator de conversão de
    tonelada para kg/s

```

```

513
514 consumo_cald_1_kg_s = consumo_cald_1*conv
515 consumo_cald_2_kg_s = consumo_cald_2*conv
516 consumo_cald_3_kg_s = consumo_cald_3*conv
517
518 ///Consumo de vapor das caldeiras em kg/s
519
520 m[11] = consumo_cald_1_kg_s
521 m[12] = consumo_cald_2_kg_s
522 m[13] = consumo_cald_3_kg_s
523
524 T[11] = 294 [°C] //dados fornecidos pela industria
525 P[11] = 22 [bar] //dados fornecidos pela industria
526 T[12] = 295 [°C] //dados fornecidos pela industria
527 P[12] = 22 [bar] //dados fornecidos pela industria
528 T[13] = 333 [°C] //dados fornecidos pela industria
529 P[13] = 22 [bar] //dados fornecidos pela industria
530
531 {entalpias e entropias para 11 - 12 - 13}
532
533 h[11]=enthalpy(Steam;T=T[11];P=P[11])
534 s[11]=entropy(Steam;T=T[11];P=P[11])
535 h[12]=enthalpy(Steam;T=T[12];P=P[12])
536 s[12]=entropy(Steam;T=T[12];P=P[12])
537 h[13]=enthalpy(Steam;T=T[13];P=P[13])
538 s[13]=entropy(Steam;T=T[13];P=P[13])
539 s[14]=entropy(Steam;T=T[14];P=P[14])
540 s[15]=entropy(Steam;T=T[15];P=P[15])
541
542 m[5]=m[11]
543 m[6]=m[12]
544
545
546 /// Foi fornecido pela usina que cada kg de bagaço
    produz 1,8 de vapor
547
548 fator_conv_vapor = 1,8
549
550 /// Consumo de bagaço na caldeira em toneladas
551
552 bagaco_1 = consumo_cald_1/fator_conv_vapor ///
    dado que cada kg de bagaço produz 1,8 de vapor
553 bagaco_2 = consumo_cald_2/fator_conv_vapor
554 bagaco_3 = consumo_cald_3/fator_conv_vapor
555
556 /// converter consumo de bagaço na caldeira de
    toneladas para kg/s

```



```

557
558 m[8] = bagaco_1*conv
559 m[9] = bagaco_2*conv
560 m[10] = bagaco_3*conv
561
562
563 /// frações molares dos produtos
564
565 R=8,314
566 C02 = 0,1146
567 H2O=0,2626
568 N2=0,5867
569 O2=0,0359
570
571 //calculo da massa molecular aparente
572
573 MMC02 = 44
574 MMH2O = 18
575 MM02 = 16
576 MMN2= 28
577 MM_ap = C02*MMC02+H2O*MMH2O+O2*MM02+N2*MMN2
578
579 /// formula da pagina 674 do shapiro e dados de Y
    retirados da tabela A1 do kotas, pagina 254 do
    pdf
580 YC02 = 3,45*10^(-4)
581 YH2O = 0,0088/1,01325
582 YO2 = 0,2099
583 YN2= 0,7803
584
585
586 bar_C02 = 20140
587 bar_H2O = 11710
588 bar_O2 = 3970
589 bar_N2 = 720
590
591 ref_C02 = bar_C02*C02 + ((hC02-h0C02)-T_0*(sC02-
    s0C02))
592 ref_H2O=bar_H2O*H2O + ((hH2O-h0H2O)-T_0*(sH2O-s0H2O
    ))
593 ref_O2=bar_O2*O2 + ((hO2-h0O2)-T_0*(sO2-s0O2))
594 ref_N2=bar_N2*N2 + ((hN2-h0N2)-T_0*(sN2-s0N2))
595 e_ch_1 = ref_C02+ref_H2O+ref_O2+ref_N2
596 e_ch_2 = R*T_0*(C02*ln(C02)+H2O*ln(H2O)+O2*ln(O2)+
    N2*ln(N2))
597 e_ch = e_ch_1+e_ch_2
598 e_ch_total = (e_ch)/(MM_ap)

```

```

599
600
601 //valores retirado da tabela A-23 - pagina 774
602 {para temp ambiente}
603 h0C02=9364
604 s0C02=213,685
605 h0H20 = 9904
606 s0H20= 188,720
607 h002 = 8682
608 s002 = 205,033
609 h0N2 = 8669
610 s0N2 = 191,502
611 {ara temp de 170 graus ~~ aproximadamente 450K}
612 hC02 = 15483
613 sC02 = 230,194
614 hH20= 15080
615 sH20 = 202,734
616 h02 = 13228
617 s02 = 217,342
618 hN2 = 13105
619 sN2 = 203,523
620
621 h_mistura450 = C02*hC02+H20*hH20+O2*h02+N2*hN2
622 s_mistura450 = C02*sC02+H20*sH20+O2*s02+N2*sN2 - R*
        (ln(C02)+ln(H20)+ln(O2)+ln(N2))
623 h_mistura_ref = C02*h0C02+H20*h0H20+O2*h002+N2*h0N2
624 s_mistura_ref = C02*s0C02+H20*s0H20+O2*s002+N2*s0N2
        - R*(ln(C02)+ln(H20)+ln(O2)+ln(N2))
625 h_mistura450kg = h_mistura450/(MM_ap)
626 h_mistura_refkg = h_mistura_ref/(MM_ap)
627 s_mistura450kg = s_mistura450/(MM_ap)
628 s_mistura_ref450kg = s_mistura_ref/(MM_ap)
629
630
631 e_ph_C02 = (hC02-h0C02)-T_0*(sC02-s0C02)
632 e_ph_H20 = (hH20-h0H20)-T_0*(sH20-s0H20)
633 e_ph_02 = (h02-h002)-T_0*(s02-s002)
634 e_ph_N2 = (hN2-h0N2)-T_0*(sN2-s0N2)
635
636
637
638 vazao_ar = m[8]*3,62
639 vazao_ar2 = m[9]*3,62
640 vazao_ar3 = m[10]*3,62
641 gases_b1 = m[8]+vazao_ar
642 gases_b2 = m[9]+vazao_ar2
643 gases_b3 = m[10]+vazao_ar3

```

```

644 m[42]=vazao_ar
645 m[43]=vazao_ar2
646 m[44]=vazao_ar3
647 m[45]=gases_b1
648 m[46]=gases_b2
649 m[47]=gases_b3
650
651
652 Q_perdido_gases_1 = gases_b1*(h_mistura_refkg-
    h_mistura450kg)
653 Q_perdido_gases_2 = gases_b2*(h_mistura_refkg-
    h_mistura450kg)
654 Q_perdido_gases_3 = gases_b3*(h_mistura_refkg-
    h_mistura450kg)
655 Q[59] = Q_perdido_gases_1
656 Q[60] = Q_perdido_gases_2
657 Q[61] = Q_perdido_gases_3
658
659 exergia_destruidagases = gases_b1*e_ch_total+
    gases_b2*e_ch_total+gases_b3*e_ch_total
660
661
662
663
664 //////////////////////////////////////
    Caldeira
    1////////////////////////////////////
665
666
667 Q_bagaco1 = m[8]*PCI_bagaco
668 Q_cald1 = m[5]*(h[11]-h[5])
669 Q_p_caldeira1 = Q_bagaco1-Q_cald1
670 Q_p_caldeira1 = Q_perdido_parede1+Q_perdido_gases_1
671 B_qp_caldeira1 = Q_perdido_parede1*(1-T_0/T_j)
672 B_q_caldeira1 = Q_perdido_gases_1*(1-T_0/T_j)
673 B_bagaco1 = m[8]*b_bagaco // exergia do bagaço
674 B_agua_caldeira1 = m[5]*e[5] // exergia que
    acompanha o fluxo de água na entrada da caldeira
675 B_vapor_caldeira1 = m[5]*e[11] // exergia que
    acompanha o vapor
676 B_destruido_caldeira_1 = B_bagaco1+
    B_agua_caldeira1-B_vapor_caldeira1-B_q_caldeira1-
    B_qp_caldeira1 // exergia destruida
677
678
679

```

```

680
681 ///////////////////////////////////////////////////
    Caldeira
    2/////////////////////////////////////////////////

682 Q_bagaco2 = m[9]*PCI_bagaco
683 Q_cald2 = m[6]*(h[12]-h[6])
684 Q_p_caldeira2 = Q_bagaco2-Q_cald2
685 Q_p_caldeira2 = Q_perdido_parede2+Q_perdido_gases_2
686 B_qp_caldeira2 = Q_perdido_parede2*(1-T_0/T_j)
687 B_q_caldeira2 = Q_perdido_gases_2*(1-T_0/T_j)
688 B_bagaco2 = m[9]*b_bagaco // exergia do bagaço
689 B_agua_caldeira2 = m[6]*e[6] // exergia que
    acompanha o fluxo de água na entrada da caldeira
690 B_vapor_caldeira2 = m[6]*e[12] // exergia que
    acompanha o vapor
691 B_destruido_caldeira_2 = B_bagaco2+
    B_agua_caldeira2-B_vapor_caldeira2-B_q_caldeira2-
    B_qp_caldeira2 + gases_b2*e_ch_total // exergia
    destruida

692
693
694
695 ///////////////////////////////////////////////////
    Caldeira
    3/////////////////////////////////////////////////

696 Q_bagaco3 = m[10]*PCI_bagaco
697 Q_cald3 = m[7]*(h[13]-h[7])
698 Q_p_caldeira3 = Q_bagaco3-Q_cald3
699 Q_p_caldeira3 = Q_perdido_parede3+Q_perdido_gases_3
700 B_qp_caldeira3=Q_perdido_parede3*(1-T_0/T_j)
701 B_q_caldeira3 = Q_perdido_gases_3*(1-T_0/T_j)
702 B_bagaco3 = m[10]*b_bagaco // exergia do bagaço
703 B_agua_caldeira3 = m[7]*e[7] // exergia que
    acompanha o fluxo de água na entrada da caldeira
704 B_vapor_caldeira3 = m[7]*e[13] // exergia que
    acompanha o vapor
705 B_destruido_caldeira_3 = B_bagaco3+
    B_agua_caldeira3-B_vapor_caldeira3-B_q_caldeira3-
    B_qp_caldeira3 + gases_b3*e_ch_total// exergia
    destruida

706
707
708
709
710 {rendimentos caldeiras}

```

```

711
712 eta_cald1 = (Q_cald1)/(m[8]*PCI_bagaco)
713 eta_cald2 = (Q_cald2)/(m[9]*PCI_bagaco)
714 eta_cald3 = (Q_cald3)/(m[10]*PCI_bagaco)
715 Efuel = m[8]*b_bagaco+m[9]*b_bagaco+m[10]*b_bagaco
716 epsilon_cald1 = m[5]*(e[11]-e[5])/(m[8]*b_bagaco)
717 epsilon_cald2 = m[6]*(e[12]-e[6])/(m[9]*b_bagaco)
718 epsilon_cald3 = m[7]*(e[13]-e[7])/(m[10]*b_bagaco)
719
720
721 //
    //////////////////////////////////////
    Equipamento 8 e 9 ---- Mixing chamber 1 e 2
    //////////////////////////////////////

722
723
724
725
726
727
728
729
730 {balanço de massa mixing chamber 1}
731
732
733 {balanço de massa}
734 m[11]+m[12]=m[14]+m[15]
735
736 m[11]*h[11]+m[12]*h[12]=m[14]*h[14]+m[15]*h[15]
737
738 h[14]=h[15]
739
740 B_destruido_mix1 = m[11]*e[11]+m[12]*e[12]-m[14]*e
    [14]-m[15]*e[15] // sum B_entrada - sum B_saida
    --- pontos 11;12;14;15:

741
742
743
744 {temperatura na saída da mixing chamber 1 - 2}
745 P[14] = 22 [bar]
746 P[15]= P[14]
747 T[14]=temperature(Steam;P=P[14];h=h[14])
748 T[15] = T[14]
749
750 {balanço de massa mixing chamber 2}
751

```

```

752 m[30] = 85,71*conv //consumo de vapor medido pela
      industria
753
754 m[13]+m[14]=m[30]
755
756 {balanço de energia para mixing chamber 2}
757
758 m[13]*h[13]+m[14]*h[14]=m[30]*h[30]
759 B_destruido_mix2 = m[13]*e[13]+m[14]*e[14]-m[30]*e[
      30]
760
761
762
763
764
765
766
767 //
      //////////////////////////////////////
      Equipamento 10 ---- Steam pipe
      //////////////////////////////////////
768
769 Q_p_steampipe = m[30]*(h[31]-h[30])
770 Q[58]=Q_p_steampipe
771 steam_pipe_temp = (T[31]+T[30])/2+273,15
772 B_destruido_heat_losses = m[30]*e[30]-m[31]*e[31]
773
774
775 //
      //////////////////////////////////////
      Equipamento 11 ao 17 ---- Turbinas 1 a Turbina
      7
      //////////////////////////////////////
776
777
778
779 {Turbinan 01}
780 T[16] = 294,5 // dado fornecido pela industria
781 P[16] = 21,5 // dado fornecido pela industria
782 T[17] = 190 // dado fornecido pela industria
783 P[17] = 2,5 // dado fornecido pela industria
784 m[16] = 18,22*conv // dado fornecido pela industria
785 m[17]=m[16]
786 W_T1 = m[16]*(h[16]-h[17])
787 h_isoT1 =enthalpy(Steam;P=P[17];s=s[16])

```

```

788 W_isoT1 = m[16]*(h[16]-h_isoT1)
789 eta_T1 = W_T1/W_isoT1
790 W_dispT1 = m[16]*(e[16]-e[17]) //trabalho
      disponível
791 W_destruidoT1 = W_dispT1 - W_T1
792 epsilon_T1 = W_T1/W_dispT1 // rendimento de segunda
      lei => trabalho real / trabalho disponível:
793 W_T1 = W[48]
794
795
796
797
798 h[16]=enthalpy(Steam;T=T[16];P=P[16])
799 s[16]=entropy(Steam;T=T[16];P=P[16])
800 h[17]=enthalpy(Steam;T=T[17];P=P[17])
801 s[17]=entropy(Steam;T=T[17];P=P[17])
802
803
804
805
806 {Turbinan 02}
807 T[18] = 290 // dado fornecido pela industria
808 P[18] = 21,2 // dado fornecido pela industria
809 T[19] = 160 // dado fornecido pela industria
810 P[19] = 2,6 // dado fornecido pela industria
811 m[18] = 23,33*conv // dado fornecido pela industria
812 m[19]=m[18]
813 W_T2 = m[18]*(h[18]-h[19])
814 W_isoT2 = m[18]*(h[18]-h_isoT2)
815 eta_T2 = W_T2/W_isoT2
816
817 W_dispT2 = m[18]*(e[18]-e[19]) //trabalho
      disponível
818 W_destruidoT2 = W_dispT2 - W_T2
819 epsilon_T2 = W_T2/W_dispT2 // rendimento de segunda
      lei => trabalho real / trabalho disponível:
820 W_T2 = W[49]
821
822 h[18]=enthalpy(Steam;T=T[18];P=P[18])
823 s[18]=entropy(Steam;T=T[18];P=P[18])
824 h[19]=enthalpy(Steam;T=T[19];P=P[19])
825 s[19]=entropy(Steam;T=T[19];P=P[19])
826 h_isoT2 =enthalpy(Steam;P=P[19];s=s[18])
827
828
829
830

```

```

831
832
833         {Turbinan 03}
834 T[20] = 280 // dado fornecido pela industria
835 P[20] = 21,6 // dado fornecido pela industria
836 T[21] = 168 // dado fornecido pela industria
837 P[21] = 2,7 // dado fornecido pela industria
838 m[20]=9,95*conv // dado fornecido pela industria
839 m[21]=m[20]
840 W_T3 = m[20]*(h[20]-h[21])
841 W_isoT3 = m[20]*(h[20]-h_isoT3)
842 eta_T3 = W_T3/W_isoT3
843
844 W_dispT3 = m[20]*(e[20]-e[21]) //trabalho
      disponível
845 W_destruidoT3 = W_dispT3 - W_T3
846 epsilon_T3 = W_T3/W_dispT3 // rendimento de segunda
      lei => trabalho real / trabalho disponível:
847 W_T3 = W[50]
848
849
850 h[20]=enthalpy(Steam;T=T[20];P=P[20])
851 s[20]=entropy(Steam;T=T[20];P=P[20])
852 h[21]=enthalpy(Steam;T=T[21];P=P[21])
853 s[21]=entropy(Steam;T=T[21];P=P[21])
854 h_isoT3 =enthalpy(Steam;P=P[21];s=s[20])
855
856
857
858
859
860
861         {Turbinan 04}
862 T[22] = 282 // dado fornecido pela industria
863 P[22] = 21,5 // dado fornecido pela industria
864 T[23] = 152 // dado fornecido pela industria
865 P[23] = 2,6 // dado fornecido pela industria
866 m[22] = 8,00*conv // dado fornecido pela industria
867 m[23] = m[22]
868 W_T4 = m[22]*(h[22]-h[23])
869 W_isoT4 = m[22]*(h[22]-h_isoT4)
870 eta_T4 = W_T4/W_isoT4
871
872 W_dispT4 = m[22]*(e[22]-e[23]) //trabalho
      disponível
873 W_destruidoT4 = W_dispT4 - W_T4
874 epsilon_T4 = W_T4/W_dispT4 // rendimento de segunda

```



```

    lei => trabalho real / trabalho disponível:
875 W_T4 = W[51]
876
877 h[22]=enthalpy(Steam;T=T[22];P=P[22])
878 s[22]=entropy(Steam;T=T[22];P=P[22])
879 h[23]=enthalpy(Steam;T=T[23];P=P[23])
880 s[23]=entropy(Steam;T=T[23];P=P[23])
881 h_isoT4 =enthalpy(Steam;P=P[23];s=s[22])
882
883
884
885
886
887
888 {Turbinan 05}
889 T[24] = 282 // dado fornecido pela industria
890 P[24] = 21,5 // dado fornecido pela industria
891 T[25] = 153 // dado fornecido pela industria
892 P[25] = 2,5 // dado fornecido pela industria
893 m[24] = 8,92*conv // dado fornecido pela industria
894 m[25]=m[24]
895 W_T5 = m[25]*(h[24]-h[25])
896 W_isoT5 = m[24]*(h[24]-h_isoT5)
897 eta_T5 = W_T5/W_isoT5
898
899 W_dispT5 = m[24]*(e[24]-e[25]) //trabalho
    disponível
900 W_destruidoT5 = W_dispT5 - W_T5
901 epsilon_T5 = W_T5/W_dispT5 // rendimento de segunda
    lei => trabalho real / trabalho disponível:
902 W_T5 = W[52]
903
904 h[24]=enthalpy(Steam;T=T[24];P=P[24])
905 s[24]=entropy(Steam;T=T[24];P=P[24])
906 h[25]=enthalpy(Steam;T=T[25];P=P[25])
907 s[25]=entropy(Steam;T=T[25];P=P[25])
908 h_isoT5 =enthalpy(Steam;P=P[25];s=s[24])
909
910
911
912
913
914
915 {Turbinan 06}
916 T[26] = 281 // dado fornecido pela industria
917 P[26] = 21,5 // dado fornecido pela industria
918 T[27] = 183 // dado fornecido pela industria

```

```

919 P[27] = 2,7 // dado fornecido pela industria
920 m[26] = 10,40*conv // dado fornecido pela industria
921 m[27] = m[26]
922 W_T6 = m[26]*(h[26]-h[27])
923
924 W_isoT6 = m[26]*(h[26]-h_isoT6)
925 eta_T6 = W_T6/W_isoT6
926
927 W_dispT6 = m[26]*(e[26]-e[27]) //trabalho
    disponível
928 W_destruidoT6 = W_dispT6 - W_T6
929 epsilon_T6 = W_T6/W_dispT6 // rendimento de segunda
    lei => trabalho real / trabalho disponível:
930 W_T6 = W[53]
931
932 h[26]=enthalpy(Steam;T=T[26];P=P[26])
933 s[26]=entropy(Steam;T=T[26];P=P[26])
934 h[27]=enthalpy(Steam;T=T[27];P=P[27])
935 s[27]=entropy(Steam;T=T[27];P=P[27])
936 h_isoT6 =enthalpy(Steam;P=P[27];s=s[26])
937
938
939
940
941
942
943
944
945         {Turbinan 07}
946 m[30] = m[31] // dado fornecido pela industria
947 P[30] = 22 // dado fornecido pela industria
948 T[30] = temperature(Water;P=P[30];h=h[30])
949 s[30] = entropy(Steam;T=T[30];P=P[30])
950 T[31] = 314 // dado fornecido pela industria
951 P[31] = 21,5 // dado fornecido pela industria
952 T[32] = 152 // dado fornecido pela industria
953 P[32] = 2,7 // dado fornecido pela industria
954 m[32]=m[31]
955 W_T7 = m[32]*(h[31]-h[32])
956 W_isoT7 = m[32]*(h[31]-h_isoT7)
957 eta_T7 = W_T7/W_isoT7
958
959 W_dispT7 = m[31]*(e[31]-e[32]) //trabalho
    disponível
960 W_destruidoT7 = W_dispT7 - W_T7
961 epsilon_T7 = W_T7/W_dispT7 // rendimento de segunda
    lei => trabalho real / trabalho disponível:

```

```

962 W_T7 = W[54]
963
964
965 h[31] = enthalpy(Steam;T=T[31];P=P[31])
966 s[31]=entropy(Steam;T=T[31];P=P[31])
967 h[32] = enthalpy(Steam;T=T[32];P=P[32])
968 s[32]=entropy(Steam;T=T[32];P=P[32])
969 h_isoT7=enthalpy(Steam;P=P[32];s=s[31])
970
971
972
973
974
975
976
977
978 //
          //////////////////////////////////////
          Equipamento 18 e 26 ---- Distribution chamber
          2 e valvula
          //////////////////////////////////////

979
980 m[15] = m[16]+m[18]+m[20]+m[22]+m[24]+m[26]+m[28]
981
982
983 m[15]*h[15] = m[16]*h[16]+m[18]*h[18]+m[20]*h[20]+m
          [22]*h[22]+m[24]*h[24]+m[26]*h[26]+m[28]*h[28]+
          Q_distribution_turbines
984
985
986 B_destruido_destrubuction = m[15]*e[15] - (m[16]*e[
          16]+m[18]*e[18]+m[20]*e[20]+m[22]*e[22]+m[24]*e[
          24]+m[26]*e[26]+m[28]*e[28])
987
988
989
990 T[28] = T[15]
991 P[28] = P[15]
992 h[28]=h[15]
993 h[29]=h[28]
994 P[29] = 2,5
995 T[29]=temperature(Steam;P=P[29];h=h[29])
996 m[28]=m[29]
997 s[28]=entropy(Steam;T=T[28];P=P[28])
998 s[29]=entropy(Steam;T=T[29];P=P[29])
999 B_destruido_valvula = m[28]*(e[28]-e[29])

```

```

1000
1001
1002
1003
1004
1005  //
      //////////////////////////////////////
      Equipamento 19  ---- Mixing chamber 3
      //////////////////////////////////////

1006
1007  B_destruido_mix3 = m[17]*e[17]+m[19]*e[19]+m[21]*e
      [21]+m[23]*e[23]+m[25]*e[25]+m[27]*e[27]+m[29]*e
      [29]+m[32]*e[32]-m[33]*e[33]

1008
1009  m[33] = m[15]+m[32]
1010  m[17]*h[17]+m[19]*h[19]+m[21]*h[21]+m[23]*h[23]+m[
      25]*h[25]+m[27]*h[27]+m[29]*h[29]+m[32]*h[32] = m
      [33]*h[33]
1011  P[33] = 2,5
1012  T[33]=temperature(Steam;P=P[33];h=h[33])
1013  s[33]=entropy(Steam;T=T[33];P=P[33])
1014
1015
1016
1017
1018
1019
1020
1021
1022  //
      //////////////////////////////////////
      Equipamento 20  ---- Distribution chamber 2
      //////////////////////////////////////

1023
1024
1025  T[34] = T[33]
1026  P[34]=P[33]
1027  T[39] = T[33]
1028  P[39]=P[33]
1029  h[34]=h[33]
1030  s[34]=s[33]
1031  h[39]=h[33]
1032  s[39]=s[33]
1033  m[39] = 35*conv // dado fornecido pela industria =
      consumo de vapor para destilaria em kg/s

```

```

1034 m[34] = m[33] - m[39]
1035
1036
1037
1038 B_destruido_camara2 = m[33]*e[33] - m[34]*e[34] - m[39
    ]*e[39]
1039
1040
1041
1042
1043 B_destruido_camara3 = m[36]*e[36] - m[37]*e[37] - m[41
    ]*e[41]
1044
1045
1046
1047
1048 //
    //////////////////////////////////////
    Equipamento 21 ---- Distilaria
    //////////////////////////////////////

1049
1050 h[40] = enthalpy(Water; x=0; P=P[39])
1051 P[40] = P[39]
1052 T[40] = temperature(Water; P=P[40]; h=h[40]) // como
    não tínhamos temperatura na saída; foi
    determinado a temperatura usando líquido saturado
    ; i.e. x=0
1053 m[40] = m[39]
1054 s[40] = entropy(Water; x=0; P=P[40])
1055 Q_destilaria = m[39]*(h[39] - h[40])
1056 T_destilaria = T[40] + 273,15
1057 B_q_destilaria = Q_destilaria*(1 - T_0/T_destilaria)
1058 B_destruido_destilaria = m[39]*e[39] - B_q_destilaria
    - m[40]*e[40]
1059 Q_destilaria = Q[62]
1060
1061
1062
1063
1064
1065
1066
1067 //
    //////////////////////////////////////
    Equipamento 22 ---- Desuperaquecedor
    //////////////////////////////////////

```

```

1068
1069
1070   T[35] = 128    ///set point fornecido pela
        industria
1071   P[35] = 2,5
1072   P[38] = 3
1073   m[34]*h[34]+m[38]*h[38]=m[35]*h[35]
1074   m[35] = m[34]+m[38]
1075
1076   h[35]=enthalpy(Steam;T=T[35];P=P[35])
1077   s[35]=entropy(Steam;T=T[35];P=P[35])
1078   s[38]=entropy(Steam;T=T[38];P=P[38])
1079
1080   B_destruido_dessuperaquecedor = m[34]*e[34]+m[38]*e
        [38]-m[35]*e[35]
1081
1082
1083
1084
1085   //
        //////////////////////////////////////
        Equipamento 23  ---- Sugar Production
        //////////////////////////////////////

1086
1087
1088
1089   T[36] = 95 // dado fornecido pela industria
1090   P[36] = P[35]
1091   m[36] = m[35]
1092   Q_sugar = m[36]*(h[35]-h[36])
1093   Q[63]=Q_sugar
1094
1095   /// mudança de fase ocorrendo a temperatura T = 128
        graus. Dessa forma a destruição de exergia foi
        dividido em duas partes.
1096   hx1 = enthalpy(Water;P=P[35];x=1)
1097   hx2 = enthalpy(Water;P=P[35];x=0)
1098
1099   Tx1=temperature(Water;P=P[35];h=hx1)
1100   {mudança de fase a T constante}
1101   Q_sugar_production = m[35]*(h[35]-hx2)
1102   T_sugar = T[35]+273,15
1103   B_q_sugar_production = Q_sugar_production*(1-T_0/
        T_sugar)
1104   {com T variável}

```

```

1105 Q_sugar_var = m[35]*(hx2-h[36])
1106 T_sugar_var = T[36] + 273,15
1107 B_q_sugar_production_var = Q_sugar_var*(1-T_0/
      T_sugar_var)
1108 {destruição de exergia}
1109 B_destruido_sugar_production = m[35]*e[35]-(
      B_q_sugar_production+B_q_sugar_production_var)-m[
      36]*e[36]
1110
1111
1112 h[36]=enthalpy(Steam;T=T[36];P=P[36])
1113 s[36]=entropy(Steam;T=T[36];P=P[36])
1114
1115
1116
1117
1118
1119
1120 //
      //////////////////////////////////////
      Equipamento 24 ---- Distribution chamber 3
      //////////////////////////////////////

1121
1122 T[37]=T[36]
1123 P[37]=P[36]
1124 T[41]=T[36]
1125 P[41]=P[36]
1126
1127 m[37]=m[38]
1128 m[41]=m[36]-m[37]
1129
1130 h[37]=h[36]
1131 s[37]=s[36]
1132 h[41]=h[36]
1133 s[41]=s[36]
1134
1135 Q_destrubution_chamber_3 = m[15]*h[15] - m[16]*h[
      16]- m[16]*h[16] - m[18]*h[18]- m[20]*h[20] - m[
      22]*h[22] - m[24]*h[24] - m[26]*h[26] - m[28]*h[
      28]
1136
1137 //
      //////////////////////////////////////
      Equipamento 27 ---- Gerador
      //////////////////////////////////////

```

```

1138
1139 W[64]=W[54]-W[57]-W[56]-W[55]
1140
1141
1142
1143
1144
1145
1146
1147 //
    //////////////////////////////////////
    Rendimentos
    //////////////////////////////////////

1148 W_mec = W_T1+W_T2+W_T3+W_T4+W_T5+W_T6
1149 W_liq=W[64]
1150 cogeraçao = (W_liq+Q[62]+W_mec+Q[63])/(Q_bagacos)
1151 cogeraçao2 = (W_liq+B_q_sugar_production+
    B_q_sugar_production_var+W_mec+B_q_destilaria)/(
    Efuel)
1152 Q_bagacos= Q_bagaco1+Q_bagaco2+Q_bagaco3
1153 eta_eletrico = 100*(W_liq)/(Q_bagacos)
1154 eta_eletrico2 = 100*(W_liq)/(Efuel)
1155
1156
1157 //
    //////////////////////////////////////
    FLUXOS DE EXERGIA UNIDADE DE MASSA
    //////////////////////////////////////

1158
1159 {exergias}
1160 e[1] = (h[1]-h[0]) - T_0*(s[1]-s[0])
1161 e[2] = (h[2]-h[0]) - T_0*(s[2]-s[0])
1162 e[3] = (h[3]-h[0]) - T_0*(s[3]-s[0])
1163 e[4] = (h[4]-h[0]) - T_0*(s[4]-s[0])
1164 e[5] = (h[5]-h[0]) - T_0*(s[5]-s[0])
1165 e[6] = (h[6]-h[0]) - T_0*(s[6]-s[0])
1166 e[7] = (h[7]-h[0]) - T_0*(s[7]-s[0])
1167 e[11] = (h[11]-h[0]) - T_0*(s[11]-s[0])
1168 e[12] = (h[12]-h[0]) - T_0*(s[12]-s[0])
1169 e[13] = (h[13]-h[0]) - T_0*(s[13]-s[0])
1170 e[14] = (h[14]-h[0]) - T_0*(s[14]-s[0])
1171 e[15] = (h[15]-h[0]) - T_0*(s[15]-s[0])
1172 e[16] = (h[16]-h[0]) - T_0*(s[16]-s[0])
1173 e[17] = (h[17]-h[0]) - T_0*(s[17]-s[0])
1174 e[18] = (h[18]-h[0]) - T_0*(s[18]-s[0])

```



```

1175 e[19] = (h[19]-h[0]) - T_0*(s[19]-s[0])
1176 e[20] = (h[20]-h[0]) - T_0*(s[20]-s[0])
1177 e[21] = (h[21]-h[0]) - T_0*(s[21]-s[0])
1178 e[22] = (h[22]-h[0]) - T_0*(s[22]-s[0])
1179 e[23] = (h[23]-h[0]) - T_0*(s[23]-s[0])
1180 e[24] = (h[24]-h[0]) - T_0*(s[24]-s[0])
1181 e[25] = (h[25]-h[0]) - T_0*(s[25]-s[0])
1182 e[26] = (h[26]-h[0]) - T_0*(s[26]-s[0])
1183 e[27] = (h[27]-h[0]) - T_0*(s[27]-s[0])
1184 e[28] = (h[28]-h[0]) - T_0*(s[28]-s[0])
1185 e[29] = (h[29]-h[0]) - T_0*(s[29]-s[0])
1186 e[30] = (h[30]-h[0]) - T_0*(s[30]-s[0])
1187 e[31] = (h[31]-h[0]) - T_0*(s[31]-s[0])
1188 e[32] = (h[32]-h[0]) - T_0*(s[32]-s[0])
1189 e[33] = (h[33]-h[0]) - T_0*(s[33]-s[0])
1190 e[34] = (h[34]-h[0]) - T_0*(s[34]-s[0])
1191 e[35] = (h[35]-h[0]) - T_0*(s[35]-s[0])
1192 e[36] = (h[36]-h[0]) - T_0*(s[36]-s[0])
1193 e[37] = (h[37]-h[0]) - T_0*(s[37]-s[0])
1194 e[38] = (h[38]-h[0]) - T_0*(s[38]-s[0])
1195 e[39] = (h[39]-h[0]) - T_0*(s[39]-s[0])
1196 e[40] = (h[40]-h[0]) - T_0*(s[40]-s[0])
1197 e[41] = (h[41]-h[0]) - T_0*(s[41]-s[0])
1198 //

```

```

////////////////////////////////////
FIM DOS FLUXOS DE EXERGIA POR UNIDADE DE MASSA
////////////////////////////////////

```

```
1199
```

```
1200
```

```
1201 //
```

```

////////////////////////////////////
EXERGIA
////////////////////////////////////

```

```
1202
```

```
1203 exergia[1] = m[1]*e[1]
```

```
1204 exergia[2] = m[2]*e[2]
```

```
1205 exergia[3] = m[3]*e[3]
```

```
1206 exergia[4] = m[4]*e[4]
```

```
1207 exergia[5] = m[5]*e[5]
```

```
1208 exergia[6] = m[6]*e[6]
```

```
1209 exergia[7] = m[7]*e[7]
```

```
1210 exergia[8] = m[8]*b_bagaco
```

```
1211 exergia[9] = m[9]*b_bagaco
```

```
1212 exergia[10] = m[10]*b_bagaco
```

```
1213 exergia[11] = m[11]*e[11]
```

```

1214 exergia[12] = m[12]*e[12]
1215 exergia[13] = m[13]*e[13]
1216 exergia[14] = m[14]*e[14]
1217 exergia[15] = m[15]*e[15]
1218 exergia[16] = m[16]*e[16]
1219 exergia[17] = m[17]*e[17]
1220 exergia[18] = m[18]*e[18]
1221 exergia[19] = m[19]*e[19]
1222 exergia[20] = m[20]*e[20]
1223 exergia[21] = m[21]*e[21]
1224 exergia[22] = m[22]*e[22]
1225 exergia[23] = m[23]*e[23]
1226 exergia[24] = m[24]*e[24]
1227 exergia[25] = m[25]*e[25]
1228 exergia[26] = m[26]*e[26]
1229 exergia[27] = m[27]*e[27]
1230 exergia[28] = m[28]*e[28]
1231 exergia[29] = m[29]*e[29]
1232 exergia[30] = m[30]*e[30]
1233 exergia[31] = m[31]*e[31]
1234 exergia[32] = m[32]*e[32]
1235 exergia[33] = m[33]*e[33]
1236 exergia[34] = m[34]*e[34]
1237 exergia[35] = m[35]*e[35]
1238 exergia[36] = m[36]*e[36]
1239 exergia[37] = m[37]*e[37]
1240 exergia[38] = m[38]*e[38]
1241 exergia[39] = m[39]*e[39]
1242 exergia[40] = m[40]*e[40]
1243 exergia[41] = m[41]*e[41]
1244 exergia[48] = W[48]
1245 exergia[49] = W[49]
1246 exergia[50] = W[50]
1247 exergia[51] = W[51]
1248 exergia[52] = W[52]
1249 exergia[53] = W[53]
1250 exergia[54] = W[54]
1251 exergia[55] = W[55]
1252 exergia[56] = W[56]
1253 exergia[57] = W[57]
1254
1255 exergia[62] = (B_q_sugar_production+
      B_q_sugar_production_var)
1256 exergia[63] = B_q_destilaria
1257
1258 exergia[64] = W[64]
1259

```

```

1260
1261 {balanço de custo exergético}
1262 B[1]=k[1]*m[1]*e[1]
1263 B[2]=k[2]*m[2]*e[2]
1264 B[3]=k[3]*m[3]*e[3]
1265 B[4]=k[4]*m[4]*e[4]
1266 B[5]=k[5]*m[5]*e[5]
1267 B[6]=k[6]*m[6]*e[6]
1268 B[7]=k[7]*m[7]*e[7]
1269 B[8]=k[8]*m[8]*b_bagaco
1270 B[9]=k[9]*m[9]*b_bagaco
1271 B[10]=k[10]*m[10]*b_bagaco
1272 B[11]=k[11]*m[11]*e[11]
1273 B[12]=k[12]*m[12]*e[12]
1274 B[13]=k[13]*m[13]*e[13]
1275 B[14]=k[14]*m[14]*e[14]
1276 B[15]=k[15]*m[15]*e[15]
1277 B[16]=k[16]*m[16]*e[16]
1278 B[17]=k[17]*m[17]*e[17]
1279 B[18]=k[18]*m[18]*e[18]
1280 B[19]=k[19]*m[19]*e[19]
1281 B[20]=k[20]*m[20]*e[20]
1282 B[21]=k[21]*m[21]*e[21]
1283 B[22]=k[22]*m[22]*e[22]
1284 B[23]=k[23]*m[23]*e[23]
1285 B[24]=k[24]*m[24]*e[24]
1286 B[25]=k[25]*m[25]*e[25]
1287 B[26]=k[26]*m[26]*e[26]
1288 B[27]=k[27]*m[27]*e[27]
1289 B[28]=k[28]*m[28]*e[28]
1290 B[29]=k[29]*m[29]*e[29]
1291 B[30]=k[30]*m[30]*e[30]
1292 B[31]=k[31]*m[31]*e[31]
1293 B[32]=k[32]*m[32]*e[32]
1294 B[33]=k[33]*m[33]*e[33]
1295 B[34]=k[34]*m[34]*e[34]
1296 B[35]=k[35]*m[35]*e[35]
1297 B[36]=k[36]*m[36]*e[36]
1298 B[37]=k[37]*m[37]*e[37]
1299 B[38]=k[38]*m[38]*e[38]
1300 B[39]=k[39]*m[39]*e[39]
1301 B[40]=k[40]*m[40]*e[40]
1302 B[41]=k[41]*m[41]*e[41]
1303 B[48]=k[48]*W[48]
1304 B[49]=k[49]*W[49]
1305 B[50]=k[50]*W[50]
1306 B[51]=k[51]*W[51]

```

```

1307 B[52]=k[52]*W[52]
1308 B[53]=k[53]*W[53]
1309 B[54]=k[54]*W[54]
1310 B[58]=k[58]
1311
1312
1313
1314 B[55]=k[55]*W[55]
1315 B[56]=k[56]*W[56]
1316 B[57]=k[57]*W[57]
1317
1318
1319
1320
1321 B[62]=k[62]*(B_q_sugar_production+
      B_q_sugar_production_var)
1322 B[63]=k[63]*B_q_destilaria
1323 B[64]=k[64]*(W_T7+W_pump1+W_pump2+W_pump3)
1324
1325 {gerador}
1326
1327
1328
1329
1330 { fluxos de entrada }
1331
1332 k[1]=1
1333 k[8]=1
1334 k[9]=1
1335 k[10]=1
1336 k[42]=1
1337 k[43]=1
1338 k[44]=1
1339 k[45]=0
1340 k[46]=0
1341 k[47]=0
1342 k[58]=0
1343 k[59]=0
1344 k[60]=0
1345 k[61]=0
1346
1347
1348 {fuel}
1349
1350 k[16]=k[17]
1351 k[18]=k[19]
1352 k[20]=k[21]

```

```

1353 k[22]=k[23]
1354 k[24]=k[25]
1355 k[26]=k[27]
1356 k[31]=k[32]
1357 k[35]=k[36]
1358
1359 {k[15]=k[16]
1360 k[15]=k[18]
1361 k[15]=k[20]
1362 k[15]=k[22]
1363 k[15]=k[24]
1364 k[15]=k[26]
1365 }
1366
1367 k[16]=k[18]
1368 k[16]=k[20]
1369 k[16]=k[22]
1370 k[16]=k[24]
1371 k[16]=k[26]
1372 k[16]=k[28]
1373 {produto}
1374
1375
1376 k[5]=k[6]
1377 k[5]=k[7]
1378 k[14]=k[15]
1379
1380
1381
1382 k[34]=k[39]
1383 k[37]=k[41]
1384
1385 k[55]=k[64]
1386 k[56]=k[64]
1387 k[57]=k[64]
1388
1389
1390 k[39]=k[40]
1391
1392
1393
1394 {Pump 1}
1395
1396 k[1]*m[1]*e[1]-k[55]*W_pump1=k[2]*m[2]*e[2]
1397
1398 {deaerator}
1399

```

```

1400 k[2]*m[2]*e[2]+k[41]*m[41]*e[41]=k[3]*m[3]*e[3]
1401
1402 {Pump 2 }
1403
1404 k[3]*m[3]*e[3]-k[56]*W_pump2=k[4]*m[4]*e[4]
1405
1406 {distribution chamber }
1407
1408 k[4]*m[4]*e[4]=k[5]*m[5]*e[5]+k[6]*m[6]*e[6]+k[7]*m
    [7]*e[7]
1409
1410 {boiler 1, 2 e 3}
1411
1412 k[5]*m[5]*e[5]+k[8]*m[8]*b_bagaco+k[42]*vazao_ar*e[
    1]=k[45]*vazao_ar*e_ch_total+k[11]*m[11]*e[11]
1413 k[6]*m[6]*e[6]+k[9]*m[9]*b_bagaco+k[43]*vazao_ar2*e
    [1]=k[46]*vazao_ar2*e_ch_total+k[12]*m[12]*e[12]
1414 k[7]*m[7]*e[7]+k[10]*m[10]*b_bagaco+k[44]*vazao_ar3
    *e[1]=k[47]*vazao_ar3*e_ch_total+k[13]*m[13]*e[13
    ]
1415
1416
1417 {mixing chamber 1 2 e 3 }
1418
1419 k[11]*m[11]*e[11]+k[12]*m[12]*e[12]=k[14]*m[14]*e[
    14]+k[15]*m[15]*e[15]
1420
1421 k[13]*m[13]*e[13]+k[14]*m[14]*e[14]=k[30]*m[30]*e[
    30]
1422
1423
1424
1425 {steam pipe}
1426
1427 k[30]*m[30]*e[30]=k[58]*0+k[31]*m[31]*e[31]
1428
1429 {turbinas}
1430
1431 k[16]*m[16]*e[16]=k[48]* W_T1+k[17]*m[17]*e[17]
1432 k[18]*m[18]*e[18]=k[49]*W_T2+k[19]*m[19]*e[19]
1433 k[20]*m[20]*e[20]=k[50]*W_T3+k[21]*m[21]*e[21]
1434 k[22]*m[22]*e[22]=k[51]*W_T4+k[23]*m[23]*e[23]
1435 k[24]*m[24]*e[24]=k[52]*W_T5+k[25]*m[25]*e[25]
1436 k[26]*m[26]*e[26]=k[53]*W_T6+k[27]*m[27]*e[27]
1437 k[31]*m[31]*e[31]=k[54]*W_T7+k[32]*m[32]*e[32]
1438
1439

```

```

1440
1441 {Valvula}
1442
1443  $k[28] * m[28] * e[28] = k[29] * m[29] * e[29]$ 
1444
1445 {mixing chamber}
1446
1447  $k[17] * m[17] * e[17] + k[19] * m[19] * e[19] + k[21] * m[21] * e[21] + k[23] * m[23] * e[23] + k[25] * m[25] * e[25] + k[27] * m[27] * e[27] + k[29] * m[29] * e[29] + k[32] * m[32] * e[32] = k[33] * m[33] * e[33]$ 
1448
1449
1450 {distribution chamber 2 e 3 }
1451
1452  $k[15] * m[15] * e[15] = k[16] * m[16] * e[16] + k[18] * m[18] * e[18] + k[20] * m[20] * e[20] + k[22] * m[22] * e[22] + k[24] * m[24] * e[24] + k[26] * m[26] * e[26] + k[28] * m[28] * e[28]$ 
1453
1454  $k[33] * m[33] * e[33] = k[34] * m[34] * e[34] + k[39] * m[39] * e[39]$ 
1455
1456 {distillery}
1457
1458  $k[39] * m[39] * e[39] = k[40] * m[40] * e[40] + k[63] * B\_q\_destilaria$ 
1459
1460
1461
1462 {desuperheater}
1463
1464  $k[34] * m[34] * e[34] + k[38] * m[38] * e[38] = k[35] * m[35] * e[35]$ 
1465
1466 {sugar production}
1467
1468  $k[35] * m[35] * e[35] = k[36] * m[36] * e[36] + k[62] * (B\_q\_sugar\_production + B\_q\_sugar\_production\_var)$ 
1469
1470
1471 {Distribtion chamber 3}
1472
1473  $k[36] * m[36] * e[36] = k[37] * m[37] * e[37] + k[41] * m[41] * e[41]$ 
1474
1475 {Pump 3}
1476

```

```
1477 k[37]*m[37]*e[37]-k[57]*W_pump3=k[38]*m[38]*e[38]
1478
1479 {gerador}
1480
1481 k[54]*W[54]-k[55]*W[55]-k[56]*W[56]-k[57]*W[57]-k[
    64]*W[64]=0
```


Annex

ANNEX A – CATALOG OF THE BPST ATTACHED TO THE GENERATOR

01 - INFORMAÇÕES GERAIS DA TURBINA

1.1 – DADOS PRINCIPAIS DA TURBINA

Número de Série	337
Tipo	TXM – 10.000/20
Ano de fabricação	2008
Acionamento	Gerador
Potência de projeto	10.000 kW
Potência de trabalho	10.000 kW
Rotação da turbina	6.000 rpm
Rotação de atuação do fecho-rápido da turbina	6.600 rpm
Pressão do vapor vivo	22 bar
Temperatura do vapor vivo	300 °C
Pressão na saída	2,5 bar
Sentido de rotação da turbina	Anti-Horário
Diâmetro da tubulação de admissão de vapor (entrada)	12 pol
Diâmetro da tubulação de escape de vapor (saída)	28 pol
Consumo específico da turbina	11,0 kg/ kWh

Figure A.1 – General information about BPST attached to the generator

ANNEX B – CATALOG OF THE BPST ATTACHED TO THE MACHINES

01 - INFORMAÇÕES GERAIS DA TURBINA

1.1 - DADOS PRINCIPAIS DA TURBINA

Número de Série	338
Tipo	TX 2040 ME/20
Ano de fabricação	2008
Acionamento	Navalha
Potência de projeto	4000 HP
Potência de trabalho	4000 HP
Rotação da turbina	6000 rpm
Rotação de atuação do fecho-rápido da turbina	6600 rpm
Pressão do vapor vivo	22 bar
Temperatura do vapor vivo	300 °C
Pressão na saída	2,5 bar
Sentido de rotação da turbina	Anti-Horário
Diâmetro da tubulação de admissão de vapor (entrada)	8"
Diâmetro da tubulação de escape de vapor (saída)	14"
Consumo específico da turbina (100% da carga)	9,25 kg/HP.h

Figure B.1 – General information about BPST

ANNEX C – GENERAL CHARACTERISTICS OF THE BOILER

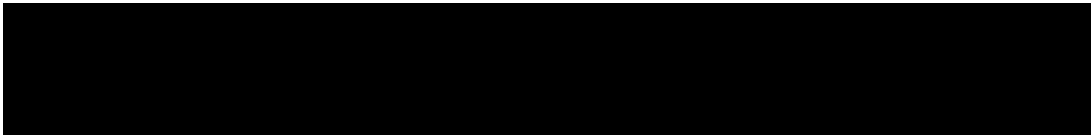


RBT_AZ-353_R0.doc


00	RS	TAMJ	TAMJ	31/07/19	EMISSÃO INICIAL	
Rev.	Elaborado	Verificado	Aprovado	Data	Descrição	
		É vedada a reprodução ou utilização total ou parcial deste documento sem prévia autorização. Sendo proibido seu uso para fins contrários aos interesses de seu proprietário.				
					Encomenda: -x-	
RELATÓRIO BALANÇO TÉRMICO CALDEIRA					Referência: CALDEIRA AZ-353	
					Grupo -----//-----	Escala -----//-----
					Código	
Projeção 1ª Diedro					Peso (kg)	Rev.
					RBT_AZ-353	00

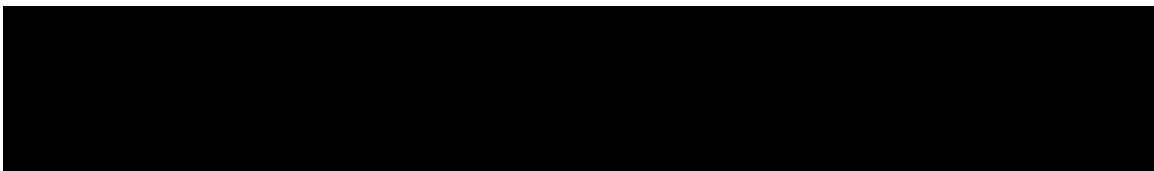
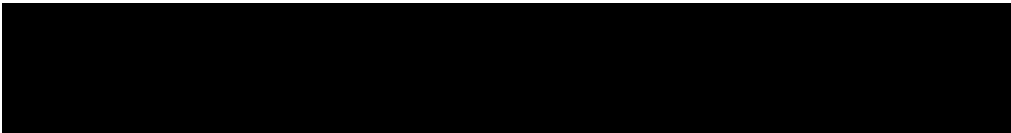
ÍNDICE

DADOS DA CALDEIRA.....	3
LOCALIZAÇÃO DA INSTALAÇÃO	3
INTRODUÇÃO	4
GERAL	4
PRODUÇÃO 70 T/H DE VAPOR; 21 KGF/CM ²	4
DADOS DE PERFORMANCE.....	7



DADOS DA CALDEIRA

Caldeira - Modelo..... AZ-353
Categoria da Caldeira "A"
Número do Registro 42.220 (Original)
Ano de Fabricação 1.983
Fabricante..... 
Produção de Vapor..... 50.000 kg/h (Original)
Produção de Vapor..... 70.000 kg/h (Otimizada)
Pressão de Operação..... 21,0 kgf/cm² man.
Temperatura do Vapor..... 320 °C
Temperatura da água de alimentação 105 °C
Combustível..... Bagaço de Cana

LOCALIZAÇÃO DA INSTALAÇÃO

INTRODUÇÃO

O relatório abaixo visa explicar de uma forma sucinta o comportamento da caldeira operando a 70 t/h de vapor, conforme projeto da otimização realizado.

GERAL

Originalmente a caldeira AZ-353 foi projetada para produzir 50 t/h de vapor, tendo 265 m³ de volume de fornalha.

Com os desenhos fornecidos pelo Cliente, nota-se que na otimização, manteve-se a elevação do tambor inferior e o centro a centro entre tambores.

A configuração das serpentinas do superaquecedor de vapor foram alteradas, modificando o sentido do fluxo do vapor e aumentando os trechos retos das serpentinas.

Em função da alteração das serpentinas do superaquecedor, a parede traseira da fornalha e screen foram alterados, com isto houve diminuição do volume de fornalha em 25 m³.

As paredes de água da fornalha, tipo espaçada, foram substituídas por paredes tipo tangentes.

As tubulações do feixe de convecção foram mantidas conforme projeto original, porem o fluxo dos gases passou de paralelo para cruzado.

Antes do pré-aquecedor de ar foi instalado um economizador do tipo tubos lisos, com 02 (dois) passes lado gás.

Após o pré-aquecedor de ar foi instalado multiciclone.

Com as informações levantadas, elaboramos o balanço térmico para verificação da caldeira.

PRODUÇÃO 70 T/H DE VAPOR; 21 KGF/CM²

Fornalha

Com tempo de residência de 1,4 segundos, há necessidade de aumentar o volume de fornalha.

- ✓ **Ideal:** Complementar as tubulações da fornalha elevando os tambores.
- ✓ **Ideal:** Instalação de sistema de ar secundário, incluso ventilador de alta pressão.



Sistema de Alimentação

Não foi possível a verificação.

- ✓ **Ideal:** Levantar dimensional dos dosadores, eixos, pinos e bandeja de espargimento para cálculo e verificação.

Quanto a liberação térmica da grelha basculante, a mesma encontra-se com os parâmetros acima do recomendado.

Screen

Em função da alteração, a velocidade dos gases encontra-se em 19,0 m/s, acima dos parâmetros recomendados.

- ✓ **Ideal:** Alteração na configuração das tubulações do screen adequando a velocidade dos gases.

Superaquecedor de Vapor

Para 70 t/h de vapor a temperatura do vapor encontra-se entre 350°C e 360°C.

A velocidade dos gases encontra-se dentro dos parâmetros recomendados.

Internos do Tambor de Vapor

Não foi possível a verificação.

- ✓ **Ideal:** Levantar qual o tipo de internos instalados para verificação de aproveitamento ou substituição.

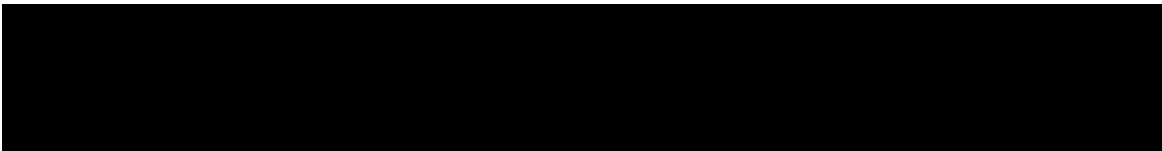
Feixe de Convecção


A velocidade média dos gases encontra-se em 13,0 m/s, pouco acima dos parâmetros recomendados.

- ✓ **Ideal:** Com as alterações do projeto da caldeira, a velocidade tende a diminuir, não sendo necessário alteração na configuração das tubulações.

Economizador

A velocidade média dos gases encontra-se em 17,0 m/s (1° passe) e 15,0 m/s (2° passe), acima dos parâmetros recomendados.



- 
- ✓ **Ideal:** Posicionar o economizador após o pré-aquecedor de ar e verificar necessidade ou não de alteração na configuração e/ou superfície de troca térmica.

Pré-Aquecedor de Ar

As velocidades mássicas encontram-se acima dos parâmetros recomendados e a temperatura do ar baixa (142°C):

- ✓ **Ideal:** Posicionar o pré-aquecedor de ar antes do economizador e verificar necessidade ou não de alteração na configuração e/ou superfície de troca térmica.

Ventiladores de Tiragem Induzida, Ar Forçado e Ar Auxiliar

Como os ventiladores foram fabricados em campo, não temos informações referentes a folha de dados para verificação.

- ✓ **Ideal:** Contatar empresa especializada para levantamento do dimensional e posterior verificação mediante Especificação Técnica com os novos dados operacionais da caldeira.

Válvulas e Acessórios

Não verificado.



DADOS DE PERFORMANCE

CARACTERÍSTICAS GERAIS					
TIPO DA CALDEIRA:		Aquatubular	SUPERFÍCIES DE TROCA DE CALOR		
CONDIÇÕES DE PROJETO			Feixe tubular (m²):		1.220
Capacidade (kg/h):	70.000		Fornalha – projetada (m²):		198
Pressão de operação (kgf/cm² g):	21		Superaquecedor (m²):		204
Temperatura do vapor (°C):	360		Economizador (m²):		382
Temperatura da água de alimentação (°C):	105		Pré-aquecedores de ar (m²):		2.000
Pressão de projeto (kgf/cm² g):	-				
Temperatura do ar ambiente (°C):	27		VOLUME / ÁREA:		
Altitude local (m):	629		Volume da fornalha (m³):		240
Umidade relativa (%):	55		Área da grelha principal (m²):		25,5
DADOS DE PERFORMANCE PREVISTOS					
DADOS DE OPERAÇÃO		PERDAS			
MCR (%):	100	PERDAS DE CARGA (mmca) (Operação)			
Temp. da água - entrada do economizador (°C):	105	Perda de carga do lado do ar:		120	
Temp. da água - saída do economizador (°C):	165	Perda de carga do lado do gás:		315	
Temp. do ar - entrada do pré-ar (°C):	27	PERDAS DE CALOR (%)			
Temp. do ar - entrada do pré-ar (°C):	142	Gás seco:		6,08	
Temp. do gás - saída da fornalha (°C):	1001	Umidade no combustível e formada:		23,03	
Temp. do gás - saída da caldeira (°C):	359	Radiação:		0,39	
Temp. do gás - saída do economizador (°C):	246	Combustível não queimado:		2,00	
Temp. do gás - saída do pré-ar (°C):	173	Não calculados:		1,00	
Excesso de ar (%):	30	Total das perdas:		32,50	
Vazão total de ar (kg/h):	109.122				
Vazão total de gás (kg/h):	138.863	DADOS DO COMBUSTÍVEL			
Liberação máx. na grelha ao PCI (kcal/h.m²):	2,10E+06	TIPO: Bagaço de cana			
Liberação volumétrica máxima ao PCI (kcal/h.m³):	222.984	ANÁLISE FINAL (% Peso)			
Eficiência estimada ao PCS (%):	67,50	C:	23,00	PODER CALORÍFICO	
Eficiência estimada ao PCI (%):	85,59	H₂:	3,25	PCI (kcal/kg):	1.775
Combustível queimado (kg/h): *	30.135	O₂:	23,00		
Produção específica (kg vapor/kg comb):	2,32	S:	0	PCS (kcal/kg):	2.250
Tempo de residência dos gases na fornalha (s):	1,40	N₂:	0		
		H₂O:	50		
		Cinzas:	0,75		